Copyright Warning & Restrictions

The copyright law of the United States (Title 17, United States Code) governs the making of photocopies or other reproductions of copyrighted material.

Under certain conditions specified in the law, libraries and archives are authorized to furnish a photocopy or other reproduction. One of these specified conditions is that the photocopy or reproduction is not to be "used for any purpose other than private study, scholarship, or research." If a, user makes a request for, or later uses, a photocopy or reproduction for purposes in excess of "fair use" that user may be liable for copyright infringement,

This institution reserves the right to refuse to accept a copying order if, in its judgment, fulfillment of the order would involve violation of copyright law.

Please Note: The author retains the copyright while the New Jersey Institute of Technology reserves the right to distribute this thesis or dissertation

Printing note: If you do not wish to print this page, then select "Pages from: first page # to: last page #" on the print dialog screen

ABSTRACT

CHARACTERIZATION OF LIGHTNING INDUCED VOLTAGES ON OVERHEAD POWER LINES

by
Wen-Ta Hsiao

The transient voltage surge caused by lightning is the major source contributed to the disturbance on power systems. The calculation of induced voltages,which is the propagated voltage surge on overhead power lines due to indirect lightning strokes, has been the subject of theoretical and experimental studies. The objective of this research is to develop a comprehensive numerical method to study the induced voltages on an overhead power line caused by a lightning return stroke with arbitrary shapes, for examples inclined lightning, zigzag lightning, etc.

A finite-length lightning channel of any direction in 3-D space has been modelled and closed-form expressions of the inducing potentials have been derived from image theory. The total inducing scalar potential and inducing vector potential caused by an arbitrarily shaped lightning stroke are evaluated by superposition. Because that the presented numerical model simulates the realistic state and takes into account the retarded-height difference between the original sources and the image sources, the bipolar characteristic of the inducing scalar potential as well as the bipolar induced voltage waves are observed.

The final induced voltage is completely composed of two components, one is the traveling voltage wave created by the inducing scalar potential, and the other is the standing voltage wave created by the vertical component of the inducing vector potential. The induced voltage on the power line is calculated by solving the partial differential

equations in which the horizontal component of the inducing vector potential is taken into consideration. A computer program has been developed to perform the comprehensive calculations with the use of the finite-difference time-domain method in which the differential equations are converted into difference equations. Through this numerical program, the induced voltage is evaluated as functions of time and space on the power line. The numerical algorithm has been validated by a simulation test on a Gaussian pulse propagation.

With the use of the program, parametric effects on the induced voltage caused by a vertical lightning stroke are inspected systematically. The comparisons of the induced voltage caused by inclined lightning strokes are made under various conditions. The effect of the horizontal component of the inducing vector potential has been illustrated. The results show that the severity of the inclined return stroke on the overhead power line is considerably harmful, especially when the return-stroke velocity gets faster or the inclined angle increases. This high voltage surge should be taken into account in the lightning protection design of transmission lines as well as distribution lines.

CHARACTERIZATION OF LIGHTNING INDUCED VOLTAGES ON OVERHEAD POWER LINES

by
Wen-Ta Hsiao

A Thesis
Submitted to the Faculty of
New Jersey Institute of Technology
in Partial Fulfillment of the Requirements for the Degree of
Master of Science in Electrical Engineering

Department of Electrical and Computer Engineering

May 1994

APPROVAL PAGE

CHARACTERIZATION OF LIGHTNING INDUCED VOLTAGES ON OVERHEAD POWER LINES

Wen-Ta Hsiao

Dr. Edwin Cohen, Thesis Adviser (Date)
Professor of Electrical and Computer Engineering, NJIT

Dr. Shih-Chang Wu, Coadviser (Date)
Assistant Professor of Electrical and Computer Engineering, NJIT

Mr. Wayne Clements, Committee Member (Date)
Associate Professor of Electrical and Computer Engineering, NJIT

BIOGRAPHICAL SKETCH

Author: Wen-Ta Hsiao

Degree: Master of Science in Electrical Engineering

Date: May 1994

Undergraduate and Graduate Education:

- Master of Science in Electrical Engineering,
  New Jersey Institute of Technology, Newark, NJ, 1994

- Bachelor of Science in Electrical Engineering,
  National Cheng Kung University, Tainan, Taiwan, R.O.C., 1984

Major: Electrical Engineering

This thesis is dedicated to
my dear parents
and lovely wife

ACKNOWLEDGMENT

At first, the author wishes to cherish the heartfelt memory of his former adviser, Dr. Khalil Denno, whose proposition incited this research idea. The author is extremely grateful to his current adviser, Professor Edwin Cohen, for his fervent assistance, invaluable suggestions, corrections, and moral support throughout this research.

The author would particularly like to acknowledge the contribution of his coadviser, Professor Shih-Chang Wu, whose guidance, constructive opinions and insightful view in electromagnetics has been a great help to this research.

The author also wants to express his sincere appreciation to Professor Wayne Clements for serving as a member of the thesis committee and his numerous comments greatly improving the final text.

Finally, deep thanks to my wife, Hsiao-Ying Kao, for her understanding and encouragement during the long hours of involvement with this research.

TABLE OF CONTENTS

LIST OF FIGURES

CHAPTER 1

LIGHTNING

1.1 Introduction

Lightning occurs when some region of the atmosphere contains electric charges sufficiently large such that the electric fields associated with the charges cause electrical breakdown of the air. Lightning can be defined as a transient, high-current electric discharge whose path length is generally measured in kilometers. The most common producer of lightning is the thundercloud. Such lightning can take place entirely within a cloud itself (intracloud or cloud discharges), between two clouds (cloud-to-cloud discharges), or between cloud and the earth (cloud-to-ground or ground discharges). Although the most frequently occurring form of lightning is the intracloud discharge, the major concern to the power system is the ground discharge, which is closer to the power lines. Cloud-to-ground lightning is sometimes referred to as streaked or forked lightning. A cloud-to-ground lightning discharge is made up of one or more intermittent partial discharges. The total discharge (whose time duration is of the order of 0.2 sec) is called a flash; and each component discharge is referred a stroke. In general, there are three or four strokes per flash, and the strokes are approximately separated by 40 millisecond. [1]

1.2 Relation between Lightning and Overhead Power Lines

The transient voltages generated either by external origins or by internally switching operations are of great concern to power systems. Among them, lightning is the largest single cause of faults. The transient high voltage caused by lightning is the major source of disturbance to overhead power lines. Such transient voltage can appear on an overhead line either by direct hit or by induction from a nearby lightning stroke. From statistic point

of view, indirect lightning strokes are as hazardous as direct strokes to the power system equipment because of their frequent occurrence.

In general, the power lines pass through many miles of territory in which there is great likelihood of lightning activities. A lightning stroke, even at a distance of 1 km away from the line, would induce a voltage surge along the line. This induced voltage surge is large enough to cause damage. It is common practice to protect overhead power lines against lightning at least in the areas where they are considered to be vulnerable. The statement, "...lightning is the greatest single cause of outages..., accounting for about 26% of the outages on 230 kV circuits and about 65% of the outages on 345 kV.", in the report issued by a Joint IEEE-EEI Committee studying outages on EHV Lines [2], appropriately described the interaction between lightning and overhead power lines.

1.3 The Return Stroke

In Chowdhuri, et al. study [3], the induced voltages had broadly been classified as follows,

(a) electrostatic effect of the cloud

(b) electrostatic effect of the stepped leader

(c) magnetic effect of the return stroke

(d) electromagnetic effect of the return stroke

It had been shown that only the electromagnetic effect of the return stroke is of any practical significance. What is a return stroke? When the stepped leader has lowered a charged column of high negative potential to near the ground, the resulting high electric field at the ground is sufficient to cause upward-moving discharges to be launched from the ground toward the leader tip. When one of these discharges contacts the leader, the bottom of the leader is effectively connected to ground potential while the remainder of the leader is at negative potential and is negatively charged. The situation is somewhat similar to a transmission line charged to a constant potential with a short circuit applied at

its end. The leader channel acts like a transmission line (nonlinear and lossy) supporting a very luminous return stroke. The return-stroke wavefront, an ionizing wavefront of high electric field intensity, carries ground potential up the path created previously by the stepped leader. The return-stroke wavefront propagates at a velocity of typically one-third to one-tenth the speed of light, making the trip between cloud base and ground in a time of the order of 50 μsec. The region between the return-stroke wavefront and ground is traversed by large currents. The excess negative charge deposited on the leader channel is effectively lowered to earth through the highly conducting channel beneath the return-stroke wavefront. The current measured at the ground rises typically to 10 to 20 kA in a few microseconds and falls to one-half of peak value typically in 20 to 60 μsec.[1]

1.4 Review of Published Studies

Induced voltages on overhead power lines caused by lightning strokes have been the subject of theoretical and experimental studies for quite some time. The early fundamental theoretical paper was published by Wagner and McCann [4]. They assumed that, prior to the return stroke, an electric charge is uniformly distributed along the lightning channel. It is, then, instantaneously neutralized as the current in the return stroke propagated upwards along the lightning path with a constant velocity. Consequently, the current behaves as a step-function. The inducing electric field was computed by Maxwell's equations and retarded potentials. Finally, the induced voltage was calculated by a numerical integration method.

In 1958, Rusck [5] published a theory on the calculation of induced voltages, which was taking into consideration both the scalar and the vector potentials of the inducing field. He gave expressions for the scalar and vector potentials caused by a uniform current propagated upwards along a linear lightning channel over a perfectly conducting earth. The line integral of the electric field from the ground to the line was

considered by Rusck to be the voltage on the line. In addition, Rusck also pointed out that the voltage caused by any other current shape may be obtained through the application of the Duhamel integral.

Chowdhuri et al. [3] realized that the induced voltage results not only from the directly radiated fields, but also from the fields from other points on the line and guided along the line. Accordingly, they solved the transmission line partial differential equations with Rusck's voltage expression for a step current as the forcing term. The method adopted by Chowdhuri and Gross for calculating the induced voltage caused by any other form of current was to apply Duhamel's theorem on the known solution for a step current propagating upwards the lightning channel. Since the publication of their analysis, several theoretical studies [6,7,8] have been successively reported to discuss this topic; and some suggestions have been made to improve the analysis. Despite of many discrepancies remained among these reported theoretical studies, there are two general assumptions were imposed on the analytic models. First, the lightning channel was assumed to be vertical. Secondly, the electric fields between the line and ground were assumed to be equal to the field at ground level because, in general, the height of the line is much smaller than that of the cloud.

Experimental investigations have also been reported by Eriksson, et al.[9] and Yokoyama, et al. [10]. Both papers utilized an experimental distribution line and instruments for measuring the induced voltage to obtain records. They compared the measured peak values and waveforms of induced voltages with the calculated results by making use of theoretical analytic models. In other words, they still adopted the two general assumptions mentioned above. In 1989, Sakakibara [11] reported the study of the induced voltages caused by the unidirectionally inclined lightning strokes. In the conclusion of his study, he pointed out that "... The voltages induced by inclined strokes are considerably higher than those by vertical ones irrespective of the progress velocity.

Higher voltages will be induced by inclined return strokes not near the lightning struck point but at locations some distance away from such point. ..."

1.5 Objective

In the above review, it is evident that, in calculating lightning induced voltages, it has been generally assumed that the lightning channel is a straight line (mostly vertical). Therefore, the characteristics of the induced voltages on an overhead power line caused by lightning strokes with arbitrary configurations is an interesting topic and worthy of investigation. The objective of this research is presenting a comprehensive numerical method to study the induced voltages on an overhead power line caused by a lightning return stroke with arbitrary shapes. To avoid confusion, two terminologies need to be clarified beforehand.

(1) Inducing potential: The electromagnetic fields produced by the charges and current in the lightning stroke will induce an electromagnetic potential on the power line. The value of this potential is relative to the ground potential (zero reference level). The electromagnetic potential is composed of two components. One is the inducing scalar potential created by the charges distributed along the lightning channel, and the other is the inducing vector potential created by the current of the return stroke.

(2) Induced voltage: The inducing potential at different points along the power line will be different. These potentials at different points of the power line tend to be correlated by the transmission-line equations. Therefore, the actual voltage measured on the power line will be different from the inducing potential. The actually measured voltage is defined as the induced voltage.

In a word, the inducing potential is the force function or the source of the induced voltage. The evaluation of the inducing potential will be presented in Chapter 2, and the evaluation of the induced voltage is demonstrated in Chapter 3. In Chapter 2, closed-form

expressions of the inducing potentials caused by a straight finite-length segment of a return stroke will be derived analytically. The total inducing potential caused by an arbitrary-shape return stroke composed of many segments is computed through superposition. In Chapter 3, the induced voltage on the power line is evaluated by solving the partial differential equations. Here, the finite-difference time-domain numerical scheme is utilized to solve the partial differential equations. A computer program has been developed to perform the comprehensive calculations. In Chapter 4, the parametric effects on the induced voltage caused by a vertical return stroke will be examined systematically. The effects of the inclined angle and direction of an arbitrary return stroke on the induced voltage are also investigated. In Chapter 5, conclusions and future research areas will be presented.

CHAPTER 2

INDUCING POTENTIAL

2.1 Introduction

A lightning return stroke, which contains time-varying current and charges, induces electromagnetic fields. These induced fields propagate out from the sources (charge and current) with the velocity of light. It is this field which can induce unexpected voltages and currents in an overhead power line. If the conductivity of the earth is assumed to be infinite, the field can be calculated by the image theory, according to which currents and charges above the ground are reflected below it and the images have the same magnitude as above the ground but opposite direction and polarity, respectively. The electromagnetic fields are generally expressed by a scalar potential V_s and a vector potential $\bar{A}_m$. The inducing potential on the power line is composed of the inducing scalar potential V_s and the potential V_{mz} produced by the vertical component of the inducing vector potential $\bar{A}_m$. The inducing potential at different points along an overhead power line will be different. In Section 2.2, some symbols are defined and basic assumptions are made. In Section 2.3, a finite-length lightning channel in 3-D space is modelled and closed-form expressions of the inducing potentials are derived from image theory. In Section 2.4, an arbitrarily shaped lightning stroke is simulated and the total inducing potentials are evaluated by superposition.

2.2 Symbols and Basic Assumptions

2.2.1 Symbols

V = voltage induced on the line

I = current induced on the line

V_i = inducing potential caused by return stroke

L = distributed inductance of the power line

C = distributed capacitance of the power line

V_s = inducing scalar potential caused by return stroke

$\vec{A}_m$ = inducing vector potential caused by return stroke

q_l = charge distributed in the lightning channel

I_m = return stroke current

I_0 = peak value of return stroke current

$\vec{E}_m$ = electric field intensity due to inducing vector potential $(-\partial\vec{A}_m/\partial t)$

E_{mx}, E_{my}, E_{mz} = x, y, and z components of $\vec{E}_m$

V_{mz} = potential on an overhead power line produced by E_{mz}

r = distance of source point from field point

l = length of a lightning channel

$\hat{l}$ = unit vector in the direction of a lightning return stroke

a, b, c = x, y, and z components of $\hat{l}$

$P(x, y, z)$ = field point in the rectangular coordinate system

$S(x, y, z)$ = source point in the rectangular coordinate system

t = time

t_f = front duration of the return stroke current

h = height of the power line above ground

h_c = height of the thundercloud above ground

v_0 = velocity of light in free space

v = progress velocity of the return stroke current

y_0 = least distance of the power line from the lightning struck point

β = ratio of velocity of the return stroke current to velocity of light in free space

ε_0 = permittivity of free space

μ_0 = permeability of free space

2.2.2 Basic Assumptions

Yokoyama [12] had proved that in untransposed lines, the induced voltages arising on a multiconductor line can essentially be handled in the manner used for single-conductor lines. In his paper, figures showed that the waveform of the middle phase in the parallel three-phase system was identical to the waveform arising in a single-conductor line at the same position. So throughout this research, just the case of a single-conductor line is considered and the basic assumptions are made as fellows,

(a) The charge distribution along the leader stroke is uniform and the polarity is negative.

(b) The waveshape of the return-stroke current is shown in Fig. 2.1, which rises rapidly before front time and falls with a drooping tail.

(c) The return stroke progresses upwards.

(d) The velocity of the return stroke is constant.

(e) The power line is lossless and the earth is perfectly conductive.

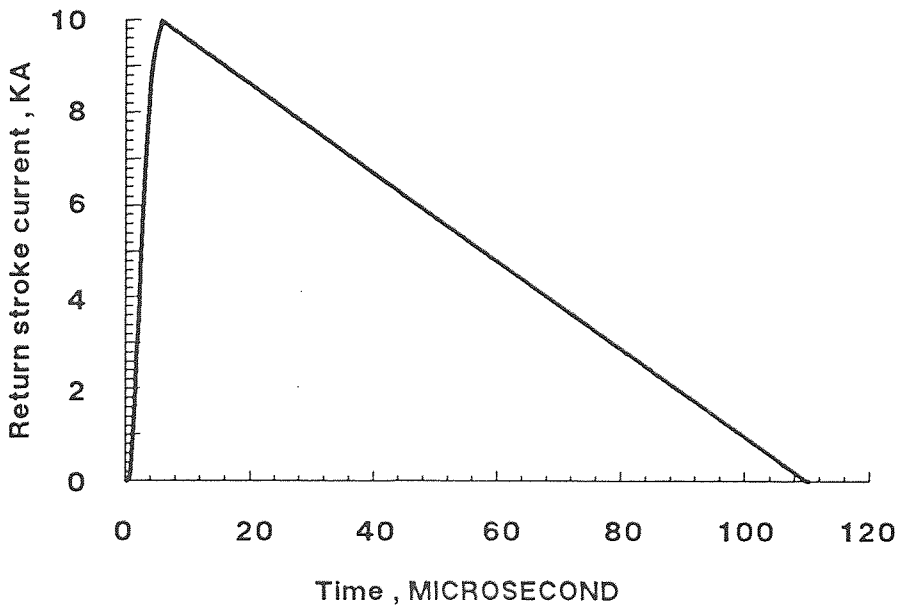

Figure 2.1 Waveshape of the return-stroke current with a 5μs front time.

2.3 Theory

As shown in Fig. 2.2, the inducing scalar potential (V_s) at the point $P(x,y,z)$ caused by one segment of charges distributed in the leader channel can be calculated as follows.

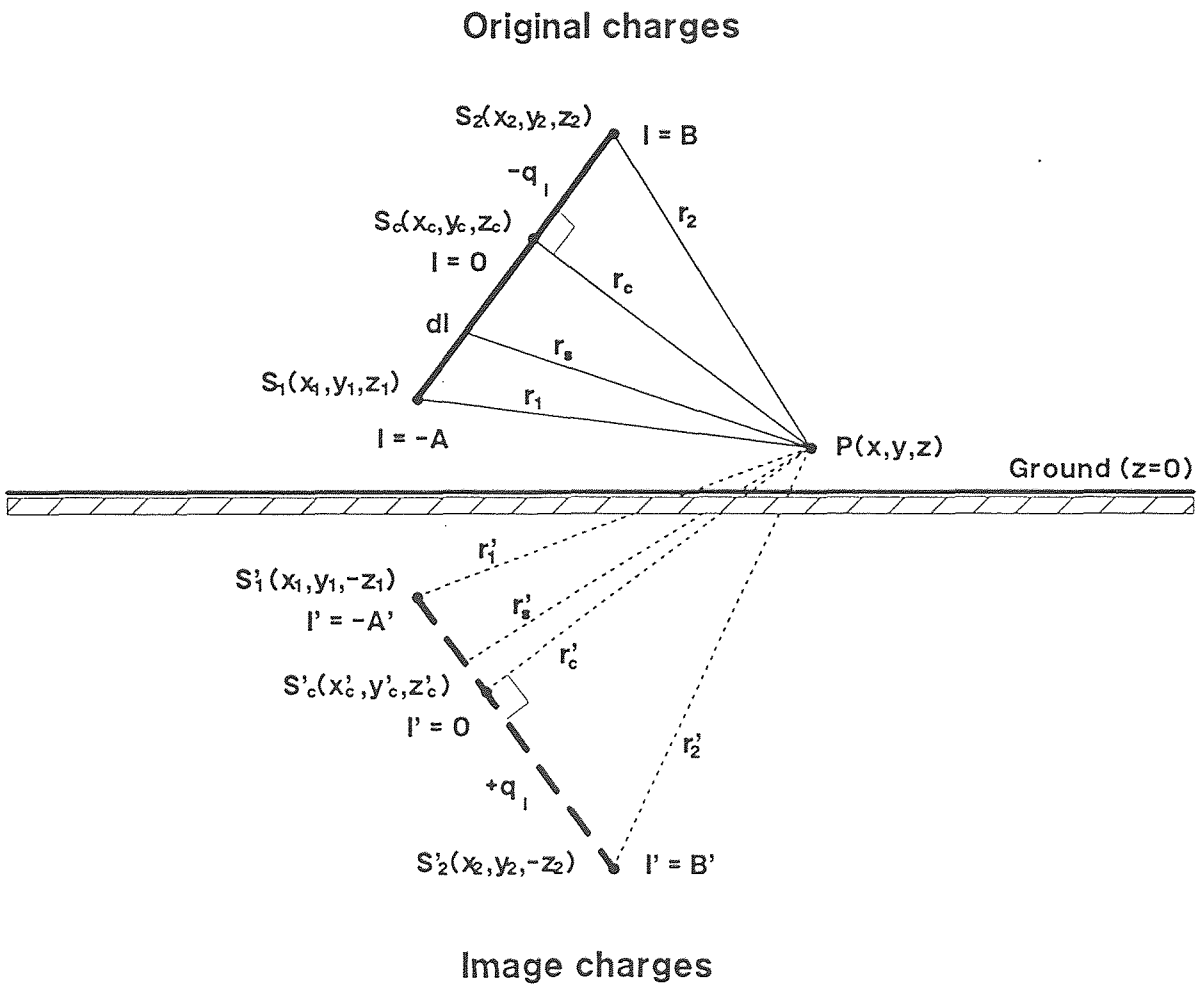

Figure 2.2 Sketch plan of one segment of charges distributed in the leader channel.

When the charge per unit length at dl is $-q_l$, the inducing scalar potential produced by original charges is expressed by equation (2.1).

$$V_s' = \frac{1}{4\pi\varepsilon_0}\int_{S_1}^{S_2}\frac{-q_l}{r_s}\,dl = \frac{-q_l}{4\pi\varepsilon_0}\ln\frac{\sqrt{r_c^2+B^2}+B}{\sqrt{r_c^2+A^2}-A} \tag{2.1}$$

where $-q_l$ is negative due to electron accumulation, the distance $\left|\overline{S_1P}\right| = r_1$, the distance $\left|\overline{S_2P}\right| = r_2$, the distance $\left|\overline{S_cP}\right| = r_c$, the distance $\left|\overline{S_1S_c}\right| = A$, the distance $\left|\overline{S_2S_c}\right| = B$, and $\overline{S_cP} \perp \overline{S_1S_2}$.

The inducing scalar potential produced by image charges is expressed by equation (2.2).

$$V_s'' = \frac{1}{4\pi\varepsilon_0}\int_{S_1'}^{S_2'}\frac{q_l}{r_s'}\,dl = \frac{q_l}{4\pi\varepsilon_0}\ln\frac{\sqrt{r_c'^2+B'^2}+B'}{\sqrt{r_c'^2+A'^2}-A'} \tag{2.2}$$

where the distance $\left|\overline{S_1'P}\right| = r_1'$, the distance $\left|\overline{S_2'P}\right| = r_2'$, the distance $\left|\overline{S_c'P}\right| = r_c'$, the distance $\left|\overline{S_1'S_c'}\right| = A'$, the distance $\left|\overline{S_2'S_c'}\right| = B'$, and $\overline{S_c'P} \perp \overline{S_1'S_2'}$.

The relationship among the charge q_l, the current I_m, and the progress velocity of the return stroke is constrained by conservation of charges as

$$q_l = I_m / v \tag{2.3}$$

From Fig. 2.2 , the following triangle relations are tenable.

$$\sqrt{r_c^2+A^2} = r_1 \;;\; \sqrt{r_c^2+B^2} = r_2 \tag{2.4}$$

$$\sqrt{r_c'^2+A'^2} = r_1' \;;\; \sqrt{r_c'^2+B'^2} = r_2' \tag{2.5}$$

Substituting equations (2.3),(2.4) and (2.5), equations(2.1) and (2.2) can be rewritten as (2.6) and (2.7), respectively.

$$V_s' = \frac{-30I_m}{\beta} \ln \frac{r_2(\pm)\sqrt{r_2^2 - r_c^2}}{r_1(\pm)\sqrt{r_1^2 - r_c^2}} \tag{2.6}$$

$$V_s'' = \frac{30I_m}{\beta} \ln \frac{r_2'(\pm)\sqrt{r_2'^2 - r_c'^2}}{r_1'(\pm)\sqrt{r_1'^2 - r_c'^2}} \tag{2.7}$$

The location of point $S_c(x_c, y_c, z_c)$ and the choice of the proper sign from the double sign ($\pm$) in equation (2.6) are determined by the following observations.

Since the point $S_c(x_c, y_c, z_c)$ lies on the line $\overline{S_1S_2}$, it can be expressed by

$$x_c = x_1 + \lambda(x_2 - x_1) \tag{2.8}$$

$$y_c = y_1 + \lambda(y_2 - y_1) \tag{2.9}$$

$$z_c = z_1 + \lambda(z_2 - z_1) \tag{2.10}$$

Because of $\overline{S_cP} \perp \overline{S_1S_2}$, the following equation is obtained.

$$(x_2 - x_1)(x_c - x) + (y_2 - y_1)(y_c - y) + (z_2 - z_1)(z_c - z) = 0 \tag{2.11}$$

Substituting equations (2.8)~(2.10) into (2.11), the parameter λ is solved.

$$\lambda = -\frac{[(x_2 - x_1)(x_1 - x) + (y_2 - y_1)(y_1 - y) + (z_2 - z_1)(z_1 - z)]}{[(x_2 - x_1)^2 + (y_2 - y_1)^2 + (z_2 - z_1)^2]} \tag{2.12}$$

x_c, y_c and z_c are obtained by substituting equation (2.12) into (2.8) ~ (2.10). The proper sign from the double sign ($\pm$) in equation (2.6) is chosen according to the following criteria,

(1) If $z_2 > z_c$, then choose sign (+) for the numerator, otherwise choose sign (−).

(2) If $z_1 > z_c$, then choose sign (+) for the denominator, otherwise choose sign (−).

The location of point $S_c'(x_c', y_c', z_c')$ and the choice of the proper sign from the double sign ($\pm$) in equation (2.7) can be determined through the same way.

As shown in Fig.2.3, the inducing vector potential ($\vec{A}_m$) at the point $P(x, y, z)$ caused by the return stroke current (I_m) can be calculated as follows.

The inducing vector potentials produced by the original current and the image current are expressed by equations (2.13) and (2.14), respectively.

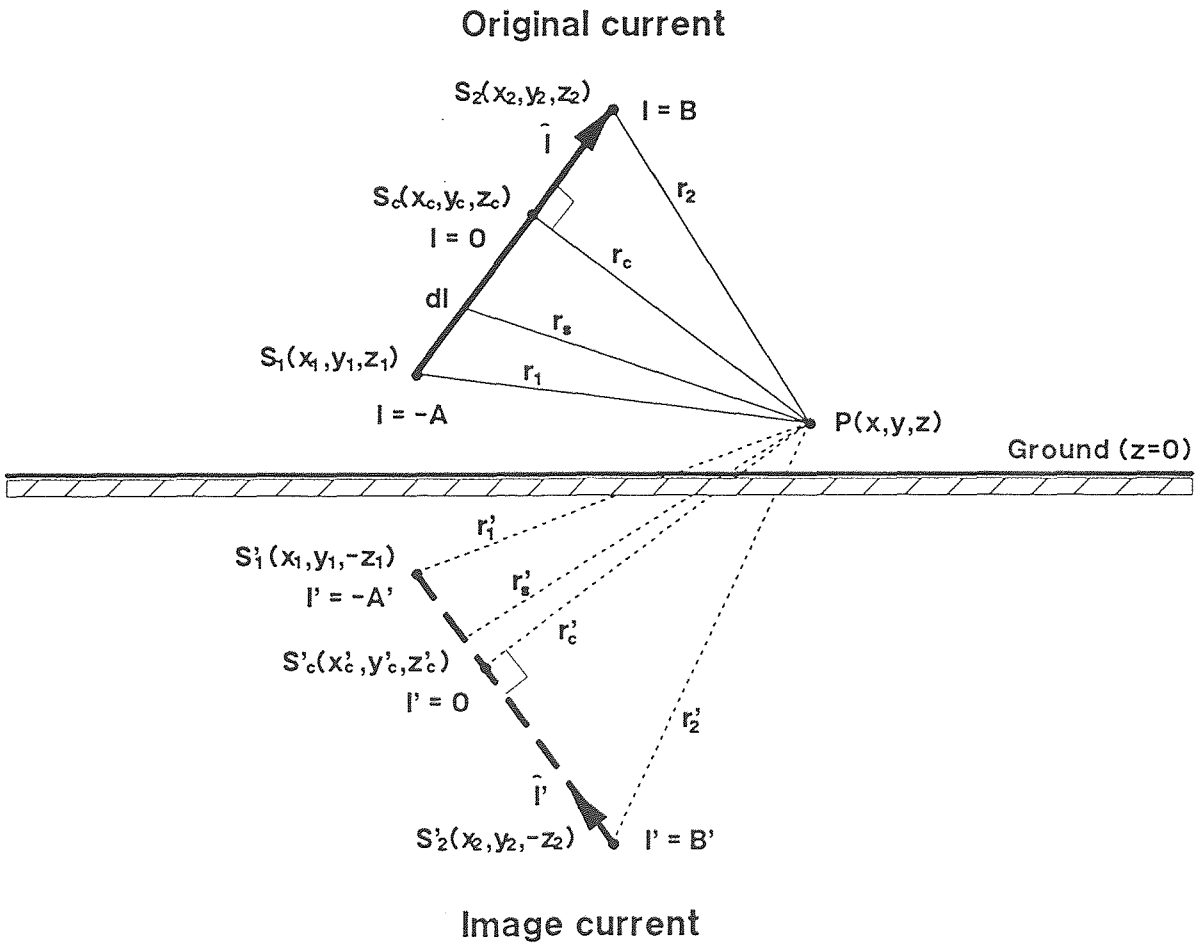

Figure 2.3 Sketch plan of one segment of the return-stroke current.

$$\vec{A}'_m = \hat{l}\,\frac{\mu_0}{4\pi}\int_{S_1}^{S_2}\frac{I_m}{r_s}\,dl = \hat{l}\,\frac{\mu_0 I_m}{4\pi}\ln\frac{\sqrt{r_c^2+B^2}+B}{\sqrt{r_c^2+A^2}-A} \tag{2.13}$$

$$\vec{A}''_m = \hat{l}'\,\frac{\mu_0}{4\pi}\int_{S_1'}^{S_2'}\frac{I_m}{r_s'}\,dl = \hat{l}'\,\frac{\mu_0 I_m}{4\pi}\ln\frac{\sqrt{r_c'^2+B'^2}+B'}{\sqrt{r_c'^2+A'^2}-A'} \tag{2.14}$$

where $\hat{l}$ is a unit vector in the progressing direction of the lightning return stroke

$$\begin{aligned}\hat{l} = \frac{\bar{l}}{l} &= \left(\frac{1}{\sqrt{(x_2-x_1)^2+(y_2-y_1)^2+(z_2-z_1)^2}}\right)\left[(x_2-x_1)\,\hat{i}+(y_2-y_1)\,\hat{j}+(z_2-z_1)\,\hat{k}\right] \\ &= a\,\hat{i}+b\,\hat{j}+c\,\hat{k}\end{aligned} \tag{2.15}$$

$$\hat{l}' = -\hat{l}^* = -a\,\hat{i}-b\,\hat{j}+c\,\hat{k} \tag{2.16}$$

where $\hat{l}^*$ is the conjugate vector of the $\hat{l}$ relative to the ground surface.

The electric field intensity due to the return stroke current is expressed by

$$\bar{E}_m = -\frac{\partial \bar{A}_m}{\partial t} \tag{2.17}$$

From equations (2.13), (2.14) and (2.17), $\bar{E}'_m$ and $\bar{E}''_m$ are expressed as

$$\begin{aligned}\bar{E}'_m = -\frac{\partial \bar{A}'_m}{\partial t} &= -\hat{l}\bullet\left(30 I_m \beta\frac{1}{r_2}+\frac{\mu_0}{4\pi}\frac{\partial I_m}{\partial t}\ln\frac{\sqrt{r_c^2+B^2}+B}{\sqrt{r_c^2+A^2}-A}\right) \\ &= (-a\,\hat{i}-b\,\hat{j}-c\,\hat{k})\bullet E'_m\end{aligned} \tag{2.18}$$

$$\begin{aligned}\bar{E}''_m = -\frac{\partial \bar{A}''_m}{\partial t} &= \hat{l}^*\bullet\left(30 I_m \beta\frac{1}{r_2'}+\frac{\mu_0}{4\pi}\frac{\partial I_m}{\partial t}\ln\frac{\sqrt{r_c'^2+B'^2}+B'}{\sqrt{r_c'^2+A'^2}-A'}\right) \\ &= (a\,\hat{i}+b\,\hat{j}-c\,\hat{k})\bullet E''_m\end{aligned} \tag{2.19}$$

Because of the retardation effect, the inducing scalar potential V_s' and vector potential $\vec{A}_m'$ at the field point $P(x,y,z)$ and at time t must be originated at the source point $S_1(x_1,y_1,z_1)$ at an earlier time $t' = t - r_1/v_0$. The quantity of r_1/v_0 is called retardation time. For the image source, its retardation time is r_1'/v_0. When the retardation time is taken into account, V_s can be expressed as

$$V_s = V_s' \bullet u(t - r_1/v_0) + V_s'' \bullet u(t - r_1'/v_0) \tag{2.20}$$

where $u(t)$: A step function, when $t < 0$, $u(t) = 0$; when $t \geq 0$, $u(t) = 1$.

Similarly, $\vec{E}_m$ is obtained by

$$\begin{aligned} \vec{E}_m &= \vec{E}_m' + \vec{E}_m'' \\ &= (-a\,\hat{i} - b\,\hat{j} - c\,\hat{k}) \bullet E_m' \bullet u(t - r_1/v_0) + (a\,\hat{i} + b\,\hat{j} - c\,\hat{k}) \bullet E_m'' \bullet u(t - r_1'/v_0) \end{aligned} \tag{2.21}$$

The x, y and z components of $\vec{E}_m$ can be expressed as

$$\left.\begin{aligned} E_{mx} &= -a[E_m' \bullet u(t - r_1/v_0) - E_m'' \bullet u(t - r_1'/v_0)] \\ E_{my} &= -b[E_m' \bullet u(t - r_1/v_0) - E_m'' \bullet u(t - r_1'/v_0)] \\ E_{mz} &= -c[E_m' \bullet u(t - r_1/v_0) + E_m'' \bullet u(t - r_1'/v_0)] \end{aligned}\right\} \tag{2.22}$$

The potential V_{mz} at point $P(x,y,z)$ derived from the vertical component of the inducing vector potential is given by

$$V_{mz} = \int_0^h (-E_{mz})\, dz \tag{2.23}$$

When h is small, E_{mz} can be assumed to be a constant. Therefore

$$\begin{aligned} V_{mz} = h \bullet (-E_{mz}) &= hc \bullet \left(30 I_m \beta \frac{1}{r_2} + \frac{\mu_0}{4\pi} \frac{\partial I_m}{\partial t} \ln \frac{\sqrt{r_c^2 + B^2} + B}{\sqrt{r_c^2 + A^2} - A} \right) \bullet u(t - r_1/v_0) \\ &+ hc \bullet \left(30 I_m \beta \frac{1}{r_2'} + \frac{\mu_0}{4\pi} \frac{\partial I_m}{\partial t} \ln \frac{\sqrt{r_c'^2 + B'^2} + B'}{\sqrt{r_c'^2 + A'^2} - A'} \right) \bullet u(t - r_1'/v_0) \\ &= V_{mz}' + V_{mz}'' \end{aligned} \tag{2.24}$$

2.4 Numerical Simulations

In practice, a lightning return stroke is composed of many inclined segments with different lengths and arbitrary orientations. As shown in Fig.2.4, the figuration of a realistic lightning return stroke is simulated by several continuous segments. For convenience, some symbols are defined as follows.

$P(x,y,z)$: a field point on the overhead power line

$S_0(x_0,y_0,0)$: originating point of the lightning return stroke

$S_i(x_i,y_i,z_i)$, $i=1...n$: turning points along the original leader channel

$S_i'(x_i,y_i,-z_i)$, $i=1...n$: turning points along the image leader channel

t_i , $i=0...n$: time when the disturbance of the original source at point S_i is felt at the field point P

t_i' , $i=1...n$: time when the disturbance of the image source at point S_i' is felt at the field point P

l_i , $i=1...n$: length of each segment of the leader channel

For a given time t , the progressing point of the return stroke can be determined by the following method.

If $t_i < t < t_{i+1}$, that means the progressing point S_t has passed the turning point S_i and lies on the segment $i+1$. As shown in Fig.2.5, the coordinate values of point $S_t(x_t,y_t,z_t)$ can be evaluated as follows,

Assuming $\Delta t = t - t_i$, it can be expressed as

$$\Delta t = \frac{\Delta l}{v} + \frac{\left|\overline{S_t P}\right|}{v_0} - \frac{r_i}{v_0} \tag{2.25}$$

The coordinate values of the progressing point S_t are given by

$$\overrightarrow{S_i S_t} = \Delta l \bullet \hat{l}_{i+1} = a_{i+1}\Delta l\,\hat{i} + b_{i+1}\Delta l\,\hat{j} + c_{i+1}\Delta l\,\hat{k} \tag{2.26}$$

$$\Rightarrow S_t(x_t,y_t,z_t) = S_t(x_i + a_{i+1}\Delta l\ ,\ y_i + b_{i+1}\Delta l\ ,\ z_{i+1} + c_{i+1}\Delta l) \tag{2.27}$$

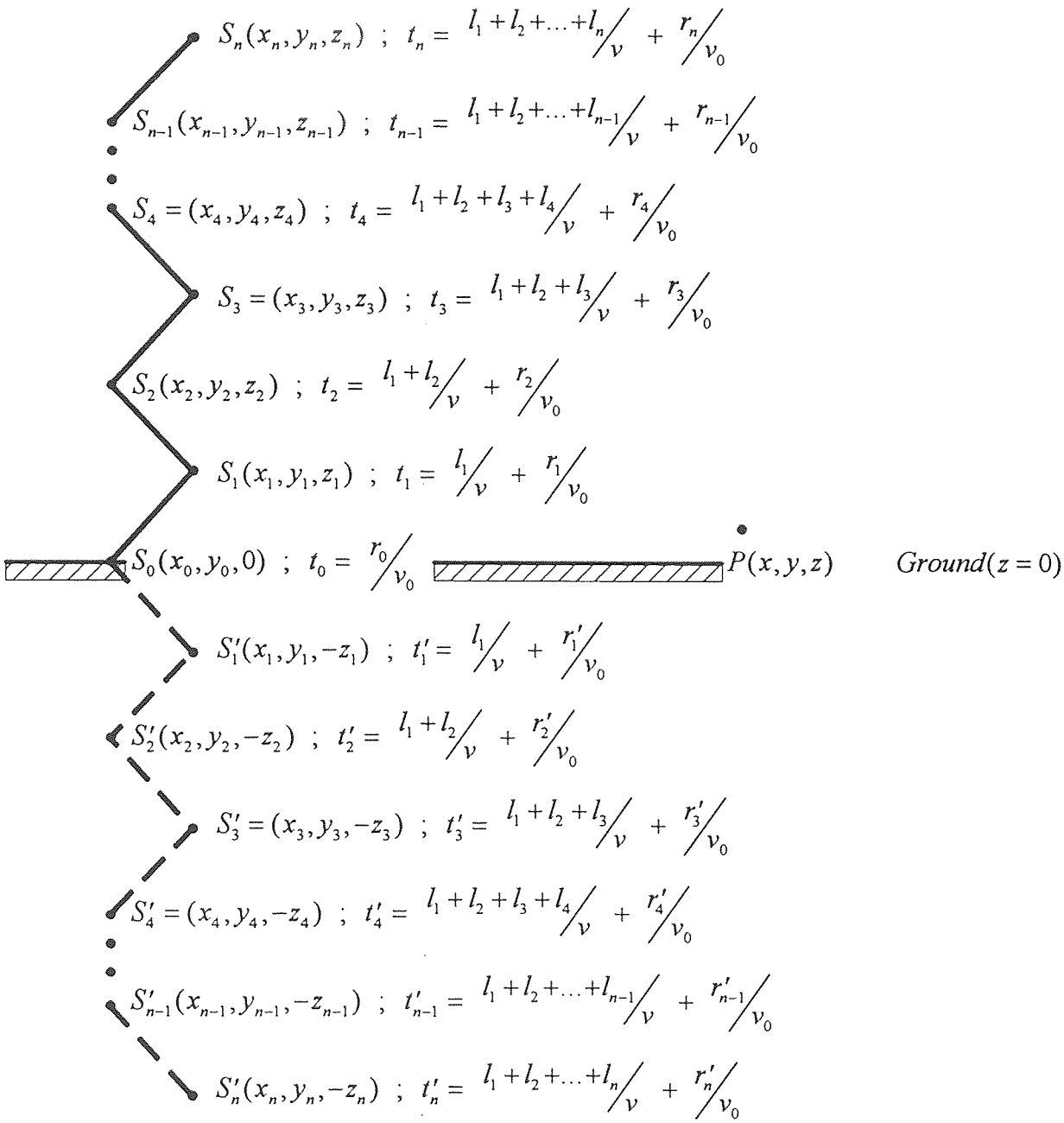

Figure 2.4 Figuration of a realistic lightning return stroke.

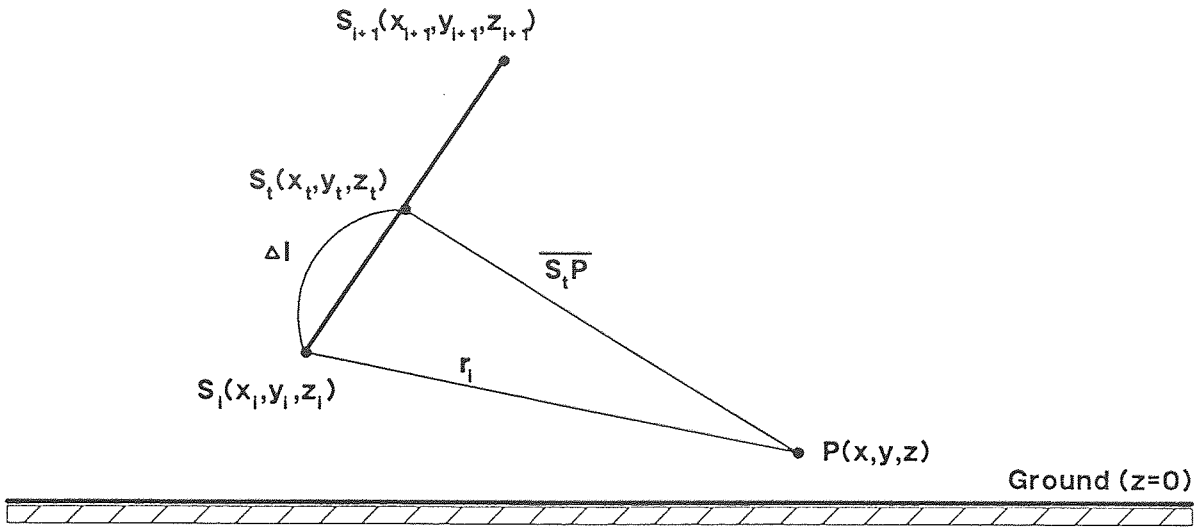

Figure 2.5 Sketch plan of the progressing point along the leader channel.

The length of segment $\overline{S_tP}$ can be expressed by

$$\begin{aligned}\overline{S_tP} &= \sqrt{(a_{i+1}\Delta l + x_i - x)^2 + (b_{i+1}\Delta l + y_i - y)^2 + (c_{i+1}\Delta l + z_i - z)^2} \\ &= \sqrt{\Delta l^2 + 2\delta\,\Delta l + r_i^2}\end{aligned} \tag{2.28}$$

where $\delta = a_{i+1}(x_i - x) + b_{i+1}(y_i - y) + c_{i+1}(z_i - z)$, $r_i = \sqrt{(x_i - x)^2 + (y_i - y)^2 + (z_i - z)^2}$

Substituting equation (2.28) into (2.25), it can be rewritten as

$$\Delta t = \frac{\Delta l}{v} + \frac{\sqrt{\Delta l^2 + 2\delta\,\Delta l + r_i^2}}{v_0} - \frac{r_i}{v_0} \tag{2.29}$$

Transform equation (2.29) and solve for Δl.

$$\Delta l = \frac{(v\Delta t + \beta r_i + \beta^2\delta) \pm \sqrt{(v\Delta t + \beta r_i + \beta^2\delta)^2 - (1-\beta^2)(v^2\Delta t^2 + 2\beta v\Delta t\, r_i)}}{(1-\beta^2)} \tag{2.30}$$

When the plus sign is given between the first and the second terms in equation (2.29) , the minus sign should be chosen from the double sign ($\pm$) in equation (2.30).

Substituting the calculated Δl into equation (2.27), the coordinate values of the progressing point S_t can be obtained immediately.

The numerical method to calculate the inducing potentials at the field point P at a given time t is described as follows,

Step 1 : Use the techniques presented in the previous paragraph to find the progressing points $S_t(x_t, y_t, z_t)$ and $S_t'(x_t', y_t', -z_t')$. Assume that the point S_t is located on segment i and the point S_t' is located on segment j'.

Step 2 : Closed-form expressions of the inducing potentials have been analytically derived in Section 2.3 for the finite-length accumulated charges and the return stroke current. The potentials due to the original and image sources are listed below.

$$V_s'(P,t) = \frac{-30I_m}{\beta}\left[\ln\frac{r_i(\pm)\sqrt{r_i^2 - r_{ic}^2}}{\overline{S_tP}(\pm)\sqrt{\overline{S_tP}^2 - r_{ic}^2}} + \sum_{k=i+1}^{n}\ln\frac{r_k(\pm)\sqrt{r_k^2 - r_{kc}^2}}{r_{k-1}(\pm)\sqrt{r_{k-1}^2 - r_{kc}^2}}\right] \tag{2.31}$$

$$V_s''(P,t) = \frac{30I_m}{\beta}\left[\ln\frac{r_j'(\pm)\sqrt{r_j'^2 - r_{jc}'^2}}{\overline{S_t'P}(\pm)\sqrt{\overline{S_t'P}^2 - r_{jc}'^2}} + \sum_{k=j+1}^{n}\ln\frac{r_k'(\pm)\sqrt{r_k'^2 - r_{kc}'^2}}{r_{k-1}'(\pm)\sqrt{r_{k-1}'^2 - r_{kc}'^2}}\right] \tag{2.32}$$

$$\begin{aligned} V_{mz}'(P,t) &= 30I_m\beta h\frac{c_i}{\overline{S_tP}} \\ &+ \frac{\mu_0}{4\pi}\frac{\partial I_m}{\partial t}\left[\sum_{k=1}^{i-1}\ln\frac{r_k(\pm)\sqrt{r_k^2 - r_{kc}^2}}{r_{k-1}(\pm)\sqrt{r_{k-1}^2 - r_{kc}^2}} + \ln\frac{\overline{S_tP} + (\pm)\sqrt{\overline{S_tP}^2 - r_{ic}^2}}{r_{i-1}(\pm)\sqrt{r_{i-1}^2 - r_{ic}^2}}\right]\bullet hc_i \end{aligned} \tag{2.33}$$

$$V''_{mz}(P,t) = 30 I_m \beta h \frac{c_j}{\overline{S'_t P}} + \frac{\mu_0}{4\pi}\frac{\partial I_m}{\partial t}\left[\sum_{k=1}^{j-1} \ln \frac{r'_k(\pm)\sqrt{r'^2_k - r'^2_{kc}}}{r'_{k-1}(\pm)\sqrt{r'^2_{k-1} - r'^2_{kc}}} + \ln \frac{\overline{S'_t P}(\pm)\sqrt{\overline{S'_t P}^2 - r'^2_{jc}}}{r'_{j-1}(\pm)\sqrt{r'^2_{j-1} - r'^2_{jc}}}\right] \bullet hc_j \quad (2.34)$$

Step 3 : The total inducing potentials at the field point P are computed by superposition. The inducing potentials consist of direct components (V'_s, V'_{mz}) and ground image components (V''_s, V''_{mz}). Thus,

$$V_s(P,t) = V'_s(P,t) + V''_s(P,t) \quad (2.35)$$

and

$$V_{mz}(P,t) = V'_{mz}(P,t) + V''_{mz}(P,t) \quad (2.36)$$

2.5 Validation of the Numerical Method

To validate the numerical method, calculations of the inducing potential were performed on two cases of return strokes. The results were compared with published results. The first case involves the calculation of the inducing potential caused by a vertical return stroke with rectangular current, and the second case with rapidly-rising current. For comparison purposes, identical conditions were applied.

2.5.1 Inducing Potential Caused by a Vertical Return Stroke with Rectangular Current

The conventional theory on the calculation of the inducing scalar and vector potential adopted by most studies is published by Rusck [5]. The calculation formulae are rewritten below.

$$V_s(\text{scalar}) = \frac{60I_0h}{\beta}\left[\frac{1}{\sqrt{h_c^2 + r^2}} - \frac{1}{\sqrt{v^2t^2 + (1-\beta^2)r^2}}\right] \tag{2.37}$$

$$V_{mz}(\text{vector}) = \frac{60I_0h}{\beta}\left[\frac{\beta^2}{\sqrt{v^2t^2 + (1-\beta^2)r^2}}\right] \tag{2.38}$$

where r is the distance of a point on the power line from the lightning return stroke measured along ground, $r = \sqrt{x^2 + y_0^{\,2}}$

In order to emphasize the significance of the height of a power line above ground in the calculation of the inducing potentials, two points were computed and their results are shown in Fig.2.6 and 2.7 (placed in Appendix), respectively. In Fig. 2.6, both waveshapes and peak values are completely identical. In Fig. 2.7, although the waveshapes still perfectly agree with each other, there exists a considerable difference in peak values between two scalar potentials. Such discrepancy derives from whether the height h is taken into account or not. In the published method, a basic assumption is imposed on the analytic model, which is stated as follows.

As the height h of the line conductor is small compared with the height of the cloud, the inducing electromagnetic fields below the line conductor can be assumed to be constant and equal to those on the ground surface.

When the distance of an overhead power line from the lightning return stroke is far enough, the variation of the field intensity with the height above the ground can be undoubtedly neglected, which is demonstrated in Fig. 2.6. However, if the lightning happens quite near to the power line, the diversity of the electromagnetic field intensity will no longer be ignored. Consequently the treatment of the published method [5] is not fully appropriate. Nonetheless, the theory is still very important and Rusck's contribution on induced voltages caused by lightning strokes is well recognized.

2.5.2 Inducing Potential Caused by a Vertical Return Stroke with Rapidly-Rising Current

Also according to Rusck's study, the inducing potential due to any current shape in the lightning return stroke can be obtained through the application of the Duhamel's theorem (convolution integral) to the known potential due to a step-function current (rectangular) in the lightning return stroke. Because in the numerical method, the inducing potential at any point P at any time t is computed by superposition, the parametric effect of the current waveshape has been considered directly. In order to verify the legitimacy of such treatment, comparisons also were made between the numerical method and the published method. The waveshape of the return stroke current shown in Fig.2.8.(A) (placed in Appendix) is applied and the calculation results are shown in Fig.2.8.(B) (placed in Appendix).

The curve obtained through the numerical method shows that the inducing scalar potential starts with a spike and diminishes with slowly approaching to zero. In fact, the curve reverses in polarity, passes through zero, rises to the reversed peak value and finally decays to zero again. Because the ratio of the positive peak value to the negative spike is too small, this phenomenon can not be seen distinctly. It is shown clearly in Fig.2.11.(B) (placed in Appendix).

The curve obtained through the published method has the same waveshape at the beginning of the return stroke, but reverses in polarity, rises continuously to the reversed peak value and finally stays at the peak value. From the viewpoint of physics, this result is out of character of the lightning return stroke. As mentioned before, the primary causes of the inducing potentials are the electrostatic and the magnetic components of the inducing electromagnetic fields. The electrostatic component is the inducing scalar potential created by the distributed charges of the lightning channel, and the magnetic component is the inducing vector potential created by the current of the return stroke. Because the inducing scalar potential depends on the amount of charges, it is impossible that when the charges

diminish to slight and keep a long distance from the power line, the inducing scalar potential still rises continuously and finally stays at the peak value. In fact, the mathematic property of convolution integral is responsible for this impractical result. In order to explain more clearly, a rapidly-rising current with constant tail shown in Fig.2.9.(A) (placed in Appendix) is applied and the response results are shown in Fig.2.9.(B) (placed in Appendix). The inconsistency of the inducing scalar potential computed through convolution integral is evident if we compare Fig.2.8.(B) with Fig.2.9.(B). At the same point and time, the inducing scalar potential caused by large charges is irrationally less than that caused by little charges. These curves are rearranged in Fig.2.10 (placed in Appendix) to show the effect of the return-stroke current tail.

From the above discussion, it is obvious that the bipolar characteristic of the inducing scalar potential is not due to the drooping tail of the return-stroke current. In fact, the bipolar phenomenon is due to the retardation height. The effect of the retardation height will be stated as follows.

As shown in Fig.2.12 (placed in Appendix), the inducing scalar potential is composed of two components, one caused by original charges and the other caused by image charges. According to the image theory, the effect of the original component is direct but the effect of the image component is reflected. The through path of the image effect is longer than that of the original effect, i.e. the retardation time of the image charges will be longer than that of the original charges. Because the inducing scalar potential is calculated at the same field point and time, the interested affair is the position of the progressing point at time t . For a vertical return stroke, the retardation height is defined as the distance of the progressing point from the ground. For the original source, the retardation height Z_t is calculated by

$$t = \frac{Z_t}{v} + \frac{\sqrt{(Z_t - h)^2 + r_0^2}}{v_0}$$
$$\Rightarrow Z_t = \frac{(vt - \beta^2 h) - \sqrt{(vt - \beta^2 h)^2 - (1-\beta^2)(v^2 t^2 - \beta^2 r_0^2 - \beta^2 h^2)}}{(1-\beta^2)} \quad (2.39)$$

For the image source, the retardation height Z_t' is calculated by

$$t = \frac{Z_t'}{v} + \frac{\sqrt{(Z_t' + h)^2 + r_0^2}}{v_0}$$
$$\Rightarrow Z_t' = \frac{(vt + \beta^2 h) - \sqrt{(vt + \beta^2 h)^2 - (1-\beta^2)(v^2 t^2 - \beta^2 r_0^2 - \beta^2 h^2)}}{(1-\beta^2)} \quad (2.40)$$

where r_0 is the distance of the field point from the lightning return stroke measured along the ground, $r_0 = \sqrt{x^2 + y_0^2}$.

At anytime t, Z_t is always longer than Z_t'. So the following inequality is established.

$$(h_c - Z_t) \leq (h_c - Z_t') \quad (2.41)$$

The inequality explicitly shows that the quantity of the image charges always outstrips that of the original charges. The effect of the difference in the charge quantity can be discussed separately in two stages.

(1) In the earlier period of the lightning return stroke

In this stage, the difference in amount of charges just occupies a very small proportion in the long leader channel. The effect of the difference in the charge quantity can be neglected. On the contrary, the distance of the sources from the power line plays a decisive role and the influence of the factor "h" is apparently important. Because the original charges are closer to the power line than the image charges, the inducing scalar potential caused by original charges dominates the

final value. Accordingly, the inducing scalar potential remains negative during the earlier period of the lightning return stroke.

(2) In the later period of the lightning return stroke

In the later stage, only a little residual charges exist in the leader channel. The difference in amount of charges will occupy an influential proportion and its effect is remarkable. On the other hand, the residual charges are quite far away from the power line in this stage. Namely, the influence of the difference in the charge quantity overcomes that of the distance. Because the image charges are more than the original charges, the inducing scalar potential changes into positive during the later period of the lightning return stroke.

The inducing scalar potential in two different stages is illustrated in Fig.2.11 (placed in Appendix). The difference in the retardation heights just causes the bipolar phenomenon of the inducing scalar potential. The other cause of the bipolar characteristic of the induced voltage is the potential V_{mz} produced by the vertical component of the inducing vector potential $\vec{A}_m$. According to equations (2.31)~(2.36), V_s and V_{mz} are of opposite polarity when the return stroke is initiated. Moreover, V_s is in inverse proportion to the parameter β, but V_{mz} is in direct proportion to it. Therefore, the higher the return-stroke velocity the more evident is the bipolar phenomenon of the induced voltage. About this topic, more details will be illustrated in Chapter 4.

CHAPTER 3

INDUCED VOLTAGE

3.1 Introduction

A lossless model is a good representation for most of the overhead power lines where ωL and ωC become very large compared to R and G. For lightning surges on an overhead power line, the study of a lossless line is a simplification that enables us to understand the phenomena of the induced voltage propagated along the power line without becoming too involved in complicated theory. Besides, a doubly infinite single-conductor line can be represented in practice by a line whose terminals are sufficiently distant from the struck point of the lightning return stroke that reflections of the induced voltage at the terminals can be neglected. This system is relatively simple to analyze, and it gives an insight into the physical nature of the lightning surges on an overhead power line caused by an arbitrarily inclined stroke.

3.2 Theory

The coordinate system of a power line and a lightning return stroke is shown in Fig.3.1. The z axis is vertical, and the x axis is parallel to the line and lies on the ground surface. The origin is chosen as the starting point of the return stroke. The line is assumed to be located at a distance y_0 meters from the origin and has a height h meters above the ground.

A lossless power line can be represented as consisting of distributed series inductance and distributed shunt capacitance. The effect of the inducing potential will then be equivalent to connecting an electromotive force along each infinitesimal section of the power line. The distribution of the line current is illustrated in Fig.3.2.

According to Sakakibara's analysis [11], the basic equations for calculating the induced voltage are expressed as

$$\frac{\partial V}{\partial x}\delta x = -L\frac{\partial I}{\partial t}\delta x + E_{mx}\delta x + \frac{\partial V_{mz}}{\partial x}\delta x \tag{3.1}$$

$$\frac{\partial I}{\partial x}\delta x = -C\frac{\partial}{\partial t}(V - V_i)\delta x \tag{3.2}$$

$$V_i = V_s + V_{mz} \tag{3.3}$$

Where L is the distributed inductance of the power line and C is the distributed capacitance. V_i is the inducing potential, V_s and V_{mz} are expressed in equations (2.31)~(2.36), and E_{mx} can be obtained by

$$E_{mx} = E'_{mx} + E''_{mx} = V'_{mz}\left(\frac{-a_i}{hc_i}\right) + V''_{mz}\left(\frac{a_j}{hc_j}\right) \tag{3.4}$$

The equations (3.1)~(3.3) can be illustrated by the equivalent circuit shown in Fig.3.3. In this circuit, the electromotive force relating to V_{mz} does not initiate a traveling wave. However, it produces a standing wave which raises the line voltage by V_{mz}. The last term in equation (3.1) can be moved to the left-hand side. Let $V_p = V - V_{mz}$ and defind V_p as a traveling wave (propagated voltage). Therefore the traveling wave V_p can be calculated by using an equivalent circuit given in Fig.3.4 wherein the electromotive force relating to V_{mz} is eliminated. The induced voltage on the line can be obtained by adding V_p and V_{mz}. Hence equations (3.1)~(3.3) can be transformed to the following equations.

$$\frac{\partial V_p}{\partial x}\delta x = -L\frac{\partial I}{\partial t}\delta x + E_{mx}\delta x \tag{3.5}$$

$$\frac{\partial I}{\partial x}\delta x = -C\frac{\partial}{\partial t}(V_p - V_s)\delta x \tag{3.6}$$

$$V = V_p + V_{mz} \tag{3.7}$$

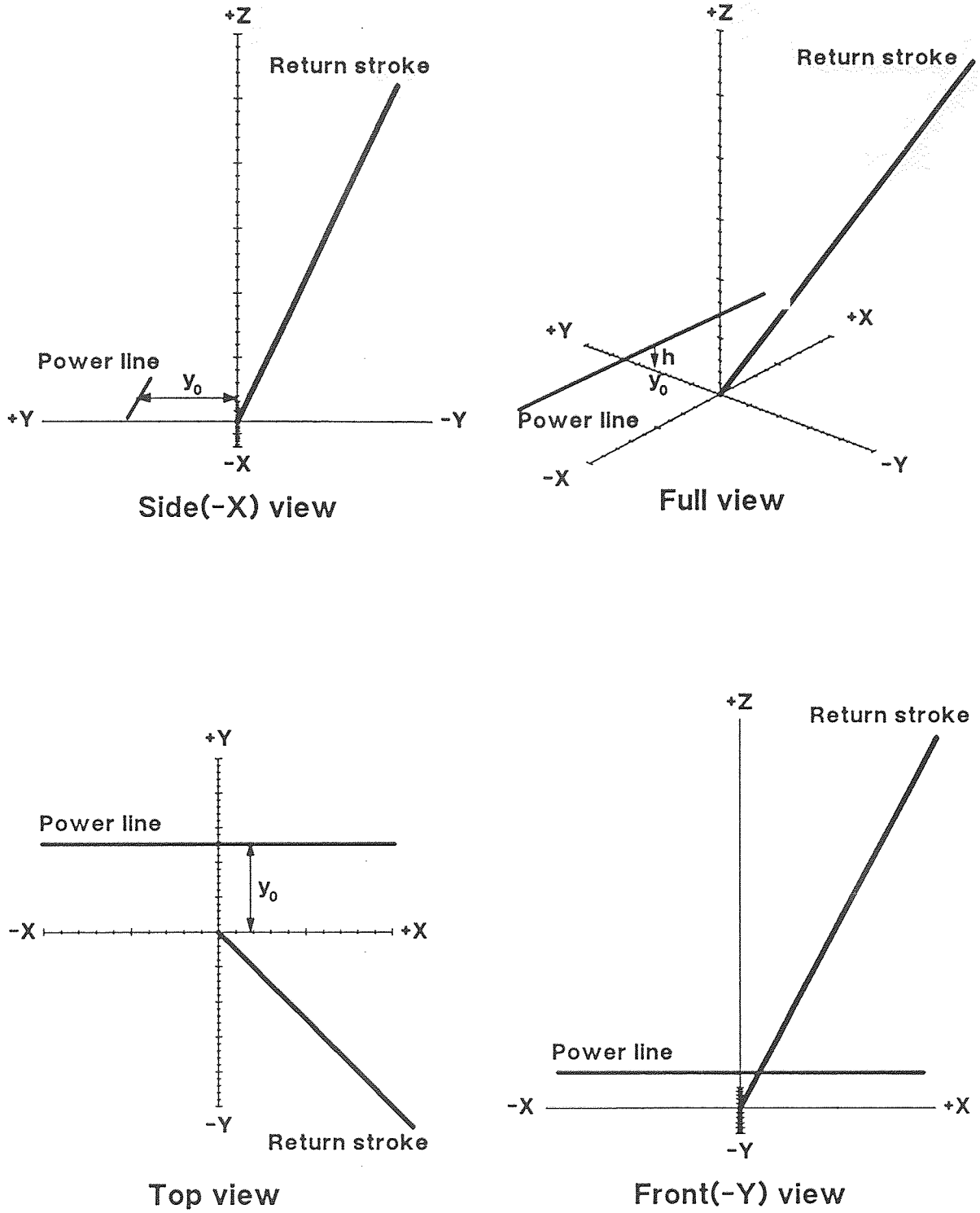

Figure 3.1 Coordinate system of a power line and a lightning return stroke

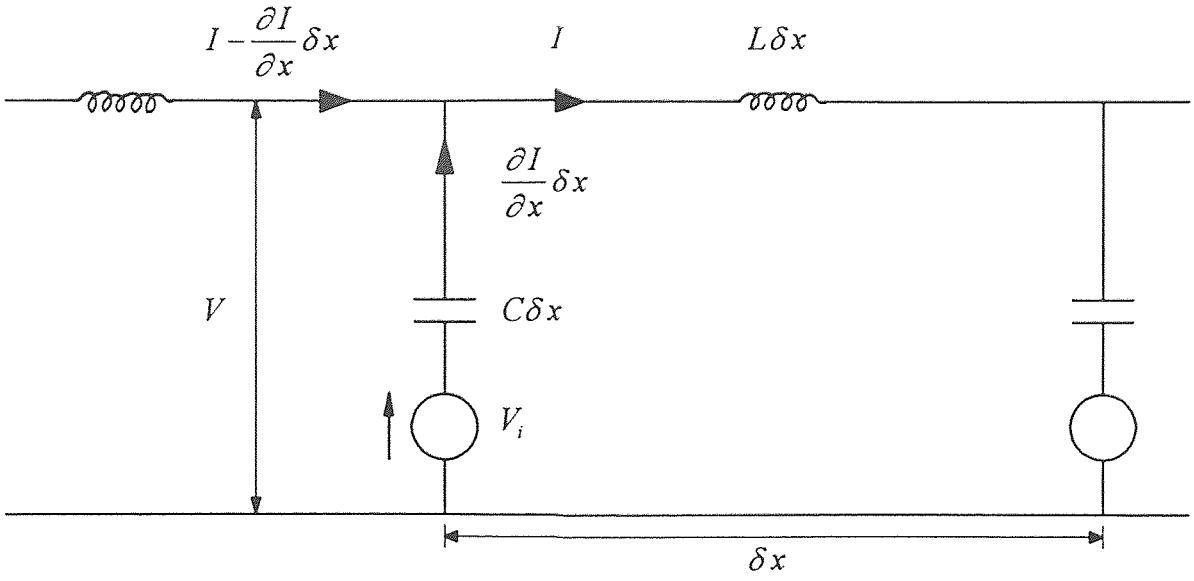

Figure 3.2 Infinitesimal section of a power line and current distribution.

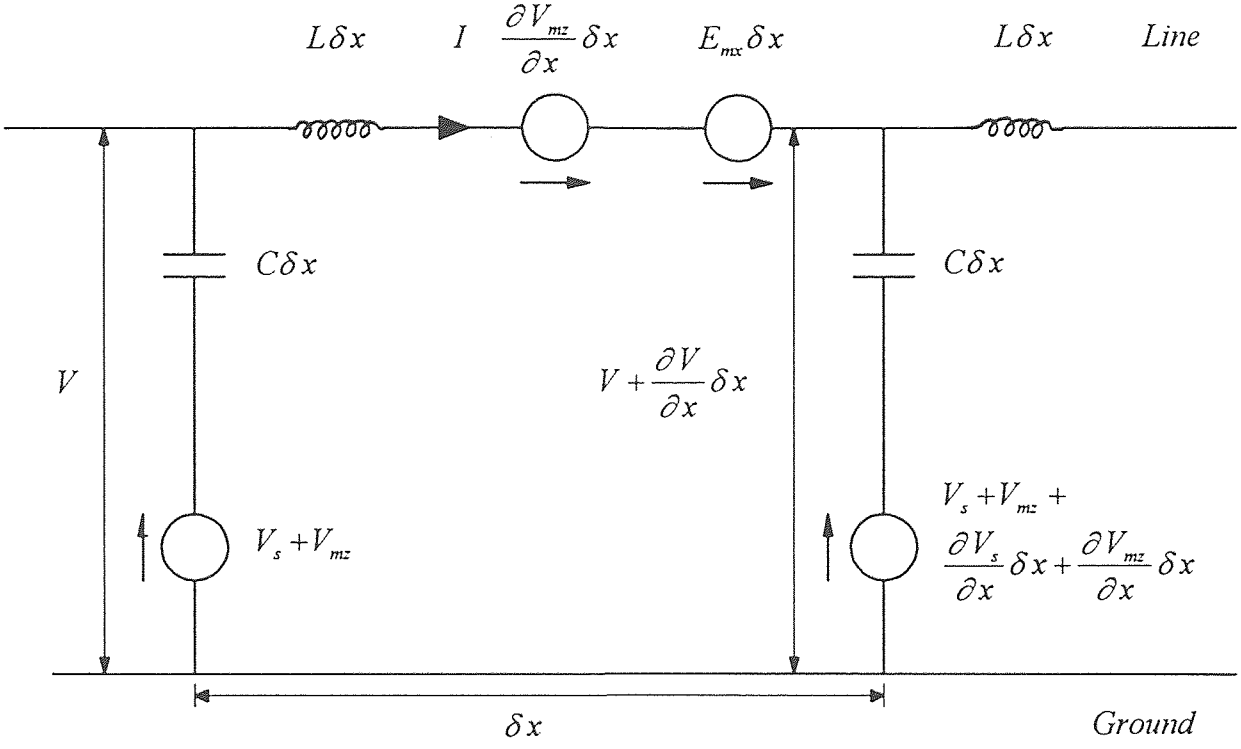

Figure 3.3 Equivalent circuit of power line under a lightning stroke.

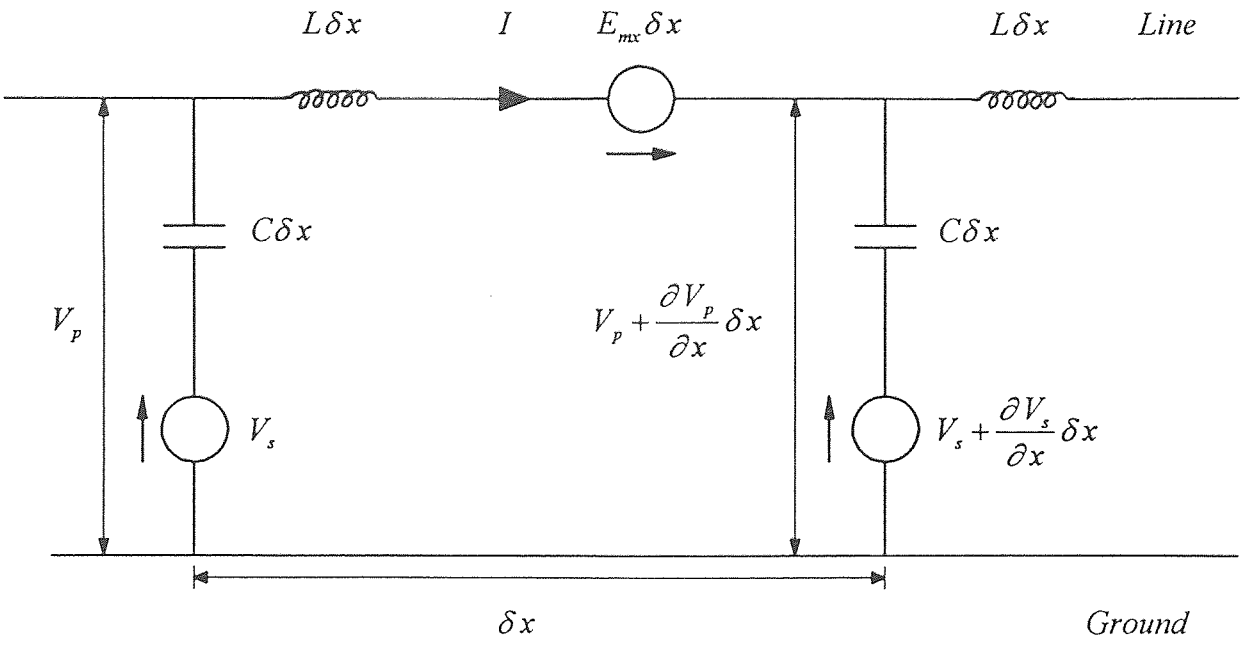

Figure 3.4 Equivalent circuit excluding V_{mz}

3.3 Numerical Method and Algorithm

The numerical method, finite-difference time-domain method, used in this study for analyzing the induced voltages on an overhead power line is based on the work described in two reported papers [13,14]. This involves converting the differential equations into difference equations, then solving the difference equations by calculating the voltages and currents for infinitesimal time units and line lengths.

By eliminating the term δx on both sides of equations (3.5) and (3.6), they can be rewritten as

$$\frac{\partial V_p}{\partial x} = -L\frac{\partial I}{\partial t} + E_{mx} \tag{3.8}$$

$$\frac{\partial I}{\partial x} = -C\frac{\partial}{\partial t}(V_p - V_s) \tag{3.9}$$

The distributed series inductance L and shunt capacitance C are determined by

$$L = \frac{\mu_0}{2\pi}\cosh^{-1}\left(h/d\right) \; ; \; C = \frac{2\pi\varepsilon_0}{\cosh^{-1}\left(h/d\right)} \tag{3.10}$$

where h is the height of the power line above the ground and d is the wire diameter of the power line.

The center-difference equation is expressed by

$$\frac{\partial f_0}{\partial x} = \frac{1}{2v}(f_{+v} - f_{-v}) + O(v^2) \tag{3.11}$$

where $O(v^2)$ represents high order terms and can be neglected.

By applying equation (3.11) on equations (3.8) and (3.9), their corresponding difference equations can be constructed respectively.

For (3.8),

$$\frac{1}{\Delta x}\left(V_p(n,t) - V_p(n-1,t)\right) = -L\frac{1}{\Delta t}\left(I(n-\frac{1}{2},t+\frac{1}{2}\Delta t) - I(n-\frac{1}{2},t-\frac{1}{2}\Delta t)\right) + E_{inc}(n-\frac{1}{2},t) \tag{3.12}$$

For (3.9),

$$\frac{1}{\Delta x}\left(I(n+\frac{1}{2},t+\frac{1}{2}\Delta t) - I(n-\frac{1}{2},t+\frac{1}{2}\Delta t)\right) = -C\frac{1}{\Delta t}\left(V_p(n,t+\Delta t) - V_s(n,t+\Delta t) - V_p(n,t) + V_s(n,t)\right) \tag{3.13}$$

where Δx is the space increment, and Δt is the time increment.

Both of equations (3.12) and (3.13) have recurrent characteristic and there is a reciprocal causation between them. Each time increment is called a iteration.

For each iteration, from equation (3.12), $I(n-\frac{1}{2},t+\frac{1}{2}\Delta t)$ can be obtained by

$$I(n-\frac{1}{2},t+\frac{1}{2}\Delta t)=I(n-\frac{1}{2},t-\frac{1}{2}\Delta t)-\frac{\Delta t}{L\Delta x}\left(V_p(n,t)-V_p(n-1,t)\right)+\frac{\Delta t}{L}E_{mx}(n-\frac{1}{2},t) \tag{3.14}$$

where $I(n-\frac{1}{2},t-\frac{1}{2}\Delta t)$, $V_p(n,t)$, and $V_p(n-1,t)$ have been calculated in the preceding iteration.

From equation (3.13), $V_p(n,t+\Delta t)$ can be given by

$$V_p(n,t+\Delta t)=V_p(n,t)+\left(V_s(n,t+\Delta t)-V_s(n,t)\right)-\frac{\Delta t}{C\Delta x}\left(I(n+\frac{1}{2},t+\frac{1}{2}\Delta t)-I(n-\frac{1}{2},t+\Delta t)\right) \tag{3.15}$$

where $I(n+\frac{1}{2},t+\frac{1}{2}\Delta t)$ and $I(n-\frac{1}{2},t+\frac{1}{2}\Delta t)$ are given by equation (3.14). $V_s(n,t+\Delta t)$ and $V_s(n,t)$ also can be computed through equations (2.31) and (2.32).

Consequently the propagated voltage V_p along the power line and the line current I are obtained step by step by applying equations (3.14) and (3.15) alternately.

Theory and equations for calculating the inducing scalar and vector potentials caused by a realistic return stroke are presented in Chapter 2. Numerical method for evaluating the propagated voltage along the power line also has been introduced in this chapter. Now a computer program will be developed to calculate the induced voltage which actually appears on an overhead power line. The flow chart in Fig.3.5 shows the major steps performed in this numerical method. The individual steps are described as follows.

(1) Read and store input data.

number of segments of leader channel and their lengths and orientations

line length, positions, height, and diameter of line conductor

lightning flash position

velocity of light in free space, v_0

progress velocity of return-stroke current, v

maximum value of return-stroke current, I_0

front time of return stroke current, t_f

(2) Treat input data.

calculate space and time increment, $\Delta x, \Delta t$

calculate min. and max. values of computing time, $t_{\min}, t_{\max}$

(3) Calculate system constants.

distributed series inductance and shunt capacitance of power line, L, C

(4) Give initial values.

set initial values of line current I, propagated voltage V_p and inducing scalar potential V_s to zero

(5) Calculate inducing scalar potential V_s and potential V_{mz} by applying equations (2.31)~(2.36).

(6) Calculate electric field intensity E_{mx} by applying equation (3.4).

(7) Calculate propagated voltage V_p along power line and line current I by using numerical method introduced in this section.

(8) Calculate induced voltage V by adding V_p and V_{mz} directly.

(9) Print out induced voltage V vs. time t for designated point.

(10) Print out induced voltage V vs. space x for fixed time.

(11) Once all the calculations have been completed for a given time t, increase the time by Δt, and repeat steps (5) through (10) until the required computing time $t_{\max}$.

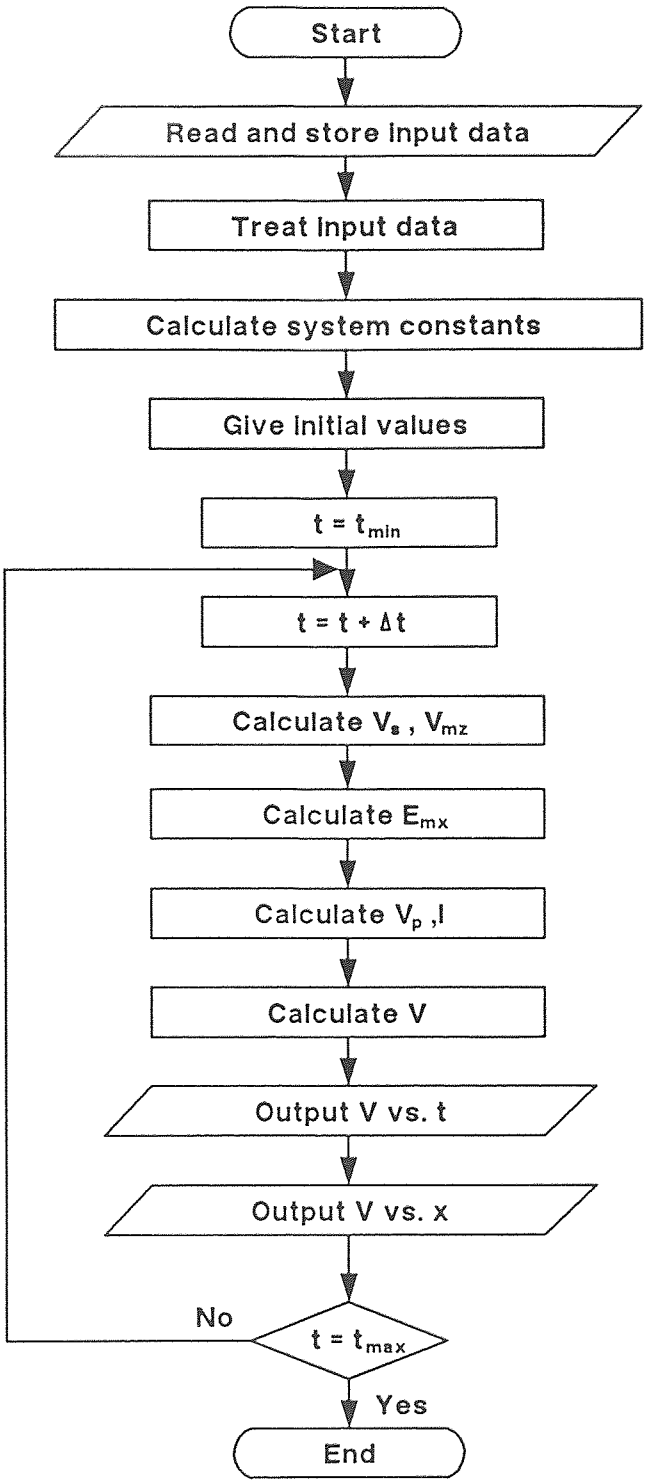

Figure 3.5 Flow chart of numerical method for evaluating the induced voltage caused by a lightning stroke.

3.4 Validation of the Numerical Method

To validate the numerical method and prove the feasibility of the developed computer program, the electromotive force in Fig.3.2 will be excluded temporarily and just consider a rather simple proposition—what happens when a uniform, isolated two-wire line is connected to a voltage source. The partial differential equations can be simplified as

$$\frac{\partial V}{\partial x} = -L\frac{\partial I}{\partial t} \tag{3.16}$$

$$\frac{\partial I}{\partial x} = -C\frac{\partial V}{\partial t} \tag{3.17}$$

Now I can be eliminated from the pair of equations by simultaneously differentiating equation (3.16) with respect to x and equation (3.17) with respect to t :

$$\frac{\partial^2 V}{\partial x^2} = -L\frac{\partial^2 I}{\partial x \partial t} \quad ; \quad \frac{\partial^2 I}{\partial x \partial t} = -C\frac{\partial^2 V}{\partial t^2}$$

Eliminating $\frac{\partial^2 I}{\partial x \partial t}$ and rearranging the terms,

$$\frac{1}{LC}\frac{\partial^2 V}{\partial x^2} = \frac{\partial^2 V}{\partial t^2} \tag{3.18}$$

Solving Equations (3.16) and (3.17) for I instead of V leads to an equation of identical form for the current :

$$\frac{1}{LC}\frac{\partial^2 I}{\partial x^2} = \frac{\partial^2 I}{\partial t^2} \tag{3.19}$$

Equations (3.18) and (3.19) are the so-called traveling-wave equations of a lossless transmission line. Consider equation (3.18), it was satisfied by the general solution

$$V = f\left[x \mp \frac{t}{\sqrt{LC}}\right] \tag{3.20}$$

where $\frac{1}{\sqrt{LC}}$ is the light velocity v_0, so that equation (3.20) can be written

$$V(x,t) = f_1(x - v_0 t) + f_2(x + v_0 t) \tag{3.21}$$

The current solution can be obtained from equation (3.17)

$$\frac{\partial I}{\partial x} = -C\frac{\partial V}{\partial t} = Cv_0\left[f_1'(x - v_0 t) - f_2'(x + v_0 t)\right] \tag{3.22}$$

Integrating both sides of equation (3.22) with respect to x,

$$I(x,t) = Cv_0\left[f_1(x - v_0 t) - f_2(x + v_0 t)\right] = \frac{f_1(x - v_0 t)}{Z_c} - \frac{f_2(x + v_0 t)}{Z_c} \tag{3.23}$$

Comparing equations (3.21) and (3.23), there exists a proportionality between voltage and current, and the proportionality factor is called the characteristic impedance Z_c of the line. Solutions expressed as the function $f_1(x - v_0 t)$ represent waves traveling in the positive direction of x. Similarly, solutions expressed as the function $f_2(x + v_0 t)$ can be interpreted as waves traveling in the negative direction of x. It is also observed that voltage and current waves traveling in the positive direction of x have the same sign, whereas those traveling the negative direction have opposite signs.

If a forward traveling voltage wave is expressed as

$$V^+(x,t) = f_1(x - v_0 t) \tag{3.24}$$

a wave of current will result from the moving charges and can be expressed as

$$I^+(x,t) = \frac{1}{Z_c} f_1(x - v_0 t) \tag{3.25}$$

Similarly for a backward traveling voltage wave where

$$V^-(x,t) = f_2(x + v_0 t) \tag{3.26}$$

the corresponding current is

$$I^{-}(x,t) = -\frac{1}{Z_c} f_2(x + v_0 t) \tag{3.27}$$

Recalling that v_0 is equal to $1/\sqrt{LC}$, so

$$Z_c = \frac{1}{C v_0} = \sqrt{\frac{L}{C}} \tag{3.28}$$

Next, a simulation test on the developed computer program will be made. Assuming,

$$D = N\,\Delta x \tag{3.29}$$

and at $t = 0^{+}$ imposing a voltage on the line,

$$V(x,0^{+}) = \exp\left(-\frac{x^2}{D^2}\right) \tag{3.30}$$

where V is a Gaussian distribution function.

Then the voltage and current waves are calculated through the computer program. The results are shown in Fig.3.6. From Fig.3.6.(A), the forward traveling waves can be expressed as

$$V^{+}(x,t) = \exp\left[-\frac{(x - v_0 t)^2}{D^2}\right] \quad kV \tag{3.31}$$

$$I^{+}(x,t) = \frac{1000}{Z_c} \exp\left[-\frac{(x - v_0 t)^2}{D^2}\right] \quad A \tag{3.32}$$

From Fig.3.6.(B), the backward traveling waves can be expressed as

$$V^{-}(x,t) = \exp\left[-\frac{(x + v_0 t)^2}{D^2}\right] \quad kV \tag{3.33}$$

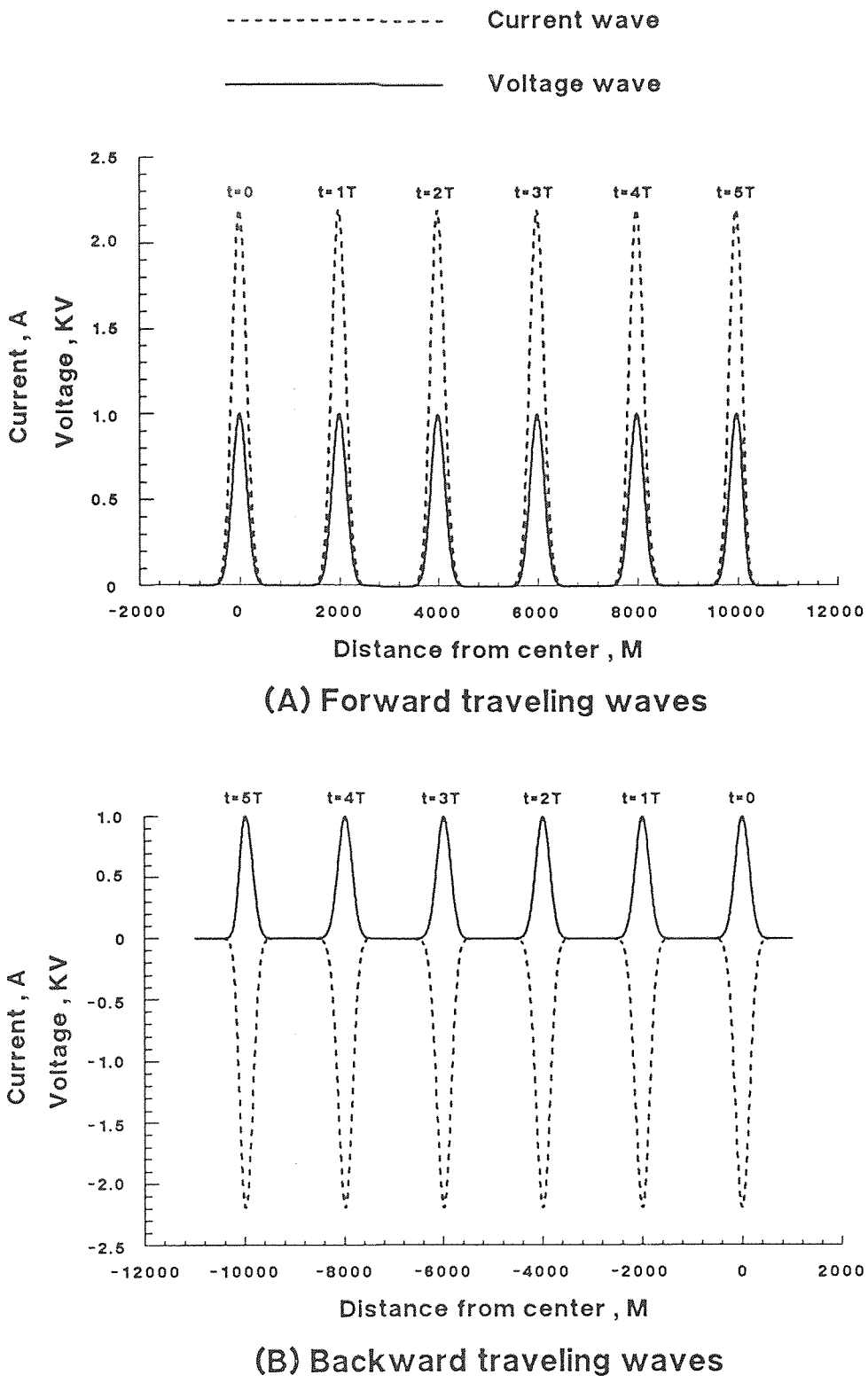

Figure 3.6 Voltage and current waves traveling along a power line which have the waveform of function $\exp\left(-x^2/D^2\right)$.

$$I^{-}(x,t) = -\frac{1000}{Z_c}\exp\left[-\frac{(x+v_0 t)^2}{D^2}\right] \quad A \tag{3.34}$$

The calculated results completely coincide with the deduced conclusion that on the lossless power line, the voltage and current waves have the same shape, being related by the characteristic impedance of the line, and travel undistorted. A current wave in the positive direction of x has the same sign as the voltage wave with which it is associated. Current wave traveling in the negative direction of x has reversal sign with respect to its voltage wave.

To ensure the accuracy of the calculated results, number N in equation (3.29) must be taken more than 20. Thus the values of V and I cannot change significantly over one space increment Δx. To ensure the stability of the time-stepping algorithm of the developed computer program, Δt is chosen to satisfy

$$\Delta t \leq \Delta x / 2v_0 \tag{3.35}$$

CHAPTER 4

APPLICATIONS

4.1 Introduction

To provide optimal protection to an overhead power line against lightning strokes, it is necessary to predict the severity of the transient overvoltage generated by such strokes. Although the complex interaction among the various line and lightning parameters, predicting the worst possible severity of indirect lightning strokes on an overhead power line is difficult, the effects of the various line and lightning parameters on the severity of induced voltage are still inspected systematically. In Section 4.2, the effects of the various parameters on the induced voltage caused by a vertical lightning stroke are discussed. In Section 4.3, the influences of the inclined angle and direction of a arbitrary return stroke will be investigated. Finally, in Section 4.4, the effects of the inducing components V_s , V_{mz} and E_{mx} on the induced voltage V are examined.

4.2 Parametric Effects on the Induced Voltage Caused by a Vertical Lightning Stroke

The effects of the following parameters on the induced voltage caused by a vertical return stroke are discussed:

(1) Lightning stroke parameters.

(a)Progress velocity of return stroke.

(b)Front time of return-stroke current.

(c)Height of cloud charge center.

(2) Power line parameters.

(a)Least distance of the power line from the lightning struck point.

(b)Height of the power line above ground.

4.2.1 Progress Velocity of Return Stroke

Uman [1] proposed that the progress velocity of the return stroke varies between 2.0×10^7 m/s to 1.4×10^8 m/s. Berger [15] suggested that it alters between 2.0×10^7 m/s to 1.1×10^8 m/s. Although no definitive knowledge exits about the progress velocity of the return stroke, it is still important to assess its sensitivity to the severity of the induced voltage. In this study, three cases are discussed by assuming the return-stroke velocity to be 10, 30 and 50 percent that of light. Recalling equation (2.3), because the amount of charge distributed along the leader channel for the same lightning is unchanged, it is necessary to pay attention to that the return-stroke current need to be changed by following the varying-ratio of the return-stroke velocity when the effect of the return-stroke velocity is discussed. Otherwise, inappropriate results will be derived as shown in Fig.4.3 (placed in Appendix) where the induced voltage is almost only one-third of that in Figs.4.1.(B) and 4.2.(B) (placed in Appendix).

In Figs.4.1 and 4.2 (placed in Appendix), although the induced voltage has the characteristic that the higher the return stroke velocity the lower is the induced voltage, the diversity of the wave form is not as apparent as anticipated. The diversity is caused by two components:

(1) Inducing scalar potential V_s

For a return stroke with higher progress velocity, its progressing point is farther away from the power line at a given time t and the retarded-height difference between original and image charges becomes larger. Therefore, when the return-stroke velocity increases, the inducing scalar potential will decrease in the period of negative polarity but increase in the period of positive polarity. Because the propagated voltage is derived from the inducing scalar potential, V_p has the same property as V_s. This is shown in Fig.4.4 (placed in Appendix). The pulsation shown

in the circle of Fig.4.4 is caused by the drop of the return-stroke current from its peak value.

(2) Induced voltage V_{mz}

From equation (3.33), (3.34) and (3.36), the higher the return stroke velocity the higher is the induced voltage V_{mz} which is also shown in Fig.4.4. Moreover, the induced voltage V_{mz} is of positive polarity.

The final induced voltage on the line is obtained by adding V_p and V_{mz}. Hence the curves $(x = 0km)$ shown in Fig.4.1 are composed of two components shown in Fig.4.4. From the above discussions, a useful conclusion is that the higher the return stroke velocity the more obvious is the bipolar phenomenon of the induced voltage wave. The progress velocity of a return stroke can be predicted by analyzing the induced voltage waveshape.

The induced voltages at various points along the overhead power line at various times are shown in Fig.4.2. It is noticed that the induced voltage at the point of least distance from the return stroke $(x = 0m)$ is the minimum. The voltage increases with increasing x up to a certain point along the power line where the sum of all contributions of propagated voltages from preceding points reaches the maximum value, then decreases slightly. If the power line is long enough, the induced voltage will be saturated a certain value. This is expectable since the line is lossless and the directly radiated fields of the lightning stroke become negligible. This conclusion is different from those presented by Liew, et al.[8] and Sakakibara [11]. According to Liew's study, it was found that the magnitude of the induced voltage increases continuously with increase in x along the power line even at $x = 75\ km$. On the contrary, Sakakibara stated that the induced voltage at the line center (nearest point to the lightning struck point) is the maximum, then decreases with increase in distance from the line center. From the physics point of view, the decay of the induced voltage cannot occur on a lossless power line over a perfect conductive earth.

Although the difference in magnitude of the induced voltage at the line center ($x = 0km$) between the slowest and the fastest return stroke velocity is 60 kV, the difference at the point $x = 5km$ diminishes to 20 kV. In other words, the higher the return stroke velocity the larger is the variation in the induced voltage between the line center and the point $x = 5km$. Recalling Fig.3.4, the flow of line current is due to the differences in inducing scalar potential at different points along the power line. For a lightning return stroke with higher velocity, in an infinitesimal section of the power line δx the value of $\partial V_s/\partial x$ will be larger than that with lower velocity. This produces higher value of $L\partial I/\partial t$ and $\partial V_p/\partial x$. Because the induced voltage is composed of V_p and V_{mz}, higher $\partial V_p/\partial x$ means higher $\partial V/\partial x$, namely, higher variation rate with space in the induced voltage. This is illustrated in Fig. 4.2.

The return-stroke velocity affects not only the magnitude of the wavefront (negative polarity) but also the peak value and decay rate of the wavetail (positive polarity). It is observable that the higher the return-stroke velocity the larger is the peak value of the wavetail and the faster is the decay rate. This property is illustrated in Fig.4.1 and 4.2.

4.2.2 Front Time of Return-Stroke Current

Fig. 4.5 and 4.6 (placed in Appendix) show the effect of the current front time t_f on the induced voltage. A shorter current front time induced higher voltages on the overhead line. Shorter front time indicates that the return-stroke current rises more quickly to its peak value and meanwhile the progressing point of return stroke is nearer to the power line. Consequently the inducing scalar potential is higher than that with longer front time. This is shown in Fig.4.7 (placed in Appendix). Moreover, from Fig.4.7, an important characteristic of the inducing scalar potential is that its peak value didn't happen at the time when the return-stroke current reached the maximum. This is reasonable because the

magnitude of the inducing scalar potential is dependent on the magnitude of the return stroke current and the distance of residual charges from the power line. These two parameters are conflicting in the period of rise time of the return-stroke current. Hence the optimal combination always happens before the return-stroke current reaches its peak value.

The effect of the current front time on the induced voltage can be described by a statement that "The induced voltage is directly proportion to the rise rate of the return-stroke current front time. In other words, a fast-rising return-stroke current will induce a fast-rising and fast-falling voltage on the overhead power line.

4.2.3 Height of Cloud Charge Center

Fig.4.8 and 4.9 (placed in Appendix) show the effect of the height of cloud charge center h_c on the induced voltage on an overhead power line. The induced voltage increases with increase in h_c but the higher the height of cloud charge center the less is the effect. Generally, the effect of the height of cloud charge center on the induced voltage is not significant. However, the waveshape of the induced voltage changes considerably for low h_c. The bipolar characteristic of the induced voltage is evident for lower h_c. The compositions of inducing scalar potential and the effect of the retardation height on the bipolar phenomenon have been introduced in Section 2.5. In the earlier period of the return stroke, the effect of the original charges outstrips that of the image charges, and lower h_c means less charges distributed along the leader channel which cause lower induced voltage as shown in Fig.4.8 (wavefront of negative polarity). In the later period of the return stroke, because the image charges are more than the original charges and lower h_c means the charges in this stage nearer to the power line, the induced voltage (wavetail of positive polarity) will be higher. Hence, the bipolar characteristic of the induced voltage is more apparent for lower h_c.

4.2.4 Least Distance of the Power Line from the Lightning Struck Point

Undoubtedly, the longer the least distance of the power line from the lightning struck point y_0 the lower is the induced voltage. The induced voltage at a point along the line away from the power line center is decided by two components. One is the directly-inducing scalar potential V_s caused by the electrostatic fields of the lightning return stroke. This induction process is delayed by the time required by the electrostatic fields to travel to the particular point from the lightning return stroke. The other is the propagated voltage V_p which is composed of voltages which have traveled along the power line from other points where the induction effects of the lightning return stroke have already taken place. For $y_0 = 100m$, because the difference in the retardation time between two points on the power line is very close to the traveling time of the propagated voltage from one point to the other, the effect of superposition is strong. Thus, the variation rate with space in the induced voltage is noticeable especially between $x = 0km$ and $x = 2.5km$. This is observable from Fig.4.10.(A) and 4.11.(A) (placed in Appendix). But for $y_0 = 5km$, the difference in the retardation time is less than the traveling time. For example, the difference in the retardation time between $x = 0km$ and $x = 2.5km$ is only $2\mu s$, but the traveling time of the propagated voltage from $x = 0km$ to $x = 2.5km$ requires $8.33\mu s$. Hence, the effect of superposition is insignificant and the variation rate with space almost approaches to zero. This is demonstrated by the unchanging magnitude of the induced voltage shown in Fig.4.10.(c) and 4.11.(c) (placed in Appendix).

The bipolar characteristic of the induced voltage is obvious for longer distance y_0. For larger y_0, the influence of the difference in the charge quantity overcomes that of the distance of the charges from the power line. The bipolar characteristic of the inducing scalar potential will be more apparent which causes the evident bipolar phenomenon of V_p as shown in Fig.4.12 (placed in Appendix). Meanwhile, the induced voltage V_{mz} occupies

an important proportion in the total induced voltage. This also increases the tendency of the bipolar characteristic.

4.2.5 Height of the Power Line above Ground

Figs.4.13 and 4.14 (placed in Appendix) show the effect of the height of the power line above ground on the induced voltage. Obviously, the induced voltage at any point along the power line is directly proportion to the height h of the line. The waveshapes of the induced voltage are identical under various h except their magnitudes.

4.3 Effects of Inclined Angle and Direction of a Arbitrary Lightning Stroke on the Induced Voltage

Thus far, the parametric effects of a vertical lightning stroke on the induced voltage have been dealt with. Now, the discussion scope will be developed over a lightning stroke in three-space. Effects of the inclined angle and direction of a arbitrary lightning stroke on the induced voltage are inspected. For convenience, some terminology about space concept need to be defined beforehand:

- Progression vector: One way of efficiently describing the progressing direction of the return stroke is to define a vector as an ordered triple $< x, y, z >$ of real numbers. It means that the return stroke progressed along the direction of vector $x\,\hat{i} + y\,\hat{j} + z\,\hat{k}$. It should be noticed that the vector is not necessary to be unit vector, because the helpful information is its direction not its magnitude.
- Inclined angle: The included angle between progression vector $< x, y, z >$ and unit vector $\hat{j}$ (in the $+y$ direction) is defined as inclined angle, $\theta_i = \tan^{-1}\left(\sqrt{x^2 + y^2}\,/z\right)$.

• Oblique angle: The quadrant angle of the projecting vector of progression vector on the xy-plane is defined as oblique angle, $\varphi = \tan^{-1}(y/x)$. The projecting vector is denoted as $< x, y, 0 >$.

• Length of lightning leader channel: In the following investigations, symbol L_c , length of the lightning leader channel, will be adopted to replace h_c, height of the thundercloud above the ground.

Comparisons will be made under various conditions which can be put into the following categories:

(1) Comparison between vertical and inclined return strokes.

(2) Effect of return-stroke oblique angle.

(3) Effect of return-stroke inclined angle.

(4) Recompare the effect of inclined angle by using multi-segment (zigzag) return stroke models.

(5) Effect of progress velocity of inclined return stroke.

4.3.1 Comparison between Vertical and Inclined Return Stroke

At first, the induced voltage caused by inclined return strokes will be compared with that caused by a vertical one. There are three return strokes, as shown in Fig.4.15, one vertical and two inclined lying on yz-plane. Undoubtedly, the nearer to the return stroke the higher is the induced voltage on the power line. As shown in Fig.4.16, the induced voltage cause by the return stroke inclined close to the power line is the highest and the difference will increase when the inclined angle increases. Because all of three return strokes are perpendicular to the power line, their induced voltage waveshapes are symmetrical and similar to each other.

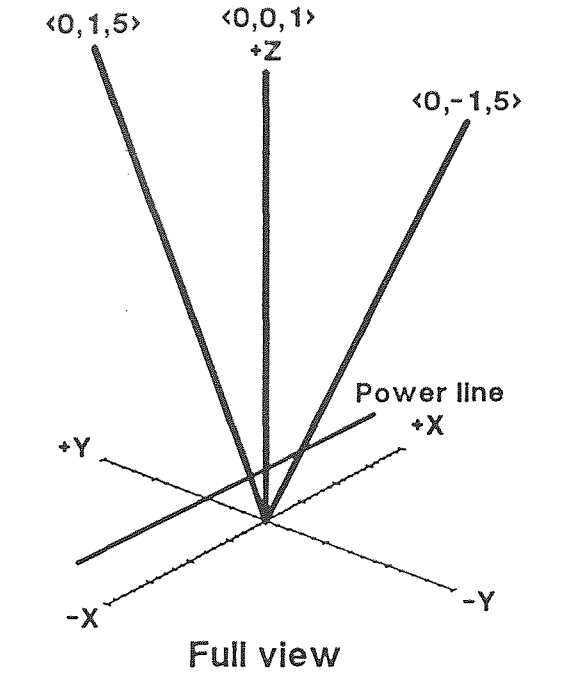

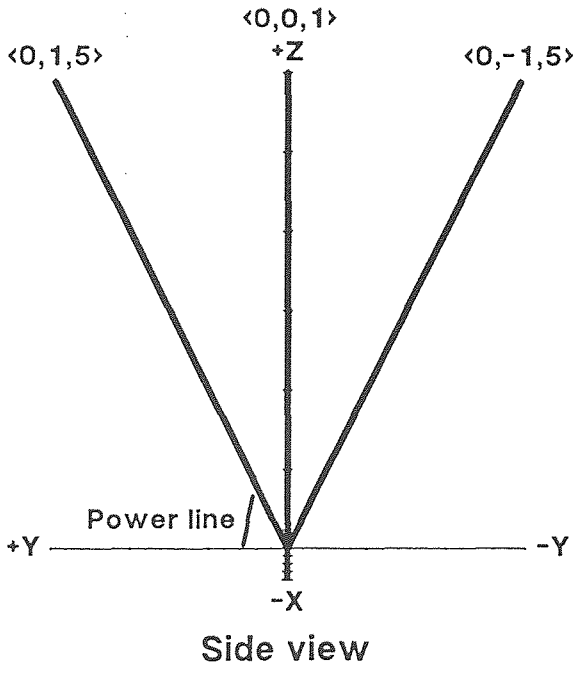

Figure 4.15 Coordinate system of a power line and three return strokes lying on the *yz*-plane.

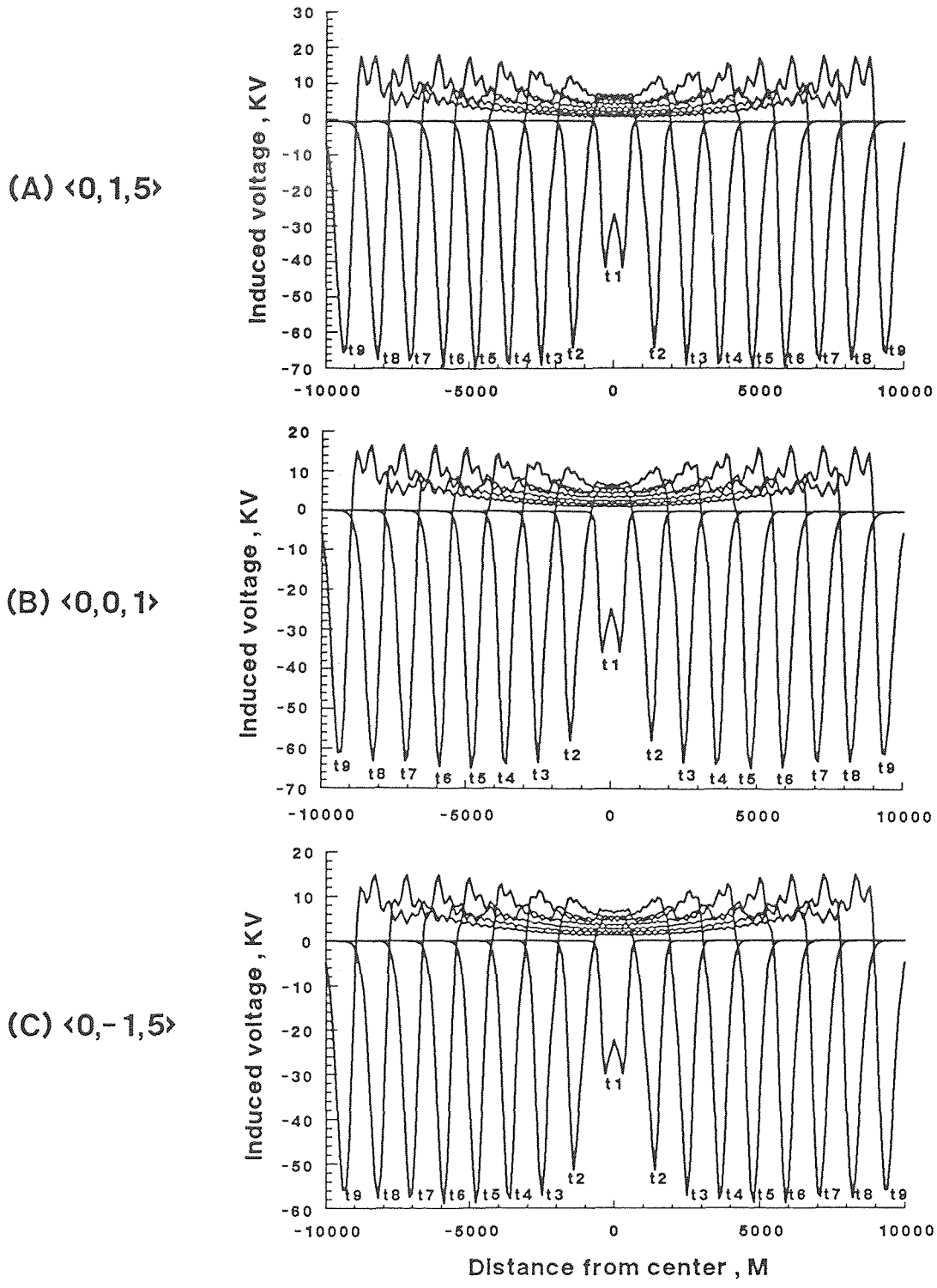

Figure 4.16 Comparison of induced voltages caused by vertical and inclined return strokes lying on the yz-plane.

$\beta = 0.3$, $I_0 = 10kA$, $t_f = 5\mu s$, $y_0 = 100m$, $h = 10m$, $L_c = 3km$

4.3.2 Effect of Return-Stroke Oblique Angle

In above subsection, inclined return strokes have been introduced but the imperfection is that the influence of the inclined angle on the induced voltage between both directions of the line can't be distinguished. In this subsection, the effect of return-stroke oblique angle on the induced voltage will be examined. To simplify the comparison, there are three inclined return strokes as shown in Fig.4.17, whose inclined angles are assumed to be the same ($\theta_i = \tan^{-1} 0.2 \cong 11.3°$)but oblique angles are –45°, 0° and 45° respectively. Fig.4.18 gives the calculation results of the induced voltages in three cases, and it shows an important information that the peak value of the voltage induced by the inclined return stroke will increases in the inclined direction but decreases in the other direction when the return-stroke oblique angle is not 90° or $-90°$. This characteristic will be clearer by comparing the figures (A), (B) and (C) between Figs.4.16 and 4.18 respectively. Moreover, the difference in the peak value of the induced voltage between both directions of the power line will increase when the oblique angle diminishes to zero. This conclusion is different from that represented by Sakakibara [11], which stated that the peak value of the voltage induced by the inclined return stroke is higher than that produced by the vertical stroke at any point along the line.

The crux of the problem can be examined by checking the induced voltage V_{mz} and propagated voltage V_p. Fig.4.19 is the case of oblique angle $\varphi = 0°$. As mentioned before, the induced voltages V_{mz} on the power line are standing waves and the propagated voltages V_p are traveling waves. From Fig.4.19, the effect of the induced component V_{mz} only happens at power line center and in the initial stage of the stroke process, besides, it is very small. Therefore, the difference in the peak value of the induced voltage is primarily caused by the inducing scalar potential V_s. Of course, as discussed in Chapter 3, the x component of the electric field intensity, E_{mx} is also a parameter affecting the induced voltage. Its effect will be discussed in Section 4.4.

The inducing scalar potentials at various points on both direction of the power line have been calculated and shown in Fig.4.20. The induced voltage at the power line center is also obtained simultaneously as reference. There are two factors affecting the peak values of the induced voltage at various points; one is the magnitude of the inducing scalar potential at the designated point, the other is the occurrence timing of the maximum inducing scalar potential. Especially, in some individual conditions, the significance of the latter is more than that of the former. From Fig.4.20, some useful informations can be observed. The initial effect of the lightning stroke reaches both sides of the power line simultaneously, because the lightning return stroke starts from the origin ($x = 0$). The difference in the induced voltages between both sides of the power line is exactly caused by the different inducing scalar potentials.

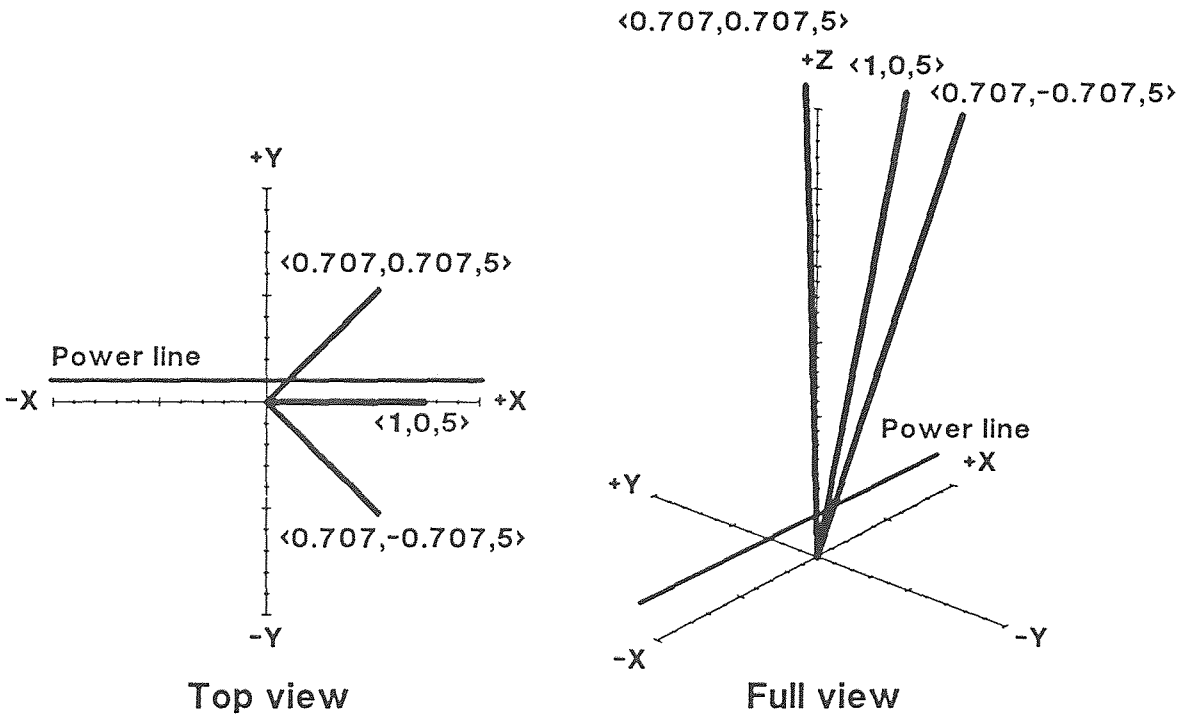

Figure 4.17 Coordinate system of a power line and three return strokes with the same inclined angle, θ_i. Effect of their oblique angles, φ.

(A)
‹0.707,0.707,5›

(B) ‹1,0,5›

(C)
‹0.707,-0.707,5›

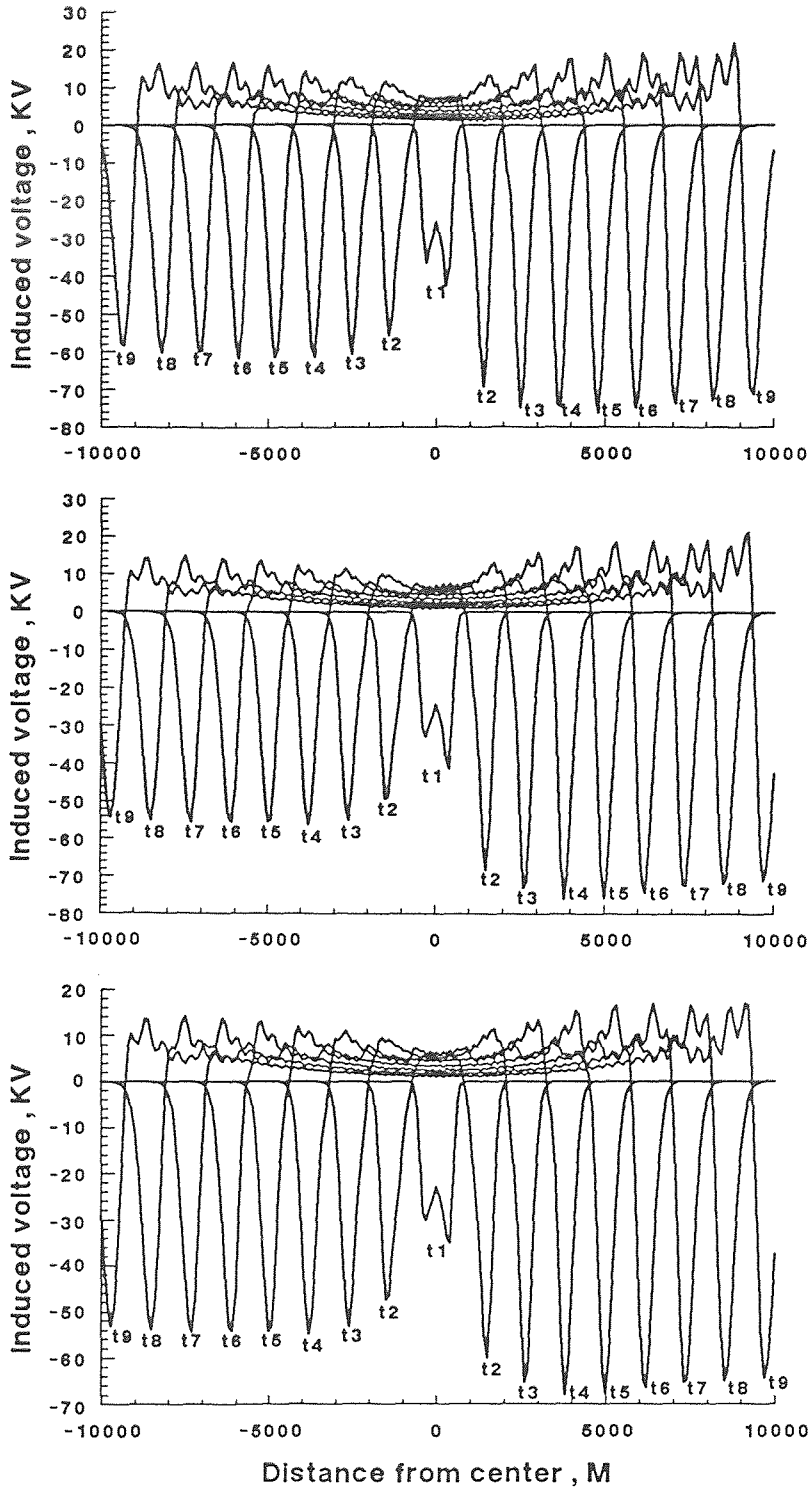

Figure 4.18 Comparison of induced voltages caused by return strokes with the same inclined angle. Effect of their oblique angles.

$\beta = 0.3$, $I_0 = 10kA$, $t_f = 5\mu s$, $y_0 = 100m$, $h = 10m$, $L_c = 3km$

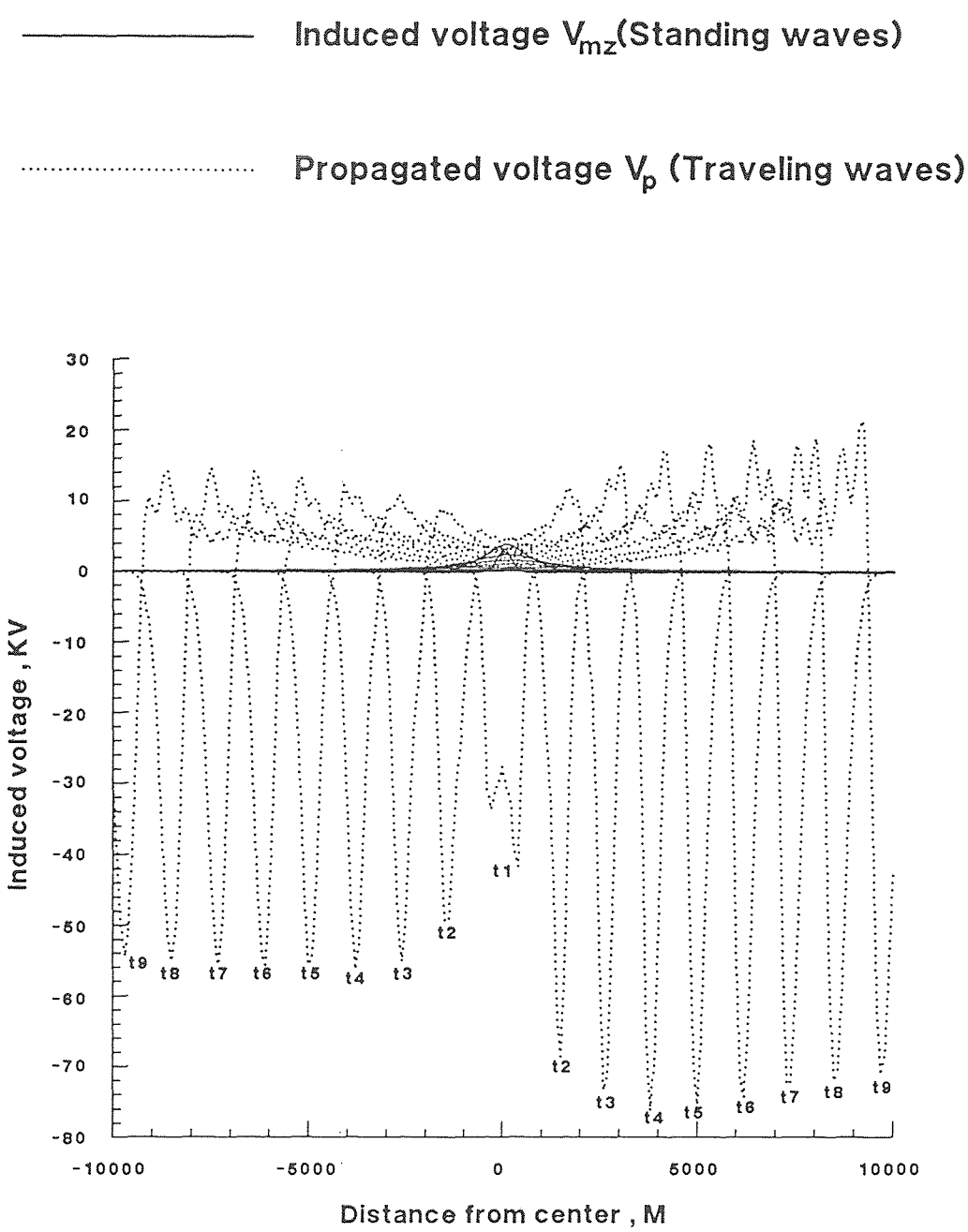

Figure 4.19 Induced voltage V_{mz} and propagated voltage V_p as a function of space at increasing time on an overhead power line caused by an inclined return stroke. $\theta_i \cong 11.3^\circ$, $\varphi = 0^\circ$

$\beta = 0.3$, $I_0 = 10kA$, $t_f = 5\mu s$, $y_0 = 100m$, $h = 10m$, $L_c = 3km$

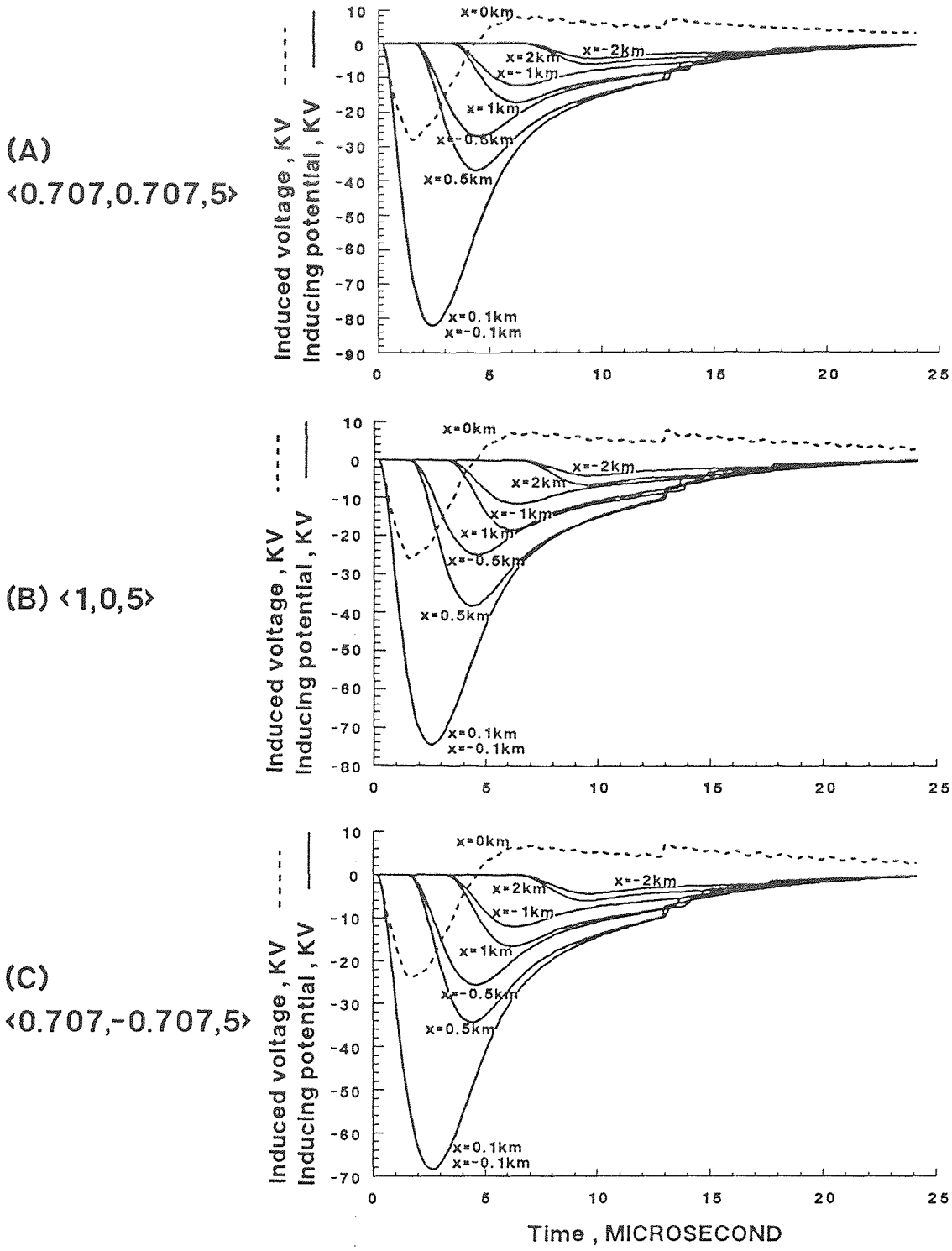

Figure 4.20 Inducing scalar potential as a function of time at various points on an overhead power line caused by inclined return strokes and the induced voltage at the line center.

$\beta = 0.3$, $I_0 = 10kA$, $t_f = 5\mu s$, $y_0 = 100m$, $h = 10m$, $L_c = 3km$

4.3.3 Effect of Return-Stroke Inclined Angle

From above investigations, it is obvious that the worst severity of indirect lightning strokes on an overhead power line occurred in the inclined direction when the return-stroke oblique angle is zero, i.e., the inclined plane is parallel to the power line. In this subsection, the investigations will concentrate on the effect of the return-stroke inclined angle on the induced voltages caused by return strokes with zero oblique angle. As shown in Fig.4.21, there are three return strokes lying on the xz-plane whose inclined angles are 11.3°, 26.6° and 45° respectively. The induced voltages under various return-stroke inclined angles are calculated and shown in Fig.4.22. The peak value of the induced voltage will increase in the inclined direction but decrease in the other direction with increase in the inclined angle. In other words, the larger the inclined angle the worse is the severity of the return stroke on the overhead power line.

The inducing scalar potentials at various points on both directions of the power line and the induced voltage at the power line center are shown in Fig.4.23. The inducing scalar potentials at points $x = 0.1km$ and $x = -0.1km$ are identical no matter what inclined angle, because the difference in the distance of the point from the return stroke is so small that the diversity cannot be distinguished. At $\theta_i = 11.3°$ and $\theta_i = 26.6°$, the magnitude of the inducing scalar potential decreases regularly with increase in the distance of the point from the power line center. But for $\theta_i = 45°$, the inducing scalar potential at point $x = 0.5km$ is higher than that at point $x = 0.1km$. The cause is that the residual charges distributed along the leader channel is nearer to the point $x = 0.5km$ when the maximum inducing scalar potential occurred (generally after the starting time about $2.8\mu s$). The inducing scalar potential at a designated point increases in the inclined direction but decreases in the other direction with increase in the inclined angle except the points $x = 0.1km$ and $x = -0.1km$. Besides, as mentioned in Section 4.2.4, if the difference in the retardation time between two points on the power line is very close to the traveling time of the propagated voltage from one point to the other, the effect of superposition will be

significant. The larger the return-stroke inclined angle the stronger is the effect of superposition for the points in the inclined direction, but the weaker for the points in the other direction. Now, both of two factors affecting the peak value of the induced voltage are favorable for the points in the inclined direction but adverse for the points in the other direction when the return-stroke inclined angle is larger. This is the reason which explains why the difference in the peak value of the induced voltage between both directions of the power line is so large when the return-stroke inclined angle reaches 45°.

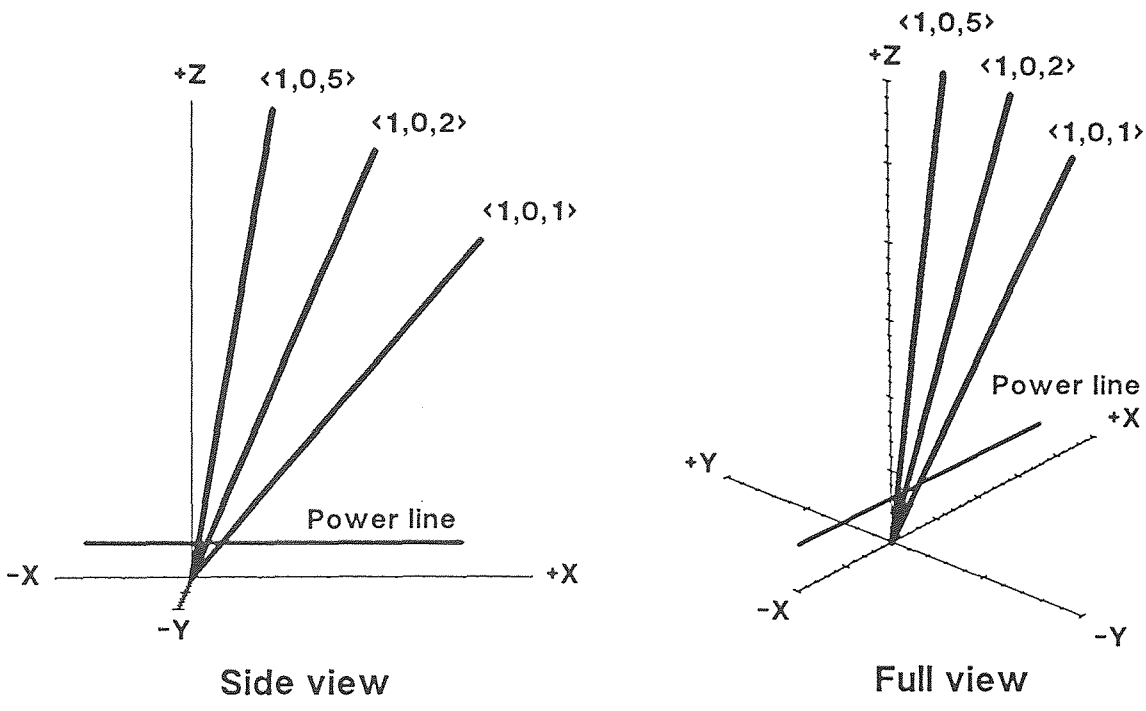

Figure 4.21 Coordinate system of a power line and three return strokes lying on the xz-plane. Effect of their inclined angles, θ_i.

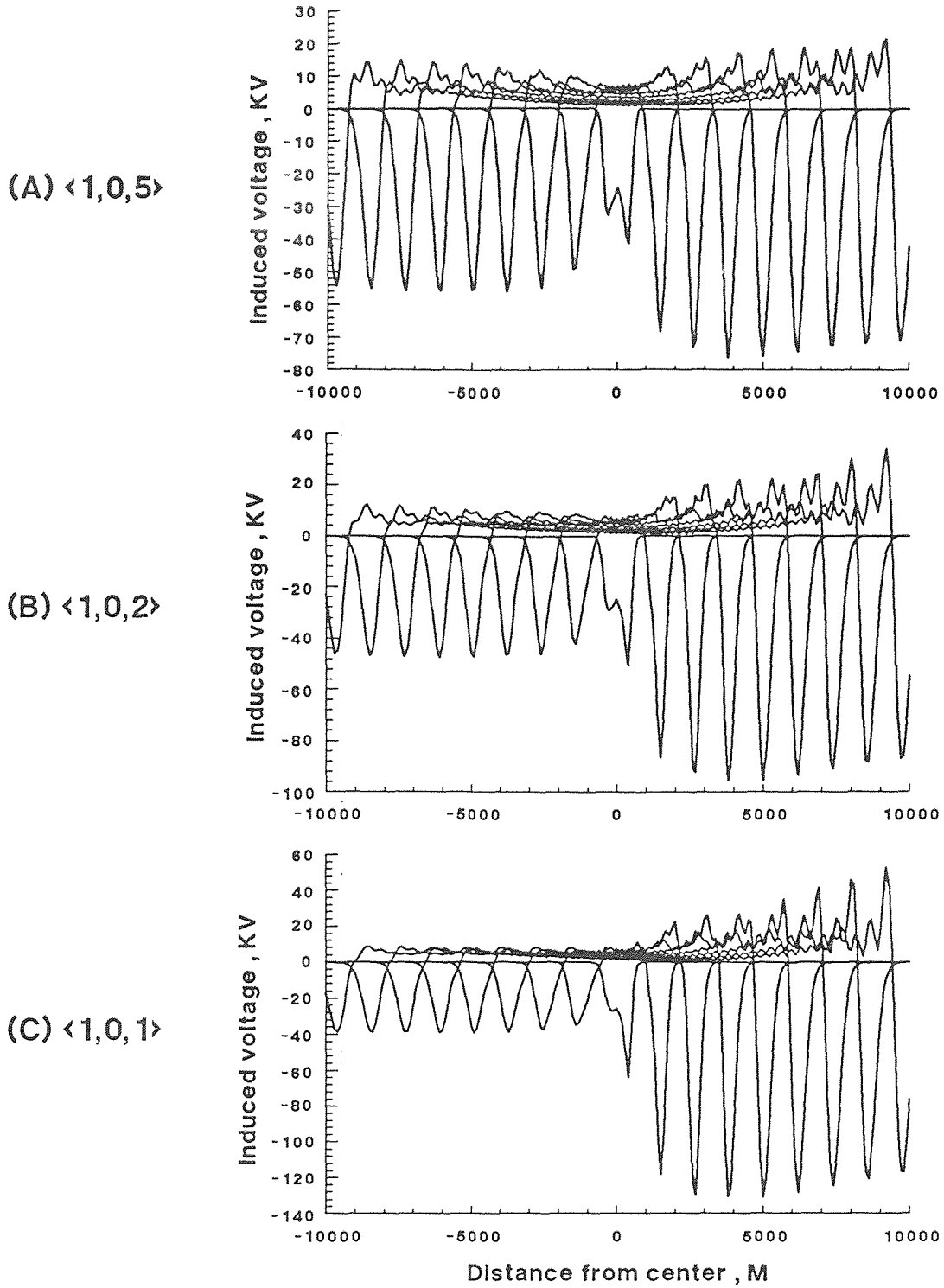

Figure 4.22 Comparison of induced voltages caused by inclined return strokes whose inclined plane is parallel to the power line. Effect of their inclined angles.

$\beta = 0.3$, $I_0 = 10kA$, $t_f = 5\mu s$, $y_0 = 100m$, $h = 10m$, $L_c = 3km$

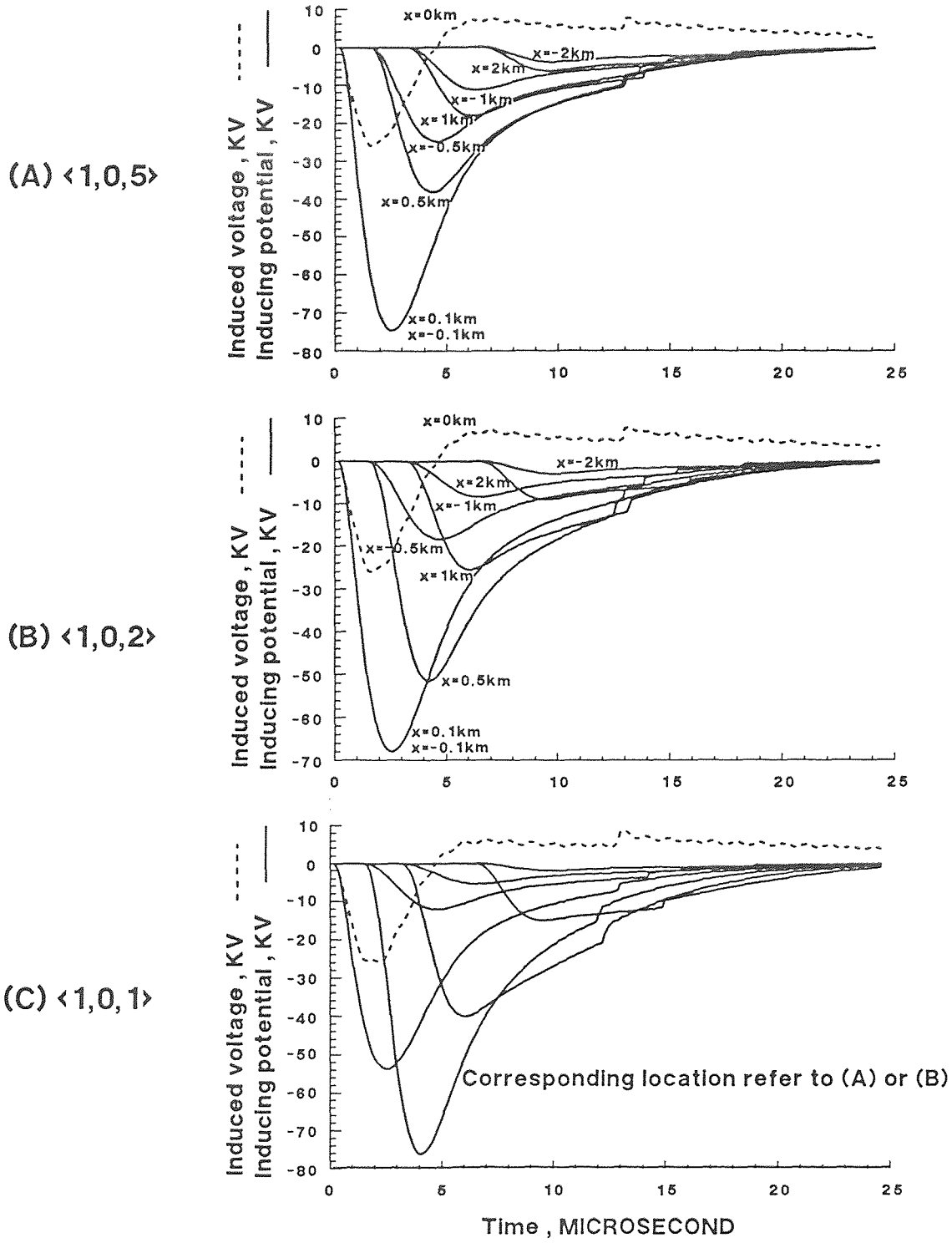

Figure 4.23 Inducing scalar potential as a function of time at various points on an overhead power line caused by inclined return strokes and the induced voltage at the line center.

$\beta = 0.3$, $I_0 = 10kA$, $t_f = 5\mu s$, $y_0 = 100m$, $h = 10m$, $L_c = 3km$

4.3.4 Recompare the Effect of Inclined Angle by Using Zigzag Return Stroke Models

Maybe someone will ask that the inclined return strokes used in the Subsection 4.3.3 are inclined in unique direction, so the comparison is not objective enough. In this subsection, the effect of the return-stroke inclined angle on the induced voltage on an overhead power line will be recompared by replacing the straight return strokes with multi-segment (zigzag) ones. There are three return strokes composed of 2, 5 and 10 segments respectively as shown in Fig.4.24. The inclined angles are the same as the straight ones. The calculation results are given in Fig.4.25. In general, the effect of the return-stroke inclined angle on the induced voltage is similar. Just on the significance of the effect, there exists some gap. The difference in the induced voltage between both sides of the power line is not so evident as those shown in Fig.4.22.

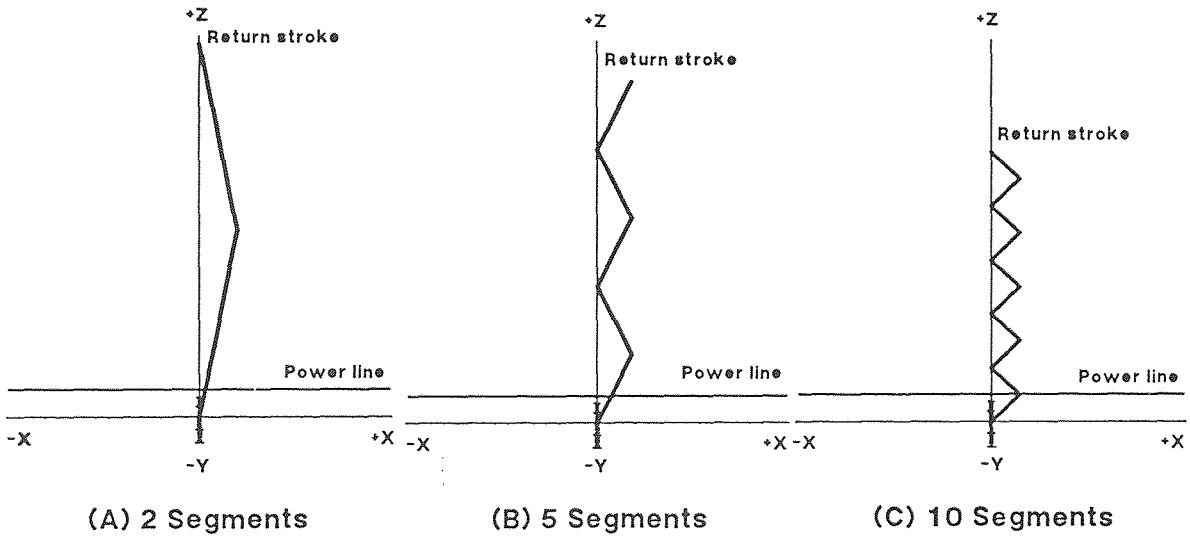

Figure 4.24 Coordinate system of a power line and return strokes composed of various segments.

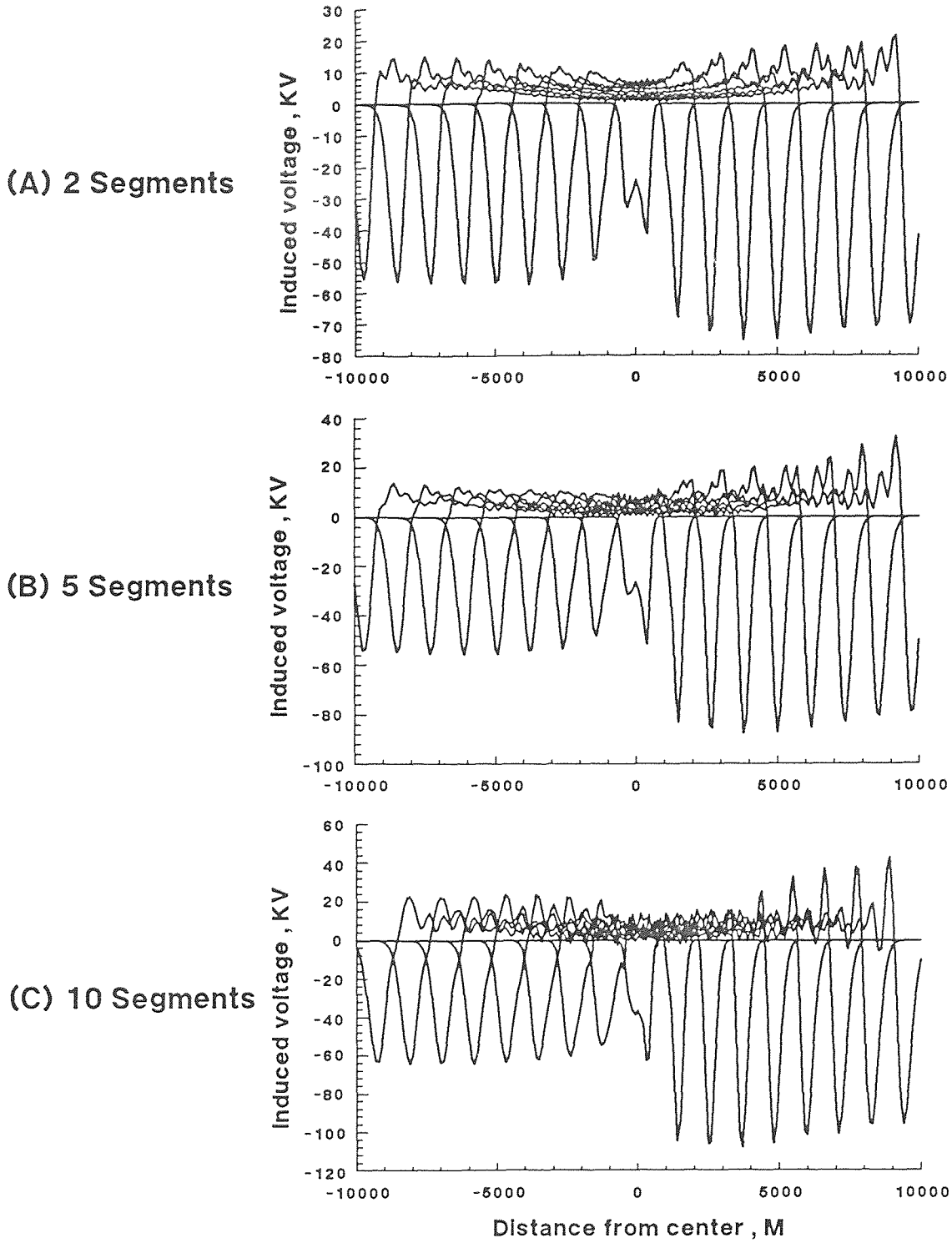

Figure 4.25 Comparison of induced voltages caused by return strokes composed of various segments. Effect of the inclined angle.

$\beta = 0.3$, $I_0 = 10kA$, $t_f = 5\mu s$, $y_0 = 100m$, $h = 10m$, $L_c = 3km$

4.3.5 Significance of the Timeliness on the Induced Voltage

To emphasize the significance of the timeliness on the induced voltage, a special return stroke composed of two segments is simulated, the former one-tenth inclined in the direction of $<1,0,1>$ and the latter nine-tenth inclined in the direction of $<-1,0,1>$. The coordinate system is shown in Fig.4.26 and the induced voltage is given in Fig.4.27.(a). The calculation results are out of anticipation. Intuitively, most people will think that the severity of the return stroke on the power line in the $-x$ direction is naturally worse than that in the $+x$ direction because the return stroke is nearer to the former. From Fig.4.27.(B), although the peak value of the inducing scalar potential at a designated point in the $+x$ direction is less than that at the relative point in the $-x$ direction, the former has better timeliness. So an important conclusion can be drawn from this special case. The magnitude of the superposition effect is determined by the value of the inducing scalar potential at a designated point when the maximum propagated voltage reached this point, but not by the peak value of the inducing scalar potential.

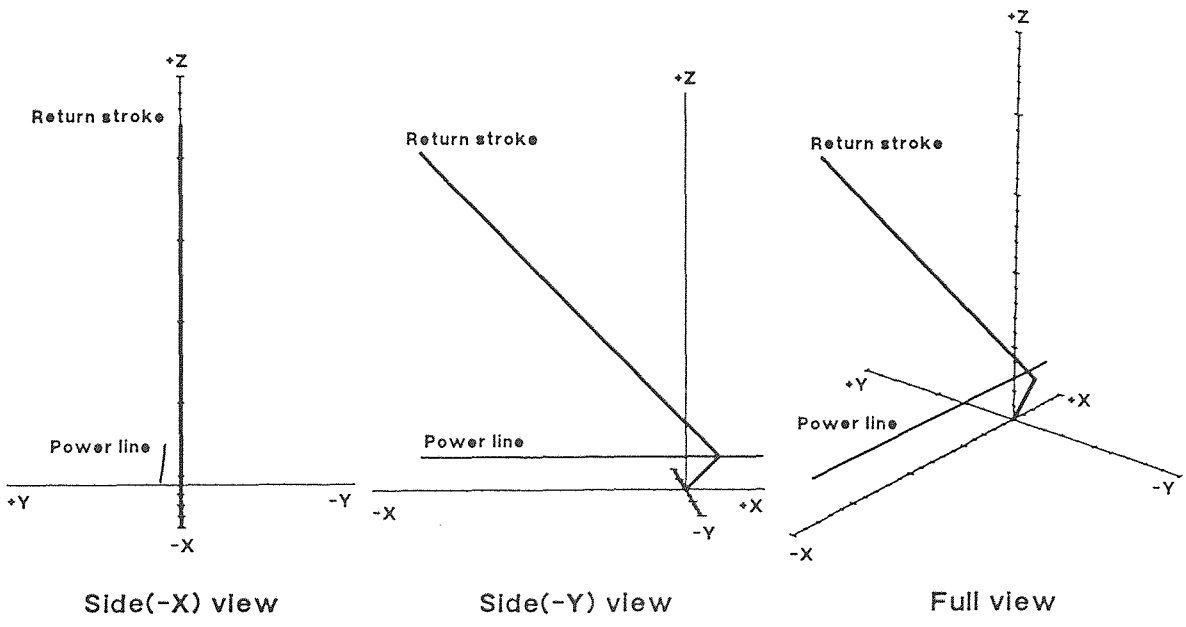

Figure 4.26 Coordinate system of a power line and a special return stroke composed of two segments.

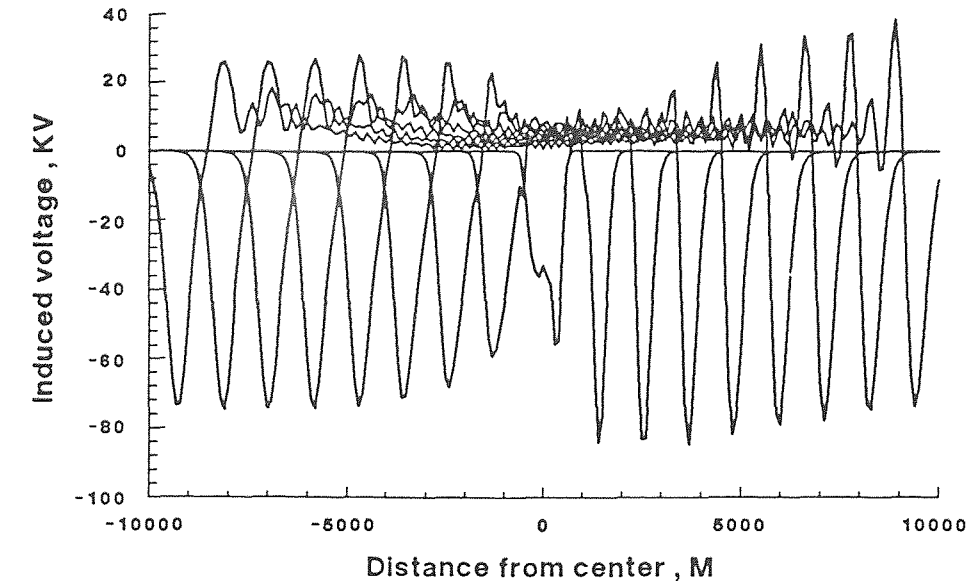

(A) Induced voltage as a function of space at increasing time

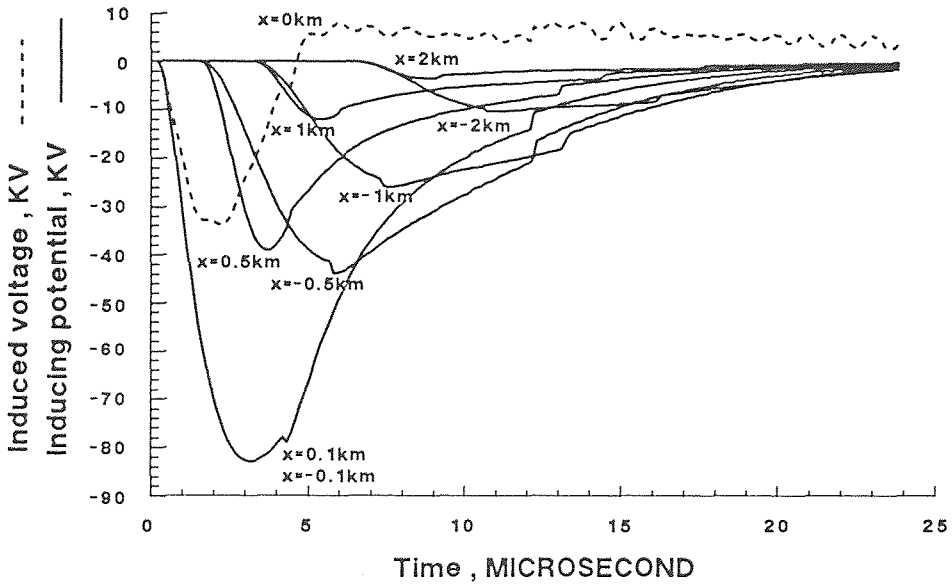

(B) Inducing potential as a function of time at different points & induced voltage at the line center

Figure 4.27 Induced voltage and inducing scalar potential on an overhead power line caused by a special return stroke.

$\beta = 0.3$, $I_0 = 10kA$, $t_f = 5\mu s$, $y_0 = 100m$, $h = 10m$, $L_c = 3km$

4.3.6 Effect of Return-Stroke Velocity on the Induced Voltage Caused by an Inclined Return Stroke

The effect of return-stroke velocity on the induced voltage caused by a vertical return stroke has been discussed in Subsection 4.2.1, and the results show that it is not very significant. Now it will be examined again by using an inclined return stroke. The case with progression vector $<1,0,1>$ shown in Fig.4.21 is adopted and three velocities, 10, 30 and 50 percent that of light, are discussed. Fig.4.28 gives the calculation results of the induced voltage. The peak value of the induced voltage on the power line increases in the inclined direction but decreases in the other direction when the return stroke velocity increases, i.e., the faster the return stroke velocity the worse is the severity of the inclined return stroke on the overhead power line. The return-stroke velocity becomes an important parameter when the lightning stroke is inclined. The primary cause is still the timeliness of the inducing scalar potential which is illustrated in Fig.4.29. The timing degree can be directly judged from the waveshapes of the inducing scalar potentials. Examining the rise time of the inducing scalar potential curve for each point, if the rise time is closer to each other, then the timeliness is better. When the rise time at various points are the same, the timeliness is perfect and the superposition effect is maximum. Of course, this is impossible in the natural world. In other words, if the waveshapes at various points look like each other, the timeliness will be well and the superposition effect is significant.

4.4 Effects of Inducing Components V_s, V_{mz} and E_{mx} on Induced Voltage V

Fig.4.19 has proved that the difference in the peak value of the induced voltage is primarily caused by the inducing scalar potential V_s. Now, an examination is made to determine the effect of the inducing component E_{mx} on the induced voltage. At first, the

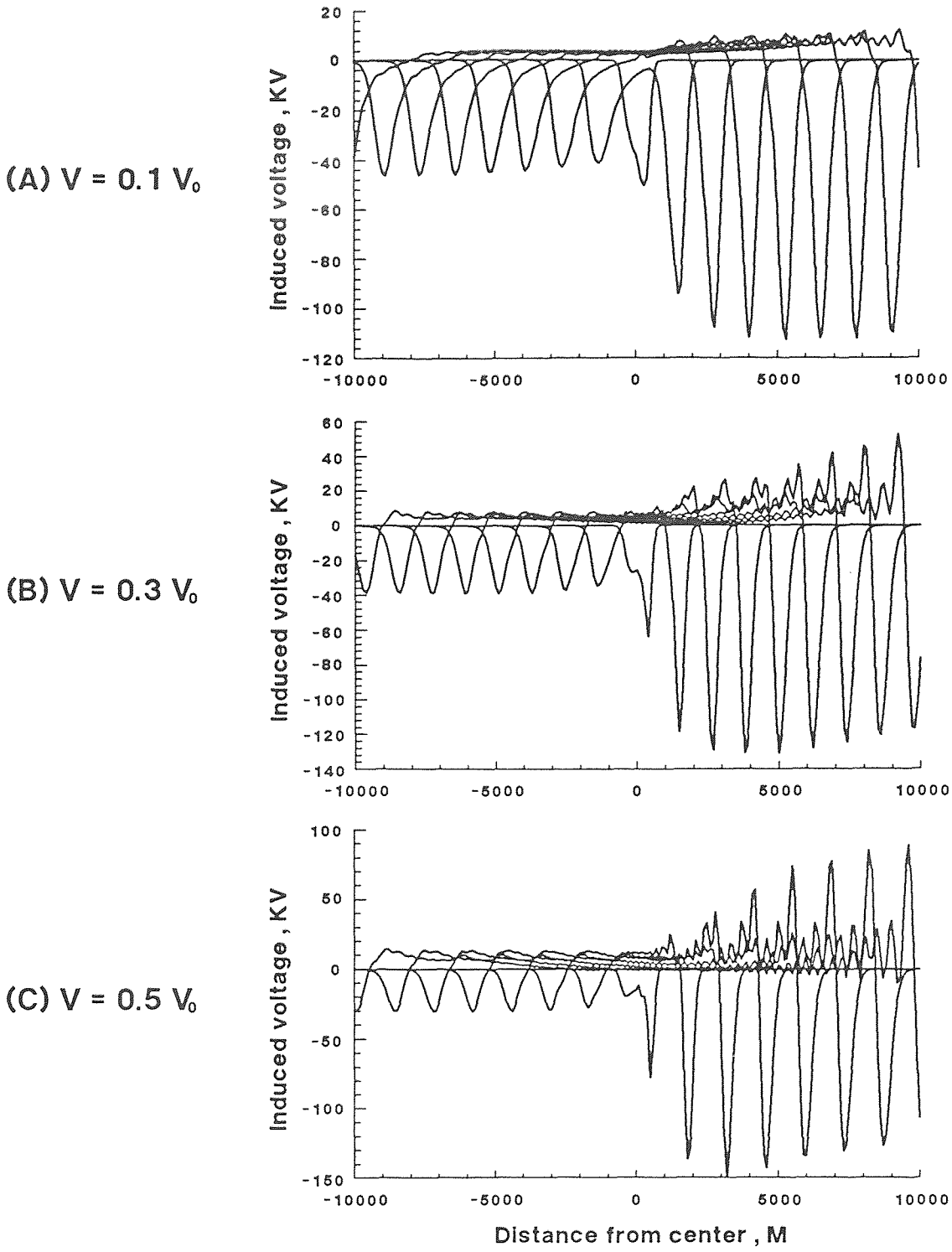

Figure 4.28 Comparison of induced voltages caused by an inclined return stroke with $\theta_i = 45^\circ$ and $\varphi = 0^\circ$. Effect of the return stroke velocity.
$\beta = 0.3$, $I_0 = 10kA$, $t_f = 5\mu s$, $y_0 = 100m$, $h = 10m$, $L_c = 3km$

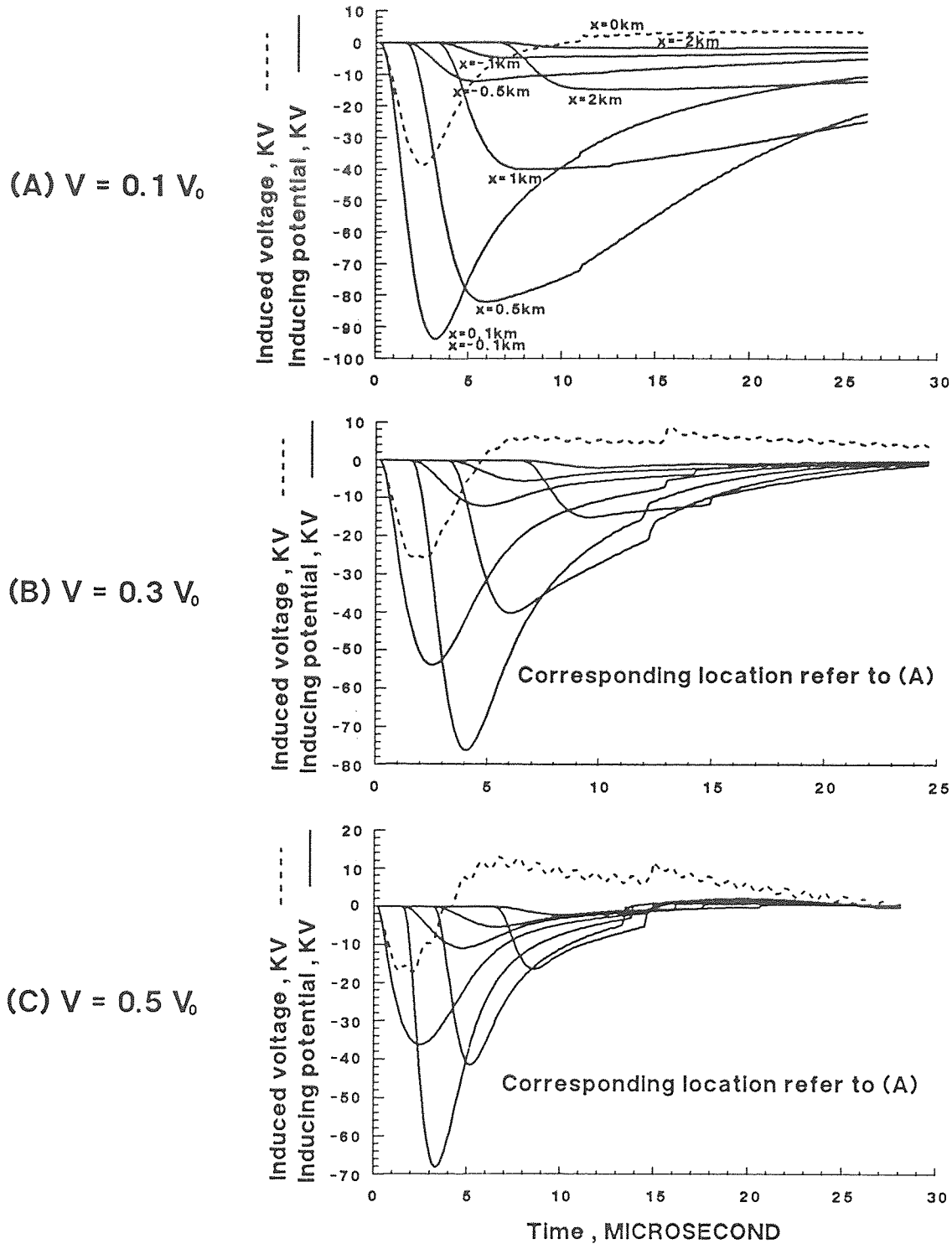

Figure 4.29 Inducing scalar potentials at various points on an overhead power line and the induced voltage at the line center caused by an inclined return stroke with $\theta_i = 45^\circ$ and $\varphi = 0^\circ$. Effect of the return stroke velocity. $\beta = 0.3$, $I_0 = 10kA$, $t_f = 5\mu s$, $y_0 = 100m$, $h = 10m$, $L_c = 3km$

inclined return stroke model with progression vector $<1,0,1>$ shown in Fig.4.21 is still adopted to discuss this topic.

The computer program is modified to exclude the effect of E_{mx} by eliminating step (6) listed in Section 3.3. The calculated V_p and V_{mz} are shown in Fig.4.30.(A), where V_p is produced by V_s only. The calculated V is shown in Fig.4.30.(B) which is the total of V_p and V_{mz}. The actual induced voltage on the power line is calculated by using the full computer program and shown in Fig.4.30(C). Comparing Fig.4.30.(C) with 4.30.(B), the contribution of E_{mx} to the induced voltage is insignificant. This is as expected from equation (2.22) in which the value of E_{mx} is very small because the inclined return stroke is straight. The values of $E_{mx}\delta x$ appearing in Fig.3.4 are calculated and shown in Fig.4.31. The maximum value is only -1.8 kV which can be neglected if compared with V_p.

Analyzing equation (2.22), E_{mx} maybe has some influence on the induced voltage under zigzag return stroke because the sign between E'_m and E''_m is changed from (-) to (+) sometimes. So the discussion is continued by using the zigzag return stroke model shown in Fig.4.24.(C). The calculations are repeated and calculated results are shown in Fig.4.32. The effect of E_{mx} is still negligible.

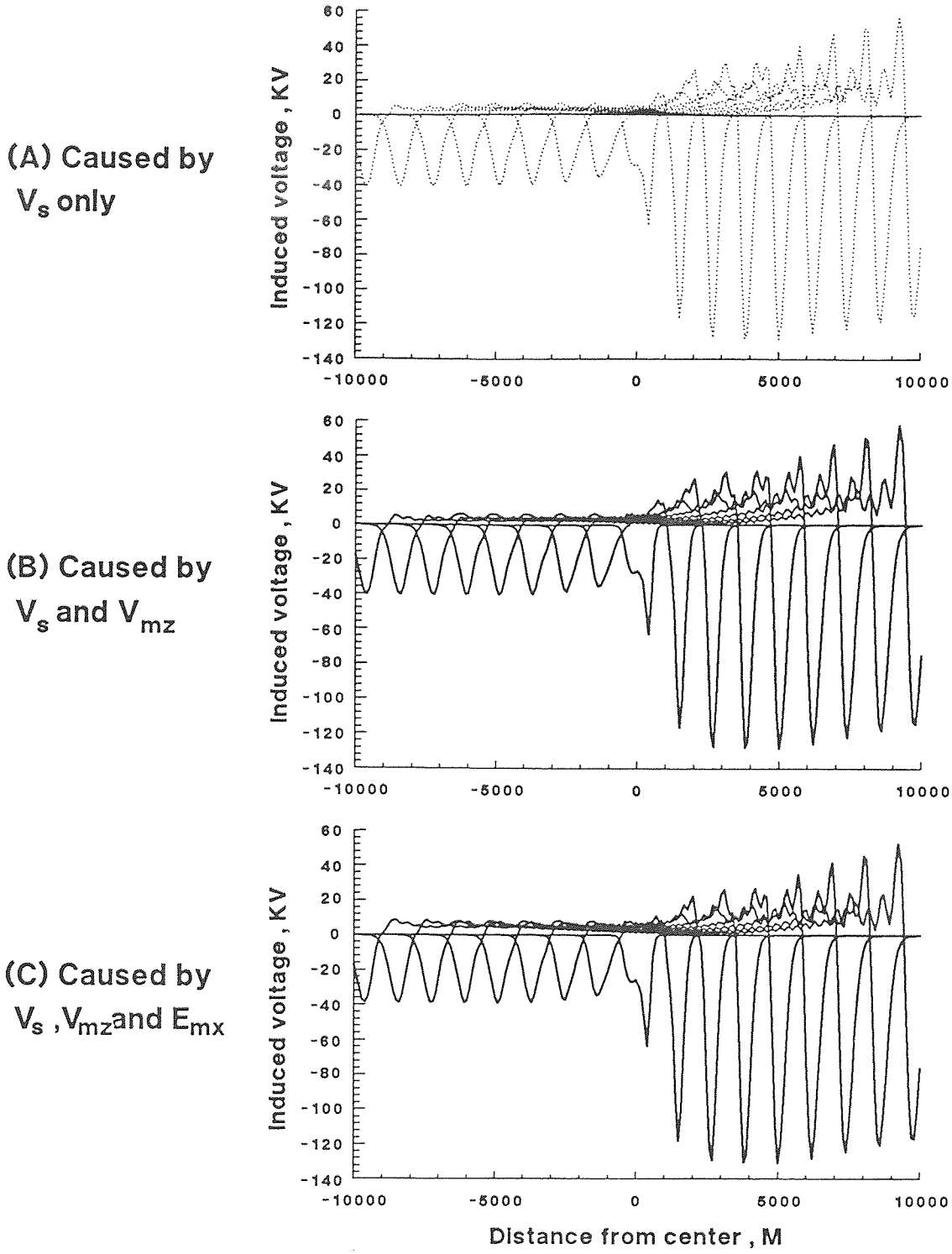

Figure 4.30 Effect of inducing components V_s, V_{mz} and E_{mx} on the induced voltage caused by a straight inclined return stroke.

$\beta = 0.3$, $I_0 = 10kA$, $t_f = 5\mu s$, $y_0 = 100m$, $h = 10m$, $L_c = 3km$

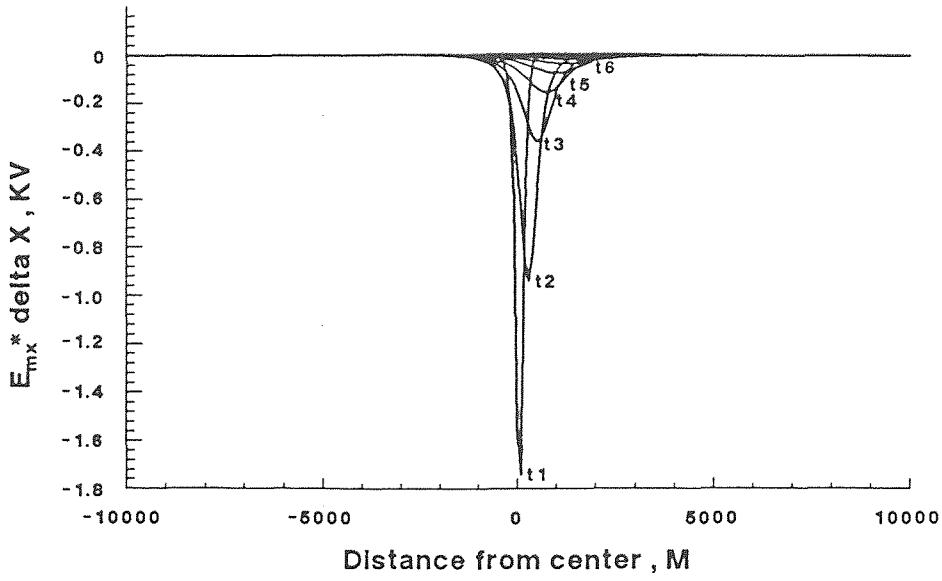

(A) Function of space at increasing time

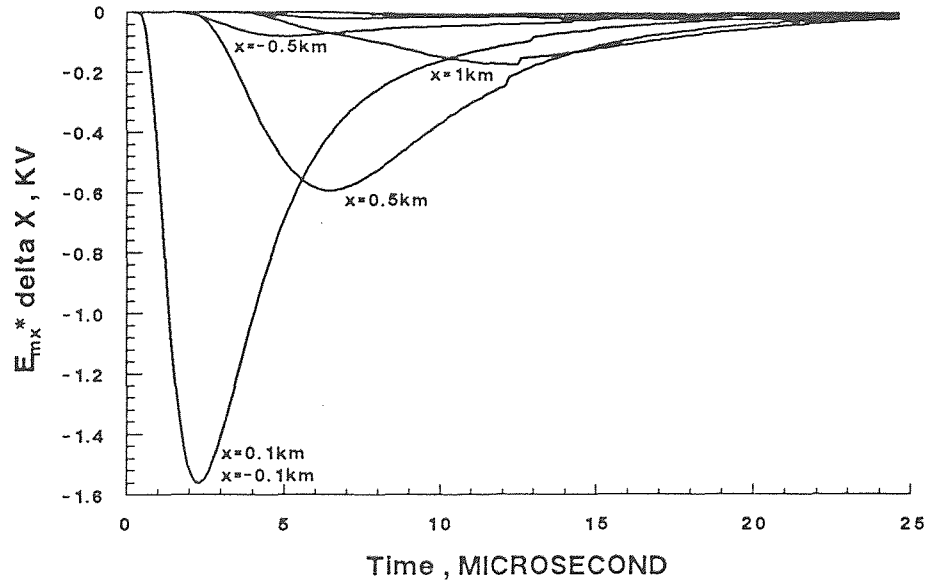

(B) Function of time at various points

Figure 4.31 Values of $E_{mx}\delta x$ induced by a straight inclined return stroke.

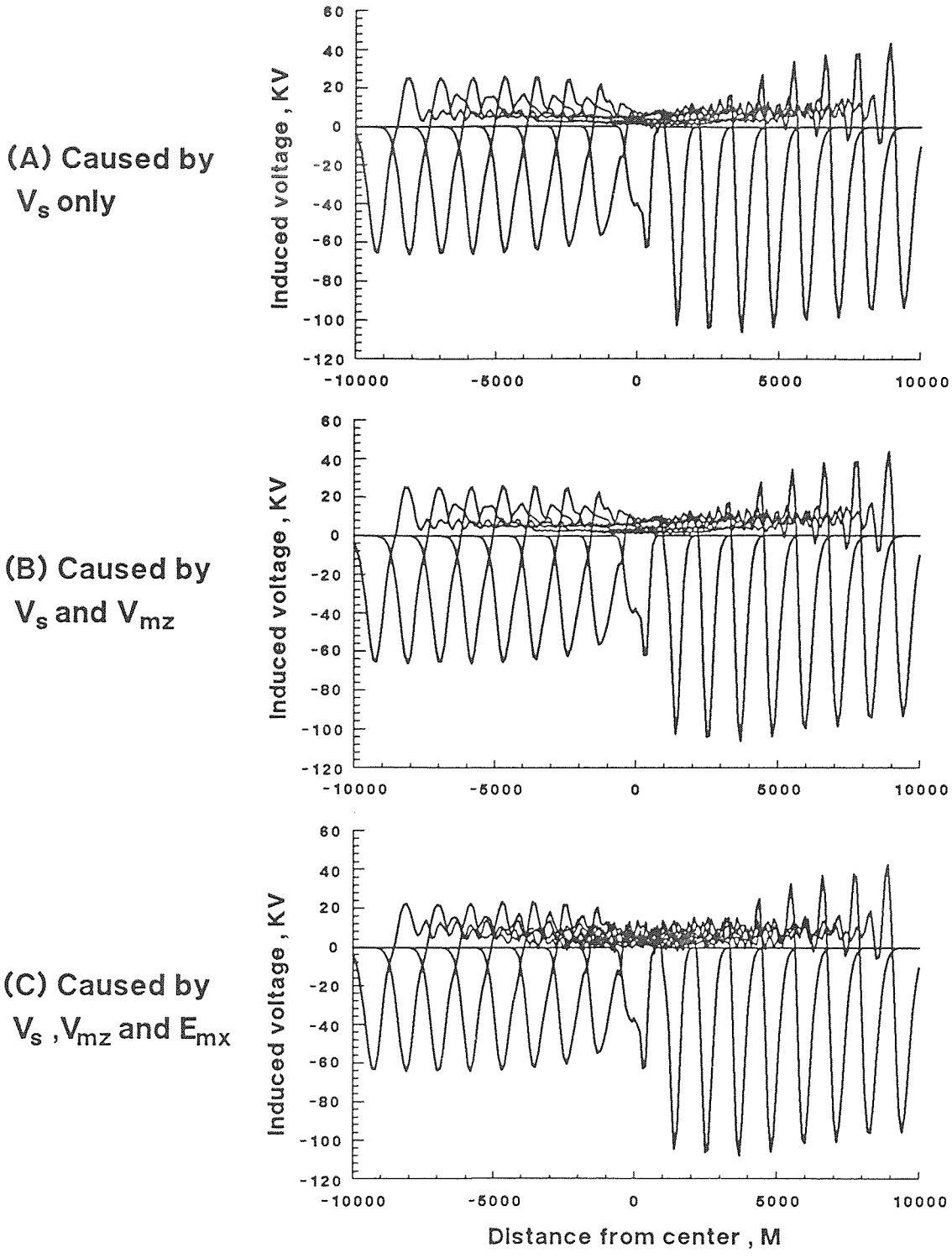

Figure 4.32 Effect of inducing components V_s, V_{mz} and E_{mx} on the induced voltage caused by a zigzag return stroke.

$\beta = 0.3$, $I_0 = 10kA$, $t_f = 5\mu s$, $y_0 = 100m$, $h = 10m$, $L_c = 3km$

CHAPTER 5

CONCLUSIONS

The following conclusions are drawn from the preceding investigations:

(1) The presented numerical model includes the most flexible capability to describe the configurations of the lightning in real systems. A finite-length lightning channel of any direction in 3-D space can be modelled and closed-form expressions of the inducing potentials have been derived. The inducing scalar potential and inducing vector potential caused by an arbitrarily shaped lightning stroke can be expressed and calculated by superposition.

(2) Taking into account the retarded-height difference between the real charges in space and the imaginary charges produced by the perfect conductive ground, we were able to explain the bipolar characteristic of the inducing scalar potential which indirectly causes the bipolar induced voltage waves.

(3) The induced voltage on an overhead power line can be calculated by solving the corresponding differential equations in which the horizontal component of the inducing vector potential is taken into consideration. A computer program has been developed with the use of the finite-difference time-domain method in which the differential equations are converted into difference equations. By means of the program, the induced voltage can be evaluated as a function of time at any point on the power line or as a function of space at various times and the results are shown up with figures. From former figure, the variation of the induced voltage with time can be examined. From latter figure, the propagation of the induced voltage along the power line can be observed.

(4) Using the program, parametric effects on the induced voltage caused by a vertical lightning stroke are discussed. According to the significance of these

parametric effects on the induced voltage, they can be arranged in order as y_0, t_f, h, h_c, β. It is out of anticipation that the effect of the return-stroke velocity is so slight. When the effect of the return-stroke velocity is inspected, the return-stroke current needs to be changed with the varying-ratio of the return-stroke velocity.

(5) With the use of the program, comparisons of the induced voltage caused by inclined lightning strokes are made under various conditions. The results show that the induced voltage caused by a inclined return stroke will increase in the inclined side of the power line but decreases in the other side when the inclined plane is not perpendicular to the power line. Moreover, the larger the inclined angle or the faster the return-stroke velocity, the larger the difference in the induced voltage between both sides of the power line. The induced voltages caused by inclined return strokes are considerably higher than those caused by vertical ones irrespective of the progress velocity. Higher voltage will be induced on an overhead power line by the inclined return stroke not near the lightning struck point but at the location some distance away from such point.

(6) Since the severity of the inclined return stroke on the overhead power line is considerably harmful, especially when the return-stroke velocity gets faster or the inclined angle increases. It should be taken into account in the lightning protection design for transmission lines as well as distribution lines.

The study has large investigative scope. The developed computer program can be extended to apply in the following areas:

(1) Analysis of multiconductor line systems.

(2) Lightning strokes with branches.

(3) Bent overhead power line.

(4) Undulating ground surface.

APPENDIX

MULTIPLE FIGURES

This appendix includes the figures validating the numerical method used to evaluate the inducing potentials, and those showing the parametric effects on the induced voltage caused by a vertical lightning stroke. For validating the numerical method, these figures include:

- Inducing potential caused by a vertical return stroke with rectangular current (Figure 2.6-Figure 2.7)
- Inducing potential caused by a vertical return stroke with rapidly-rising current (Figure 2.8-Figure 2.12)

For showing the parametric effects, these figures include:

- Progress velocity of return stroke (Figure 4.1-Figure 4.4)
- Front time of return-stroke current (Figure 4.5-Figure 4.7)
- Height of cloud charge center (Figure 4.8-Figure 4.9)
- Least distance of the power line from the lightning struck point (Figure 4.10-Figure 4.12)
- Height of the power line above ground (Figure 4.13-Figure 4.14)

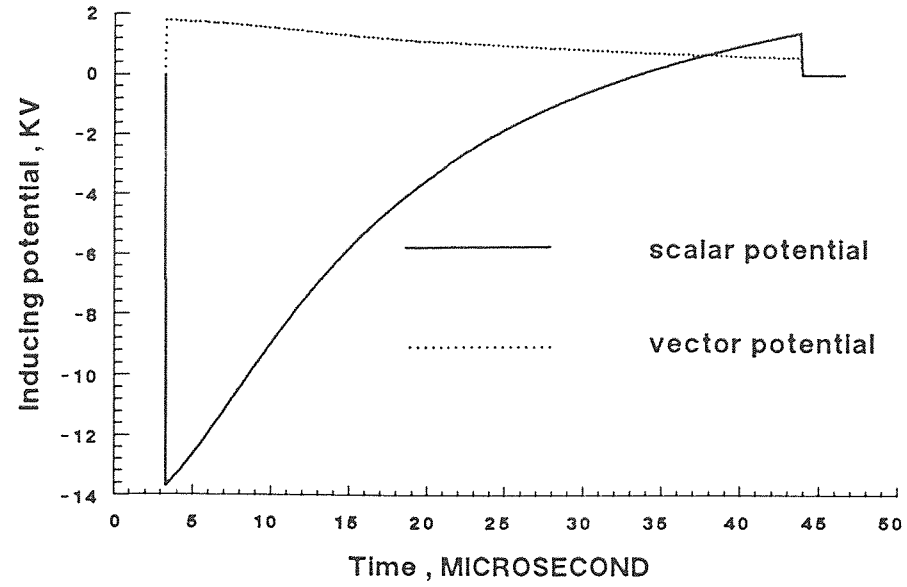

(A) Numerical method , x = 5 km

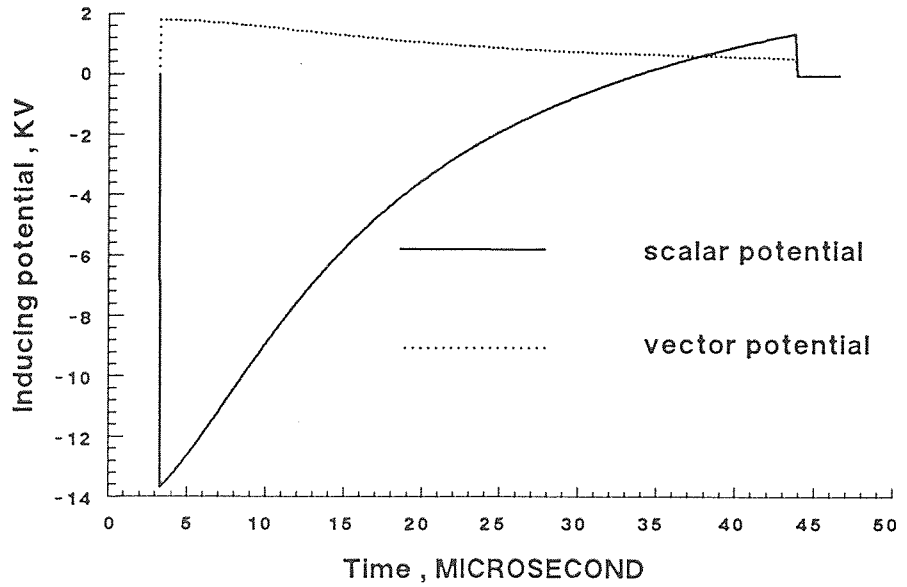

(B) Published method , x = 5 km

Figure 2.6 Comparison between numerical method and published method to calculate the inducing potential on an overhead power line caused by a vertical return stroke with rectangular current.

$x = 5km$, $y_0 = 10m$, $\beta = 0.3$, $I_0 = 10kA$, $h = 10m$, $h_c = 3km$

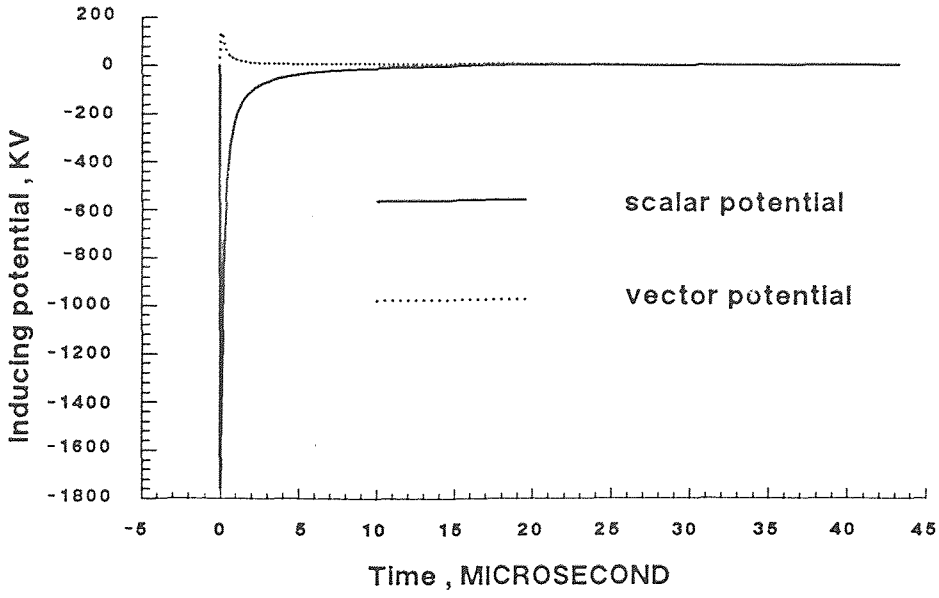

(A) Numerical method , x = 0 km

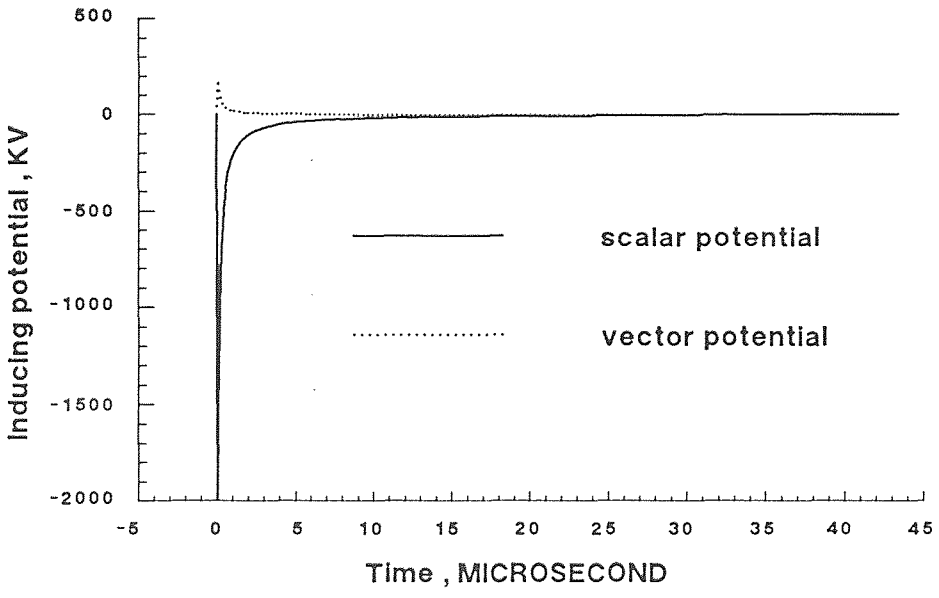

(B) Published method , x = 0 km

Figure 2.7 Comparison between numerical method and published method to calculate the inducing potential on an overhead power line caused by a vertical return stroke with rectangular current.

$x = 0m$, $y_0 = 10m$, $\beta = 0.3$, $I_0 = 10kA$, $h = 10m$, $h_c = 3km$

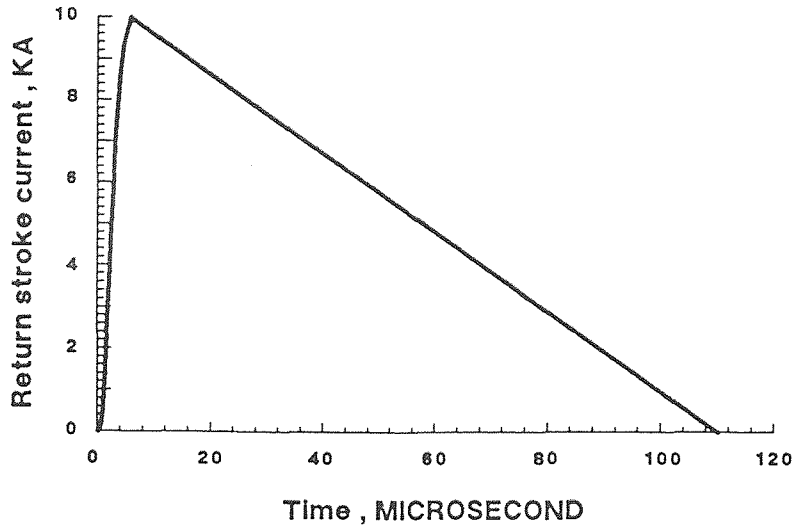

(A) Waveshape of the return stroke current

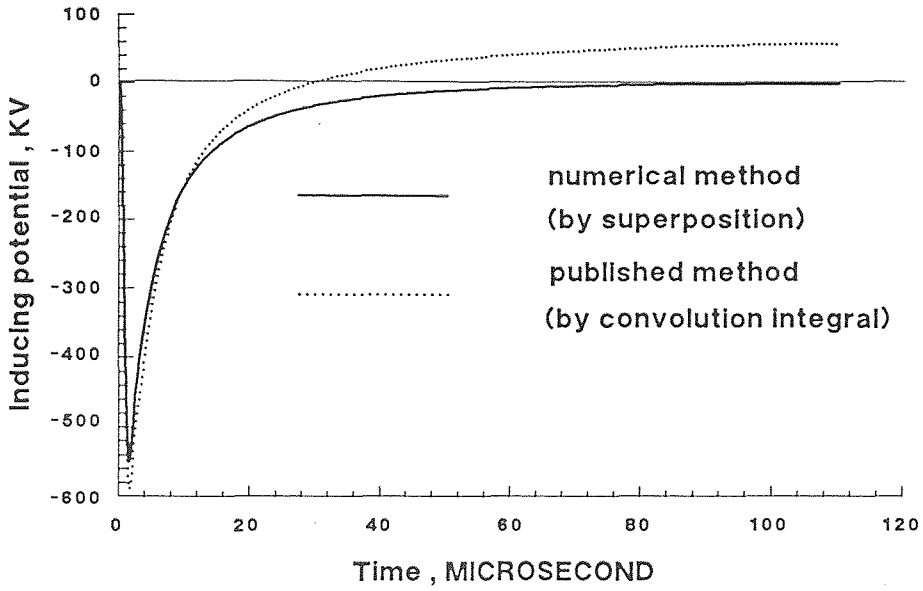

(B) Inducing scalar potential at point x = 0 m

Figure 2.8 Comparison between numerical method and published method to calculate the inducing potential on an overhead power line caused by a vertical return stroke with rapidly-rising current possessing drooping tail.

$x = 0m$, $y_0 = 100m$, $\beta = 0.1$, $I_0 = 10kA$, $t_f = 2\mu s$, $h = 10m$, $h_c = 3km$

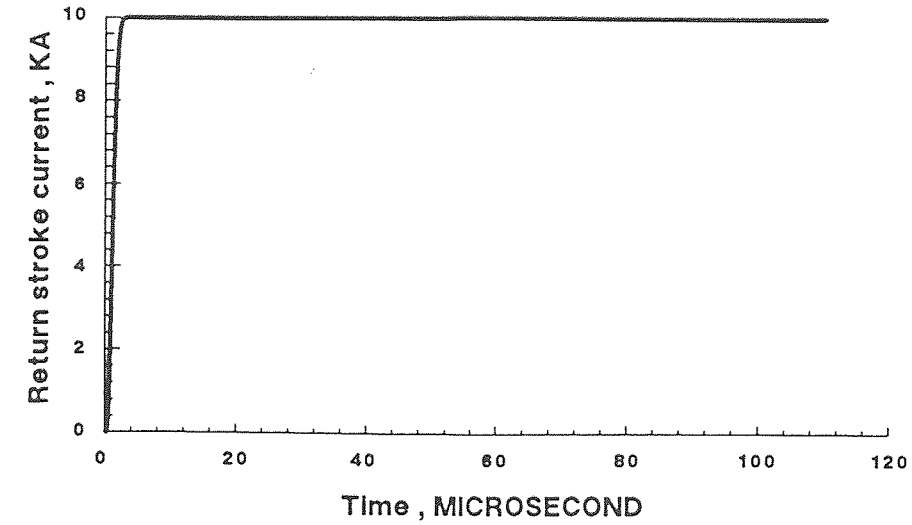

(A) Waveshape of the return stroke current

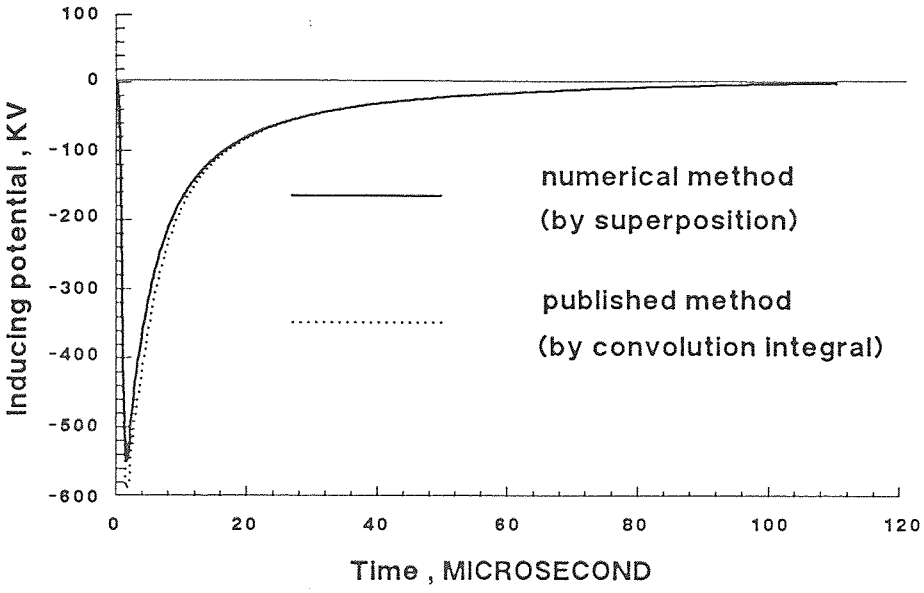

(B) Inducing scalar potential at point x = 0 m

Figure 2.9 Comparison between numerical method and published method to calculate the inducing potential on an overhead power line caused by a vertical return stroke with rapidly-rising current possessing constant tail.

$x = 0m$, $y_0 = 100m$, $\beta = 0.1$, $I_0 = 10kA$, $t_f = 2\mu s$, $h = 10m$, $h_c = 3km$

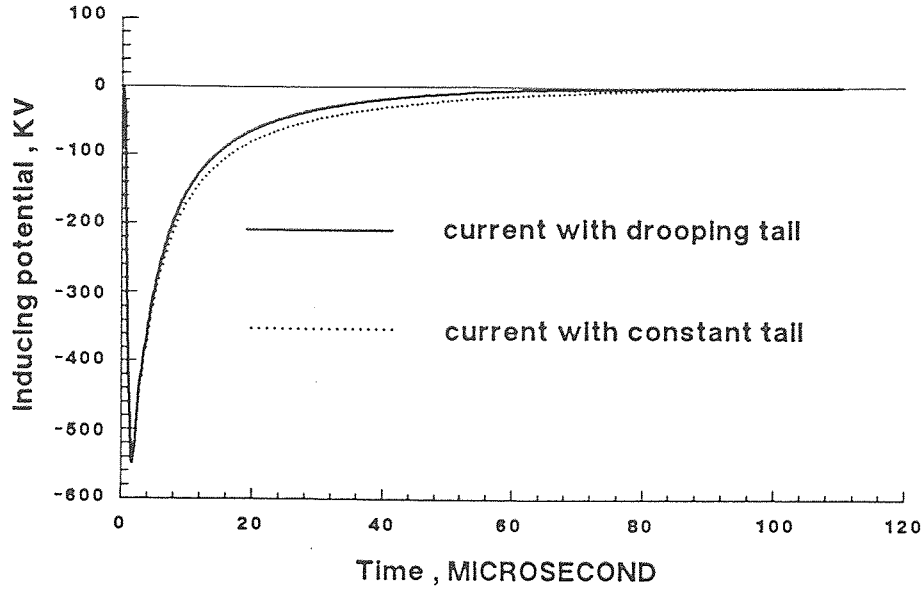

(A) Method through superposition

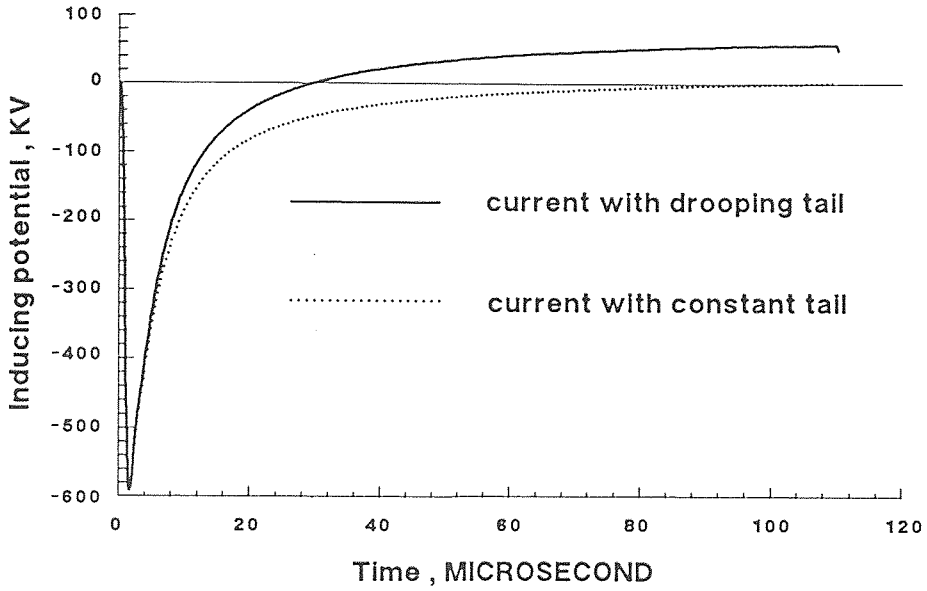

(B) Method through convolution integral

Figure 2.10 Effect of the tail variety of the lightning return-stroke current. $x = 0m$, $y_0 = 100m$, $\beta = 0.1$, $I_0 = 10kA$, $t_f = 2\mu s$, $h = 10m$, $h_c = 3km$

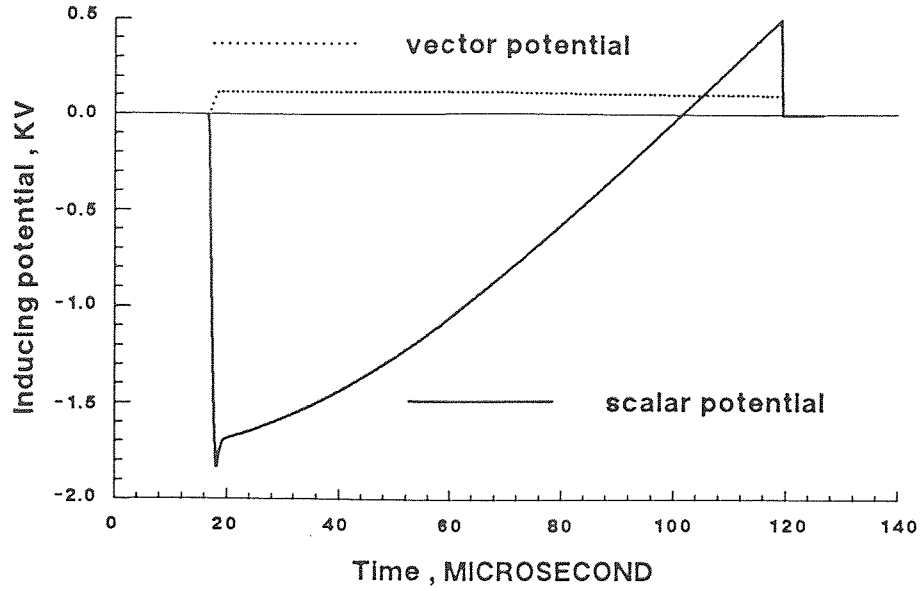

(A) Current with constant tail

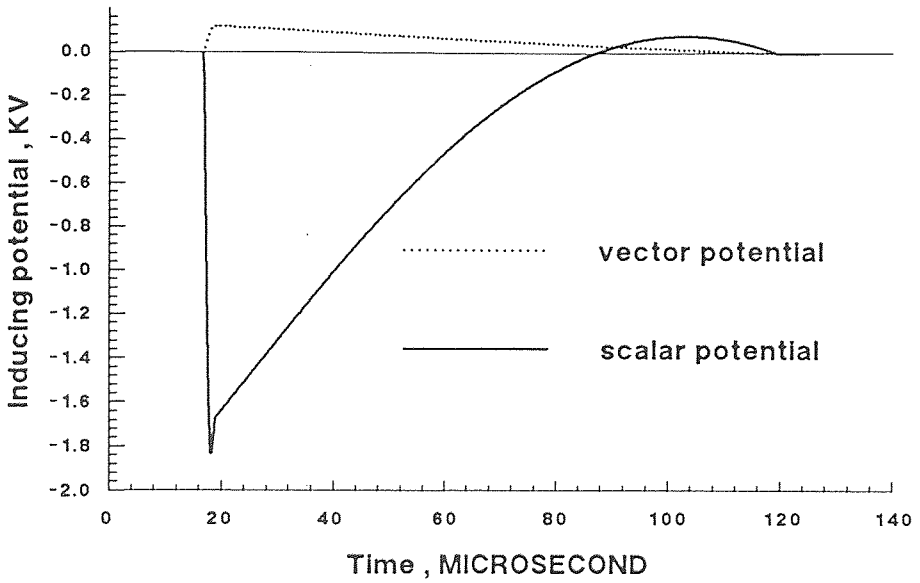

(B) Current with droping tail

Figure 2.11 Bipolar characteristic of the inducing scalar potential.
$x = 5km$, $y_0 = 100m$, $\beta = 0.1$, $I_0 = 10kA$, $t_f = 2\mu s$, $h = 10m$, $h_c = 3km$

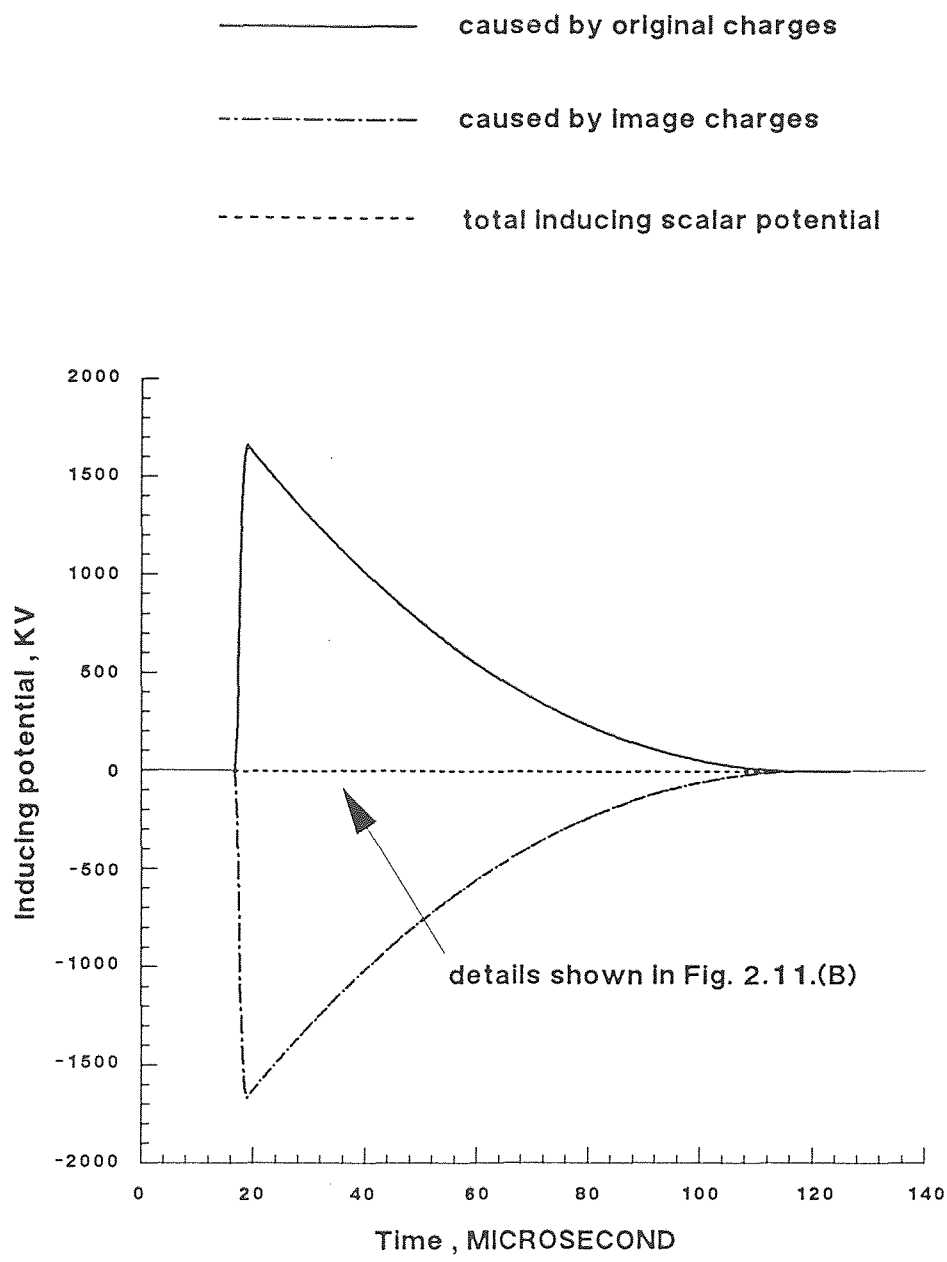

Figure2.12 Composition of the inducing scalar potential caused by a vertical return stroke with rapidly-rising current possessing drooping tail.

$x = 5km$, $y_0 = 100m$, $\beta = 0.1$, $I_0 = 10kA$, $t_f = 2\mu s$, $h = 10m$, $h_c = 3km$

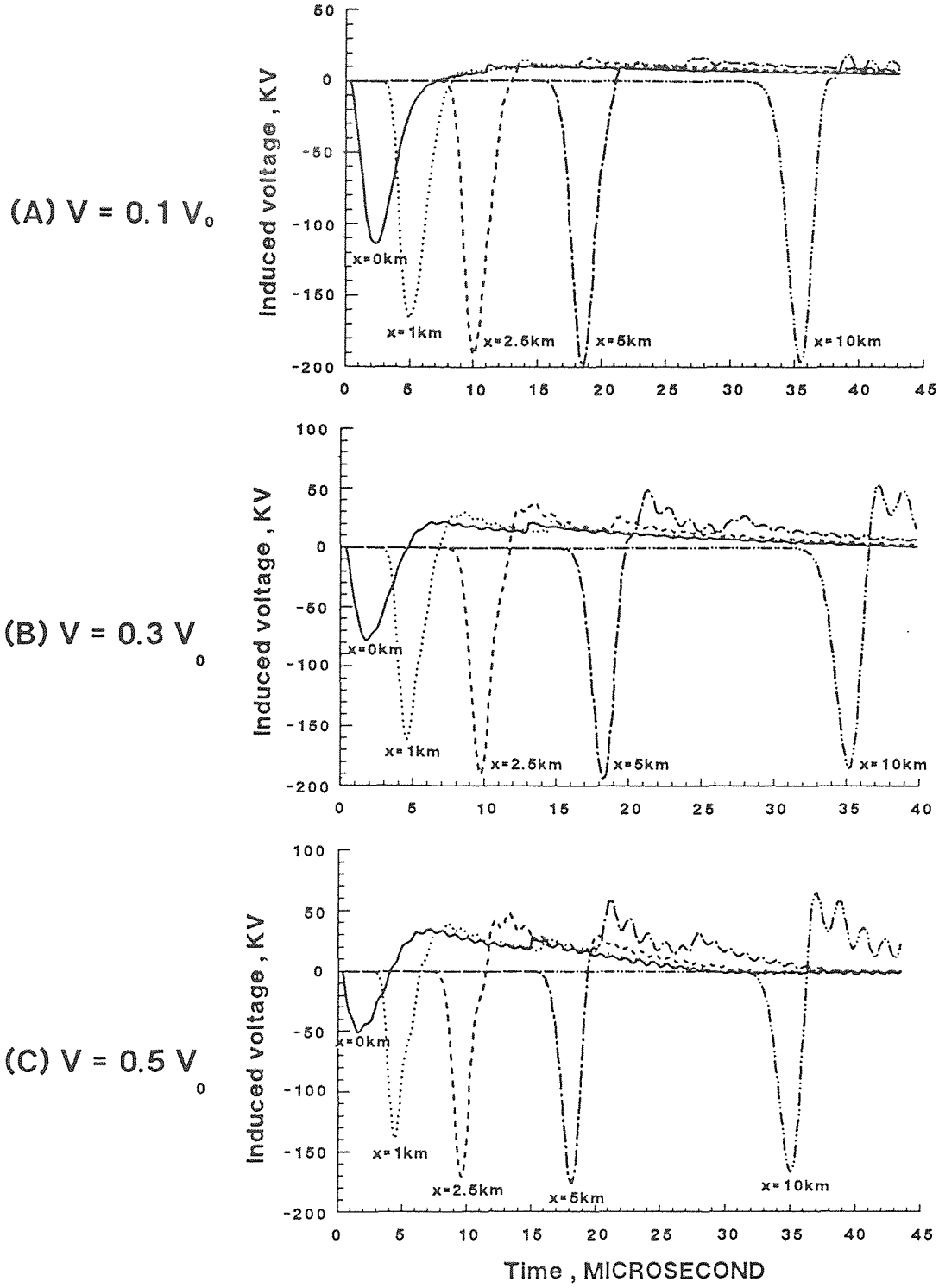

Figure 4.1 Induced voltage as a function of time at different points on an overhead power line caused by a vertical lightning stroke. Effect of return stroke velocity, β.

1: $\beta = 0.1, I_0 = 10kA$; 2: $\beta = 0.3, I_0 = 30kA$; 3: $\beta = 0.5, I_0 = 50kA$

$t_f = 5\mu s$, $y_0 = 100m$, $h = 10m$, $h_c = 3km$

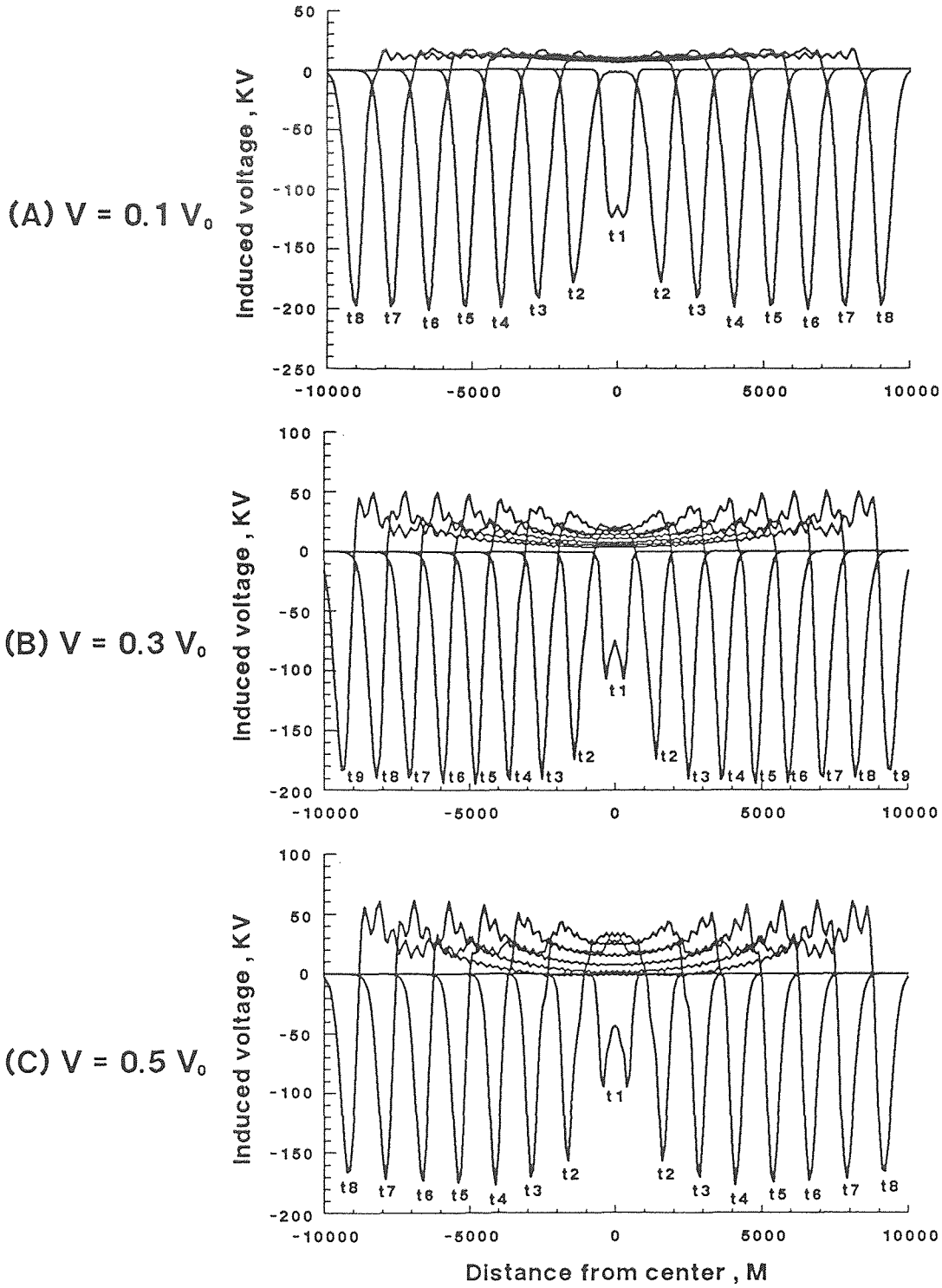

Figure 4.2 Induced voltage as a function of space at various times on an overhead power line caused by a vertical lightning stroke. Effect of return stroke velocity, β.

1: $\beta = 0.1, I_0 = 10kA$; 2: $\beta = 0.3, I_0 = 30kA$; 3: $\beta = 0.5, I_0 = 50kA$

$t_f = 5\mu s$, $y_0 = 100m$, $h = 10m$, $h_c = 3km$

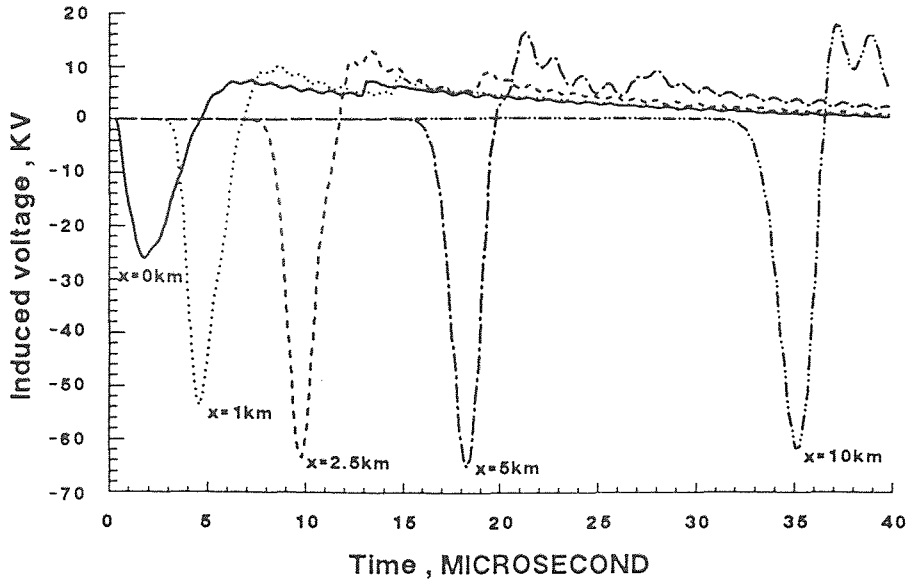

(A) Induced voltage as a function of time at different points

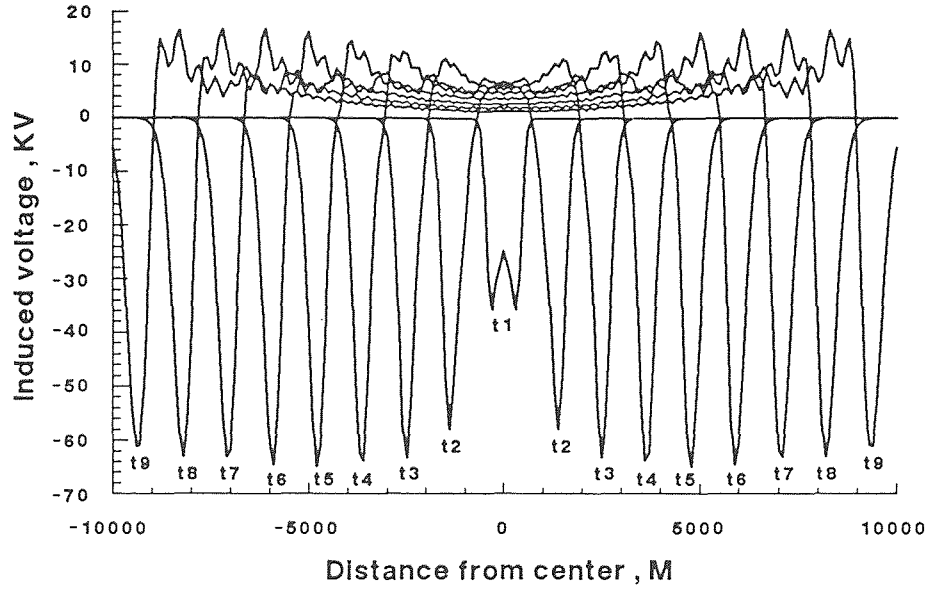

(B) Induced voltage as a function of space at various times

Figure 4.3 Induced voltage on an overhead power line caused by a vertical lightning stroke. Current is not changed with the varying- ratio of the return stroke velocity.

$\beta = 0.3$, $I_0 = 10kA$, $t_f = 5\mu s$, $y_0 = 100m$, $h = 10m$, $h_c = 3km$

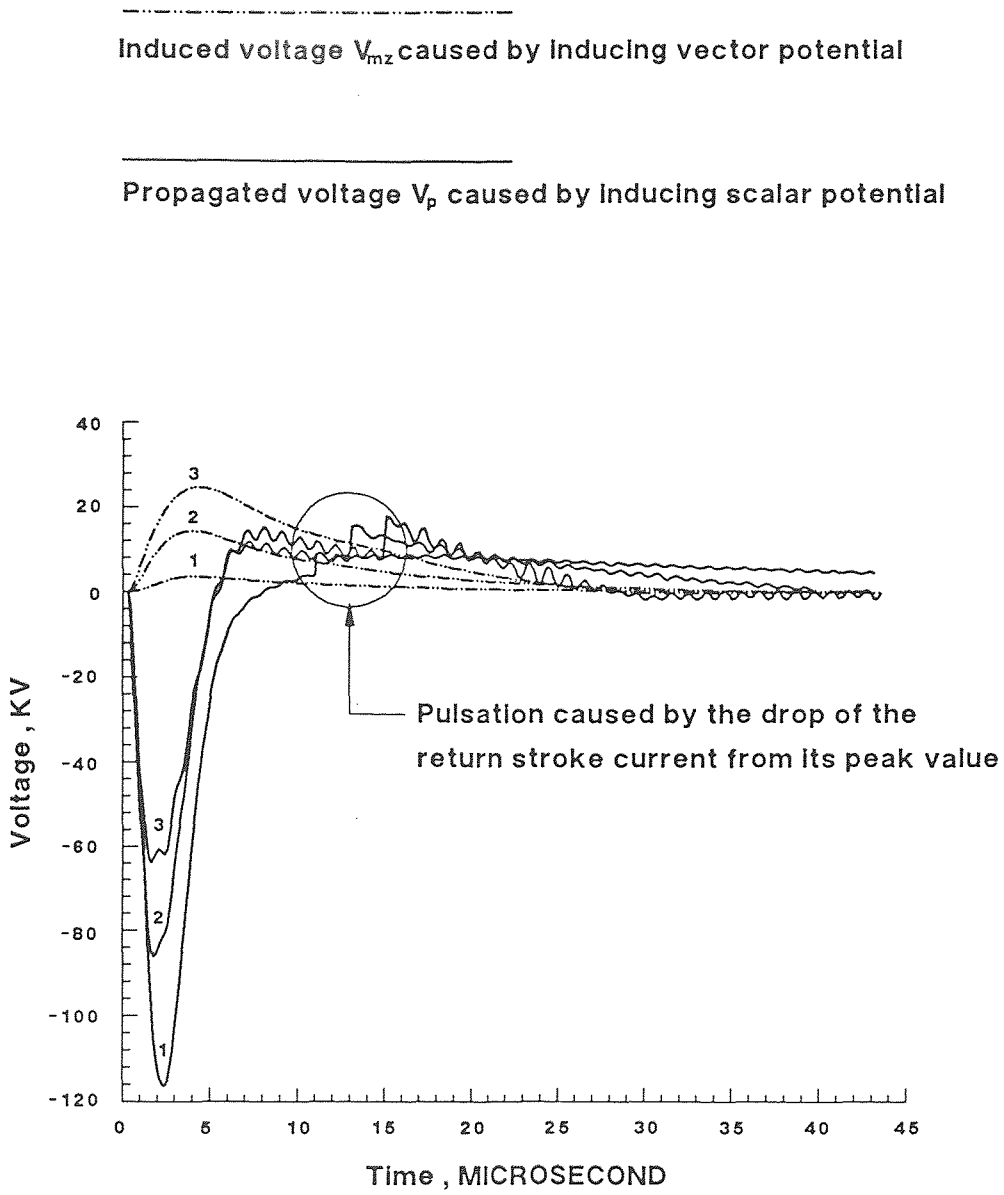

Figure4.4 Components of induced voltage. Effect of return stroke velocity.

1: $\beta = 0.1, I_0 = 10kA$; 2: $\beta = 0.3, I_0 = 30kA$; 3: $\beta = 0.5, I_0 = 50kA$

$t_f = 5\mu s$, $x = 0m$, $y_0 = 100m$, $h = 10m$, $h_c = 3km$

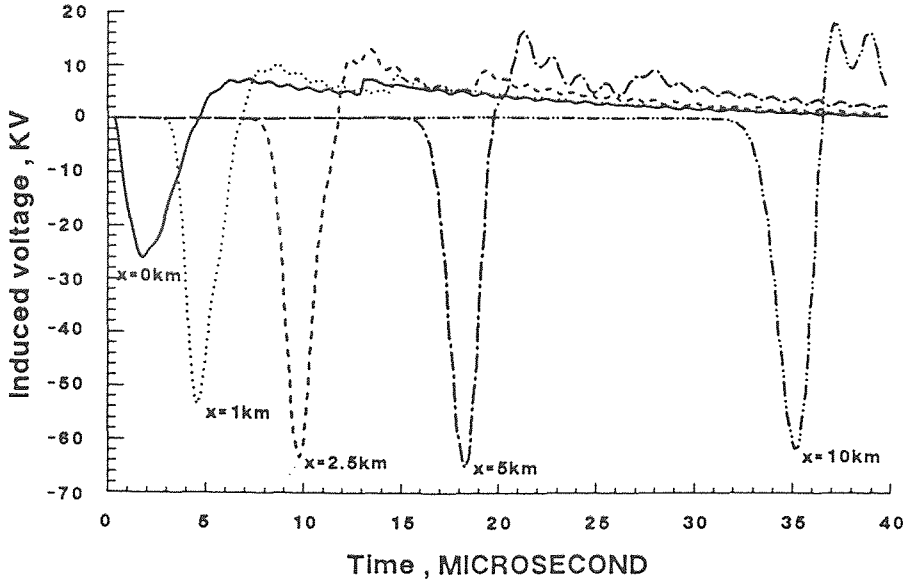

(A) Front time t_f = 5 microsecond

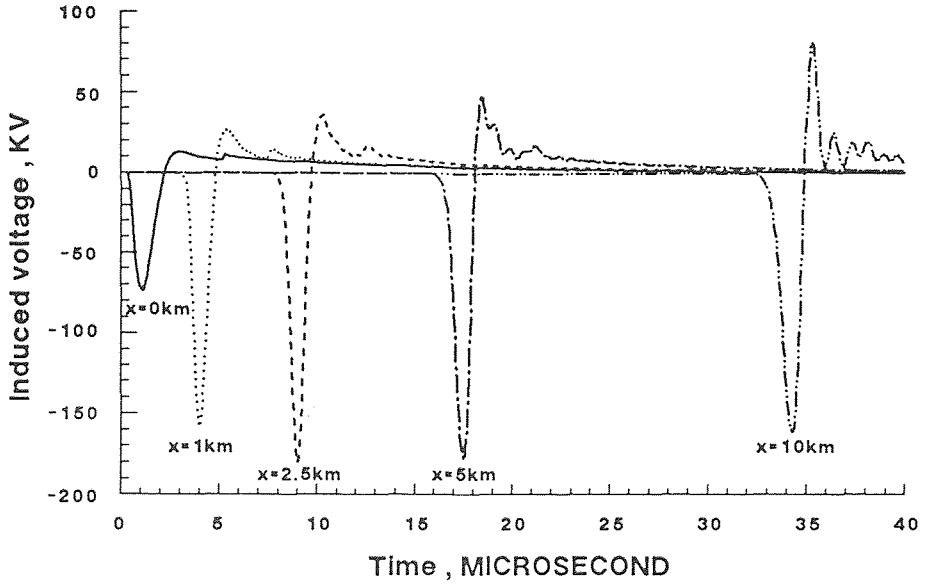

(B) Front time t_f = 2 microsecond

Figure 4.5 Induced voltage as a function of time at different points on an overhead power line caused by a vertical lightning stroke. Effect of current front time, t_f.

$\beta = 0.3$, $I_0 = 10kA$, $y_0 = 100m$, $h = 10m$, $h_c = 3km$

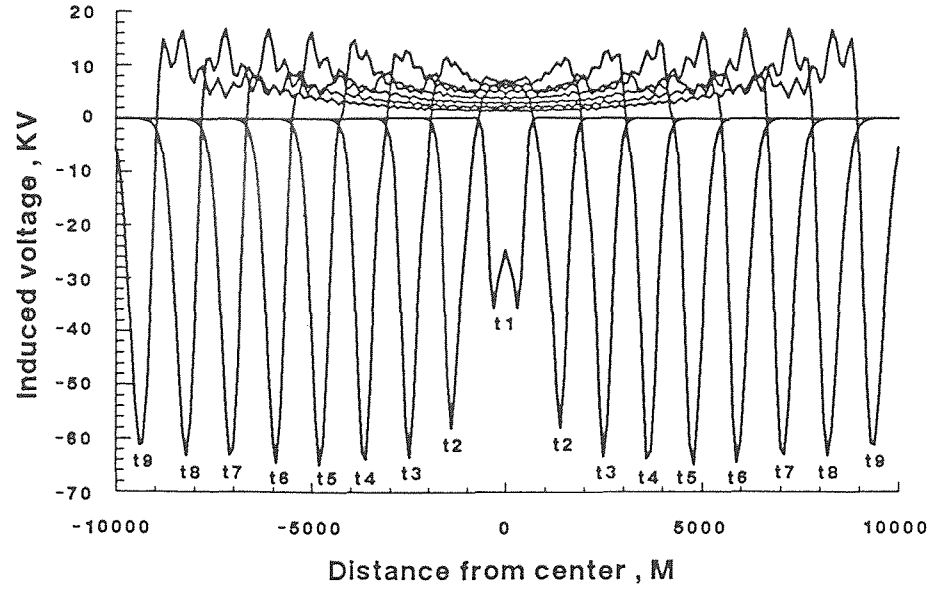

(A) Front time t_f = 5 microsecond

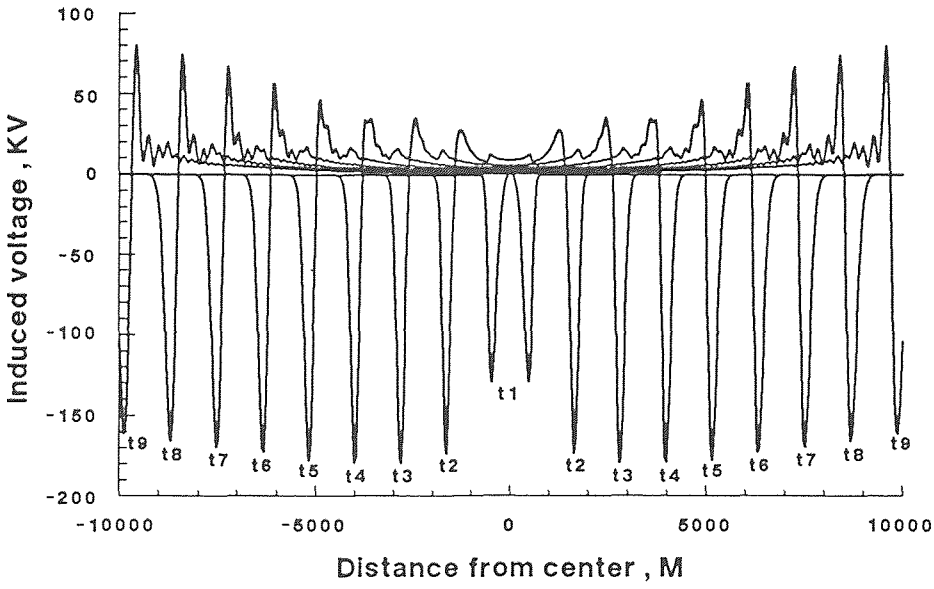

(B) Front time t_f = 2 microsecond

Figure 4.6 Induced voltage as a function of space at various times on an overhead power line caused by a vertical lightning stroke. Effect of current front time, t_f.

$\beta = 0.3$, $I_0 = 10kA$, $y_0 = 100m$, $h = 10m$, $h_c = 3km$

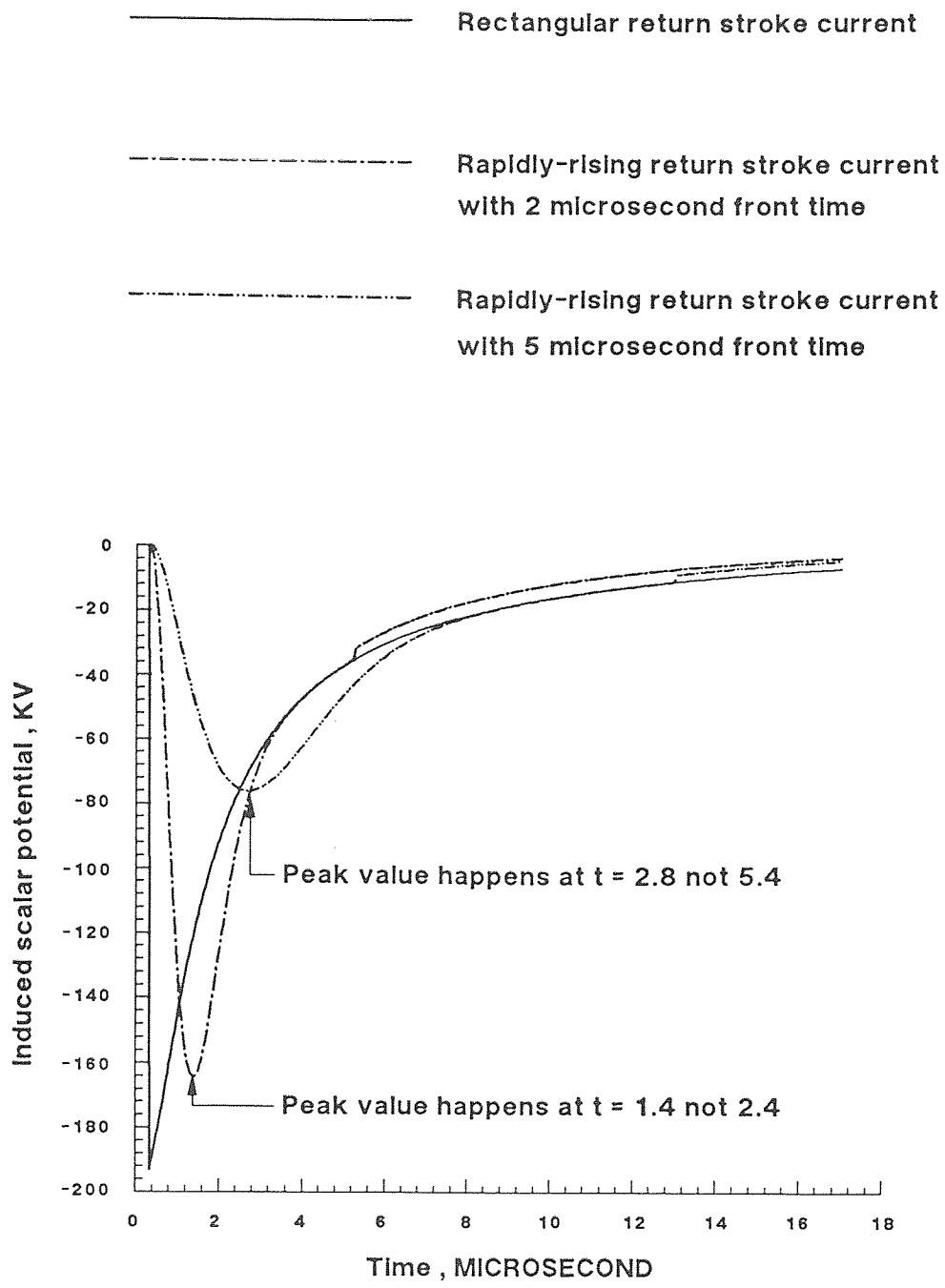

Figure 4.7 Effect of current front time on inducing scalar potential, V_s.
$\beta = 0.3$, $I_0 = 10kA$, $x = 0m$, $y_0 = 100m$, $h = 10m$, $h_c = 3km$

(A) h_c = 1 km

(B) h_c = 3 km

(C) h_c = 5 km

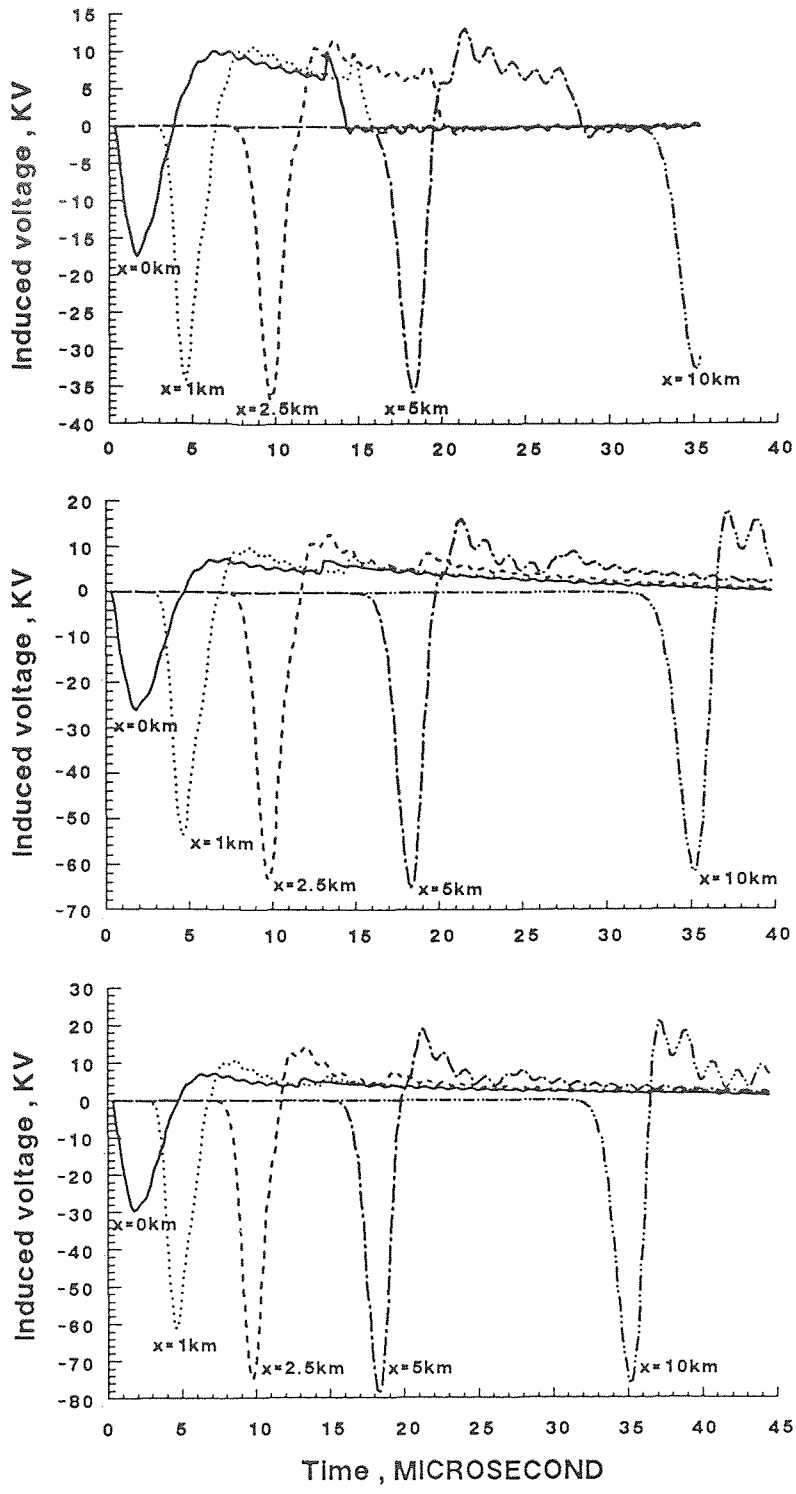

Figure 4.8 Induced voltage as a function of time at different points on an overhead power line caused by a vertical lightning stroke. Effect of height of cloud charge center, h_c.

$\beta = 0.3$, $I_0 = 10kA$, $t_f = 5\mu s$, $y_0 = 100m$, $h = 10m$

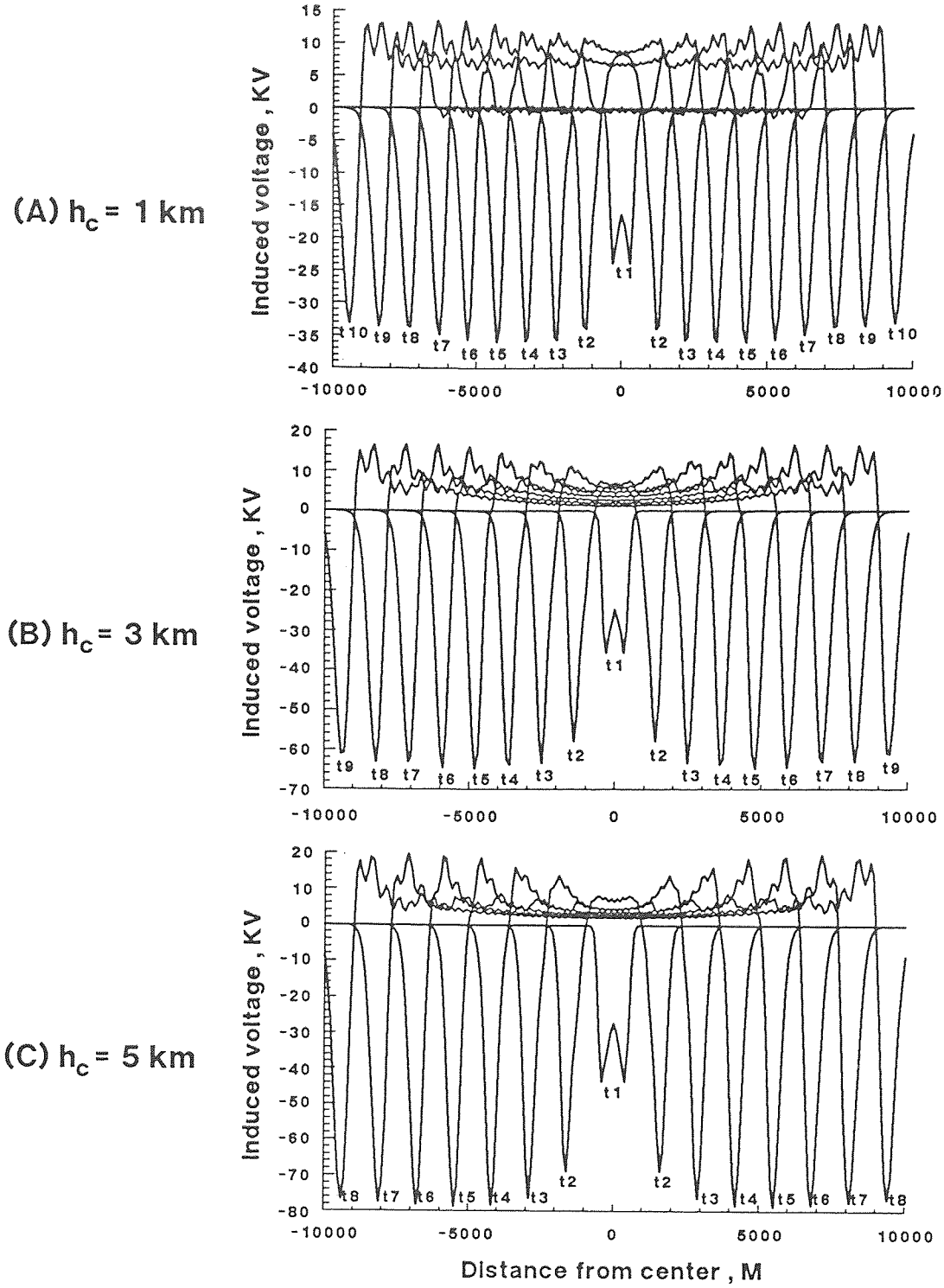

Figure 4.9 Induced voltage as a function of space at various times on an overhead power line caused by a vertical lightning stroke. Effect of height of cloud charge center, h_c.

$\beta = 0.3$, $I_0 = 10kA$, $t_f = 5\mu s$, $y_0 = 100m$, $h = 10m$

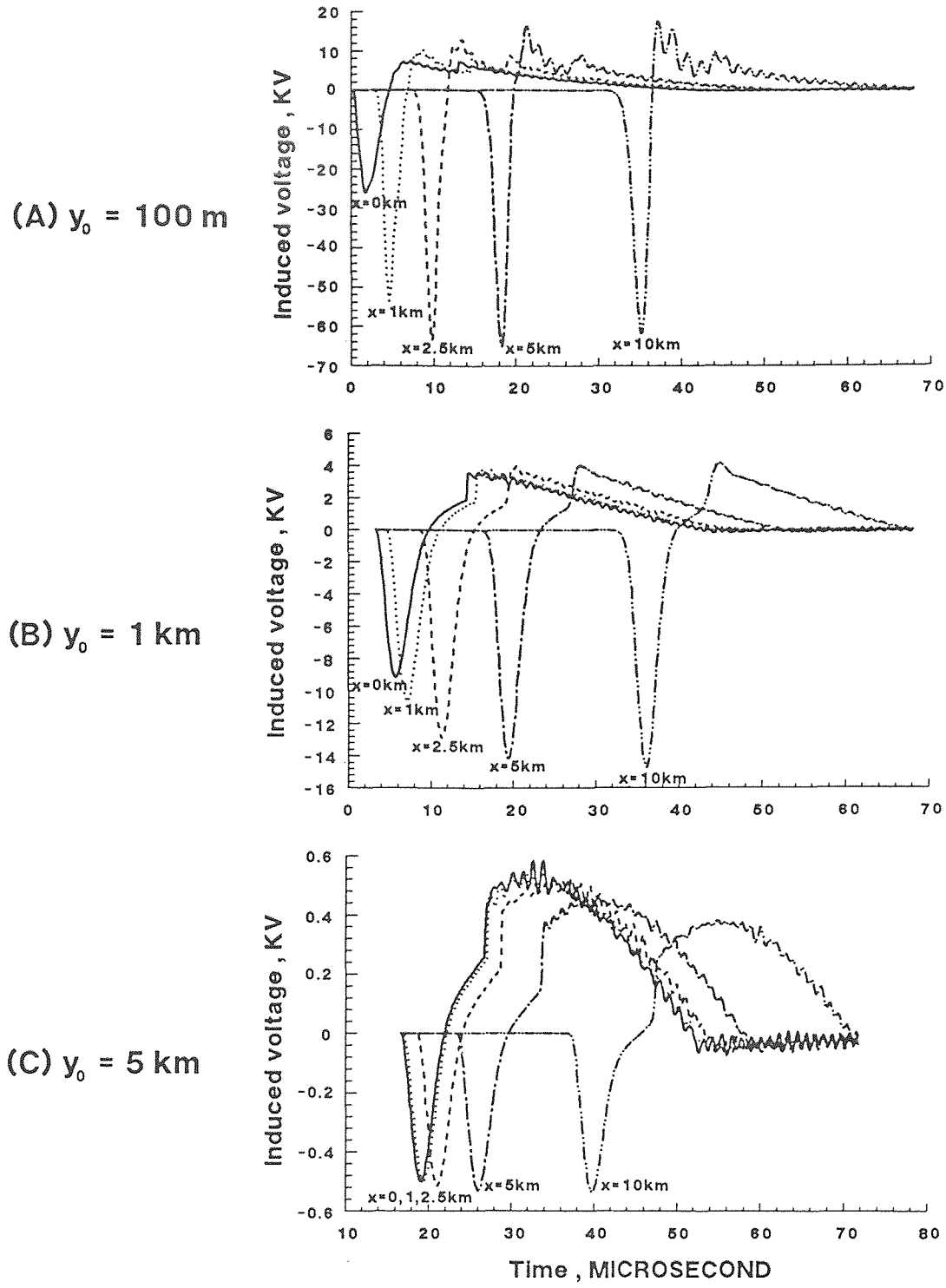

Figure 4.10 Induced voltage as a function of time at different points on an overhead power line caused by a vertical lightning stroke. Effect of least distance of the power line from the struck point, y_0.

$\beta = 0.3$, $I_0 = 10kA$, $t_f = 5\mu s$, $h = 10m$, $h_c = 3km$

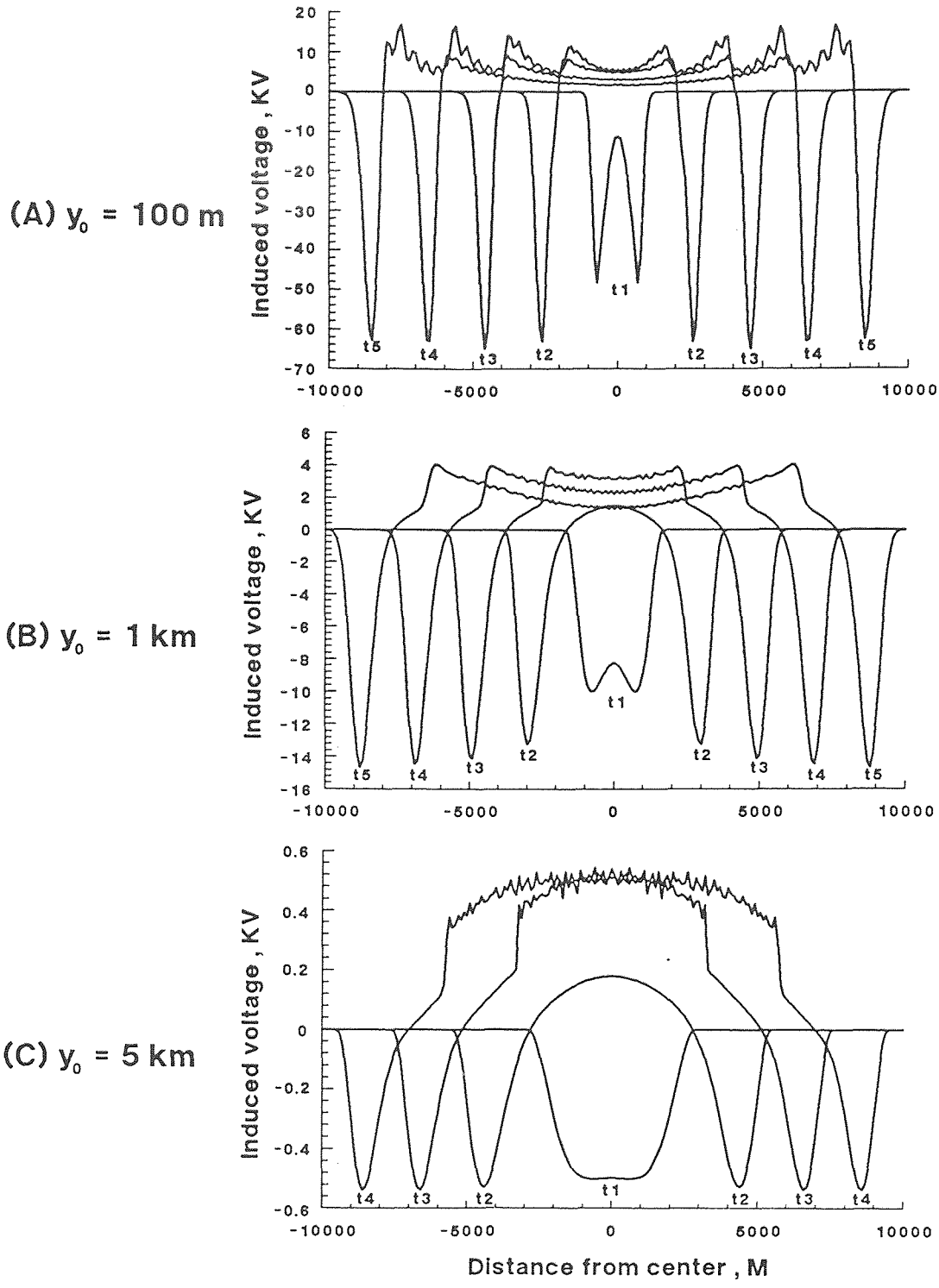

Figure 4.11 Induced voltage as a function of space at various times on an overhead power line caused by a vertical lightning stroke. Effect of least distance of the power line from the struck point, y_0.

$\beta = 0.3$, $I_0 = 10kA$, $t_f = 5\mu s$, $h = 10m$, $h_c = 3km$

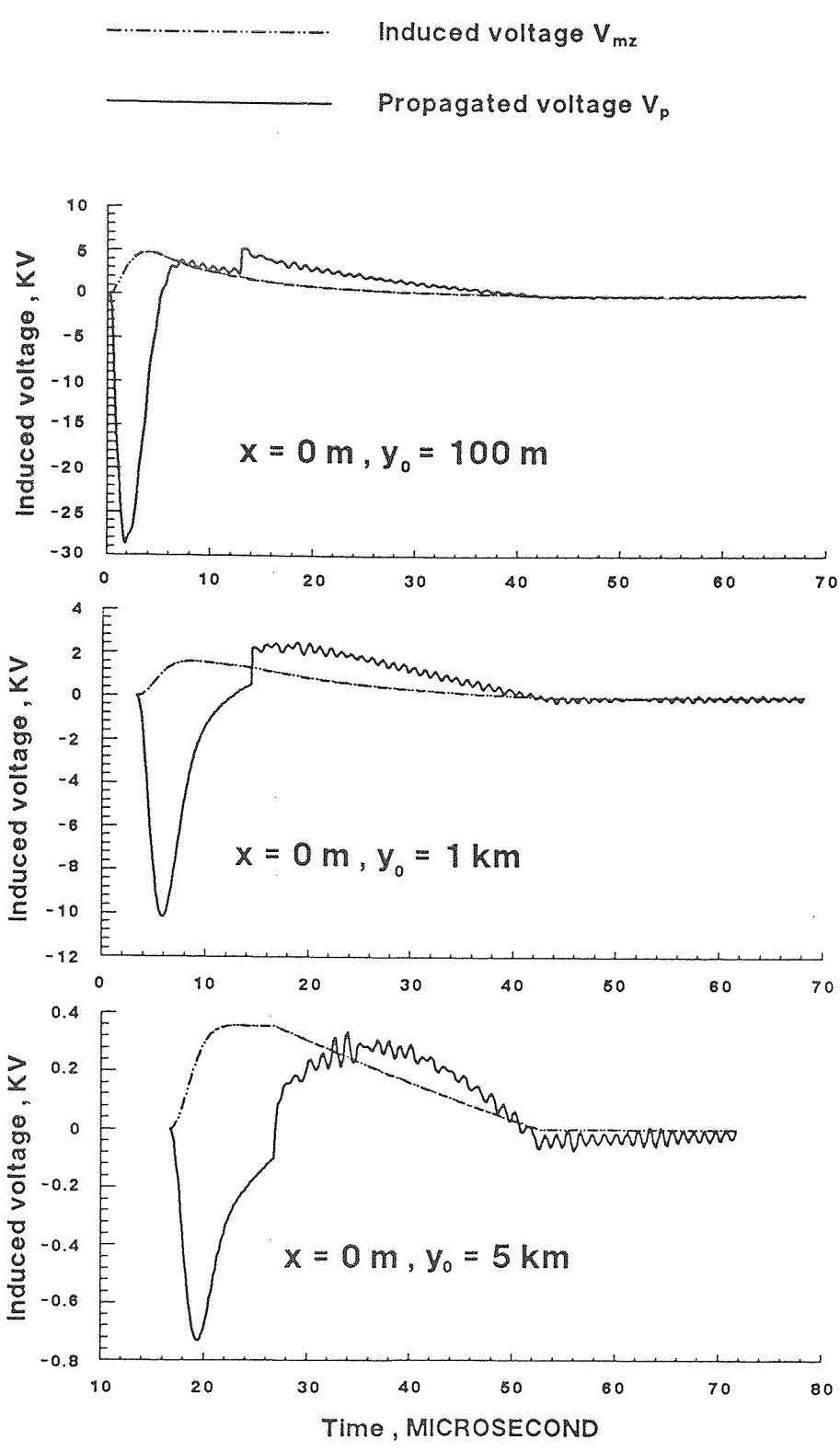

Figure 4.12 Components of induced voltage. Effect of least distance of the power line from the struck point, y_0.

$\beta = 0.3$, $I_0 = 10kA$, $t_f = 5\mu s$, $h = 10m$, $h_c = 3km$

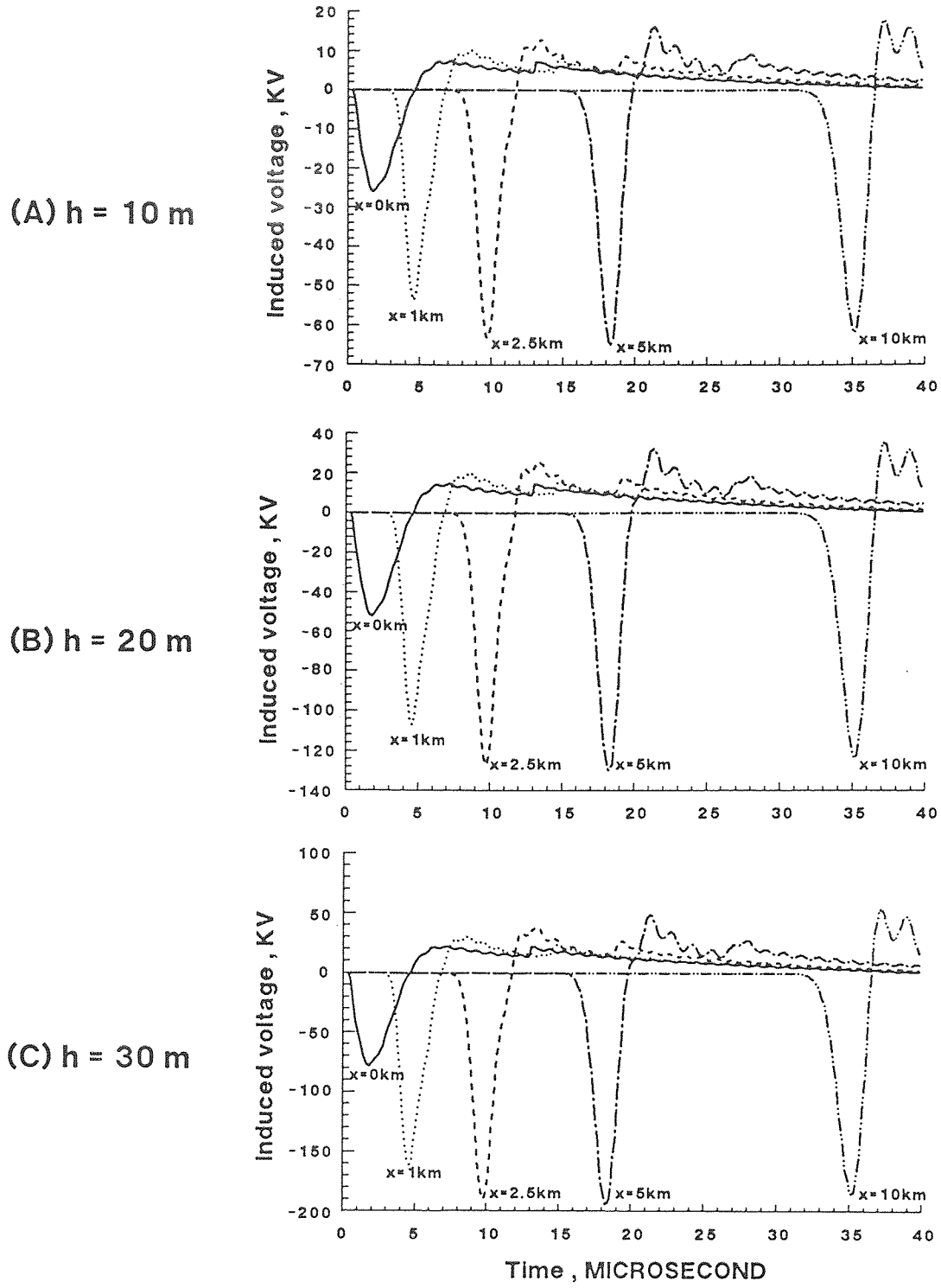

Figure 4.13 Induced voltage as a function of time at different points on an overhead power line caused by a vertical lightning stroke. Effect of height of the power line above ground, h.

$\beta = 0.3$, $I_0 = 10kA$, $t_f = 5\mu s$, $y_0 = 100m$, $h_c = 3km$

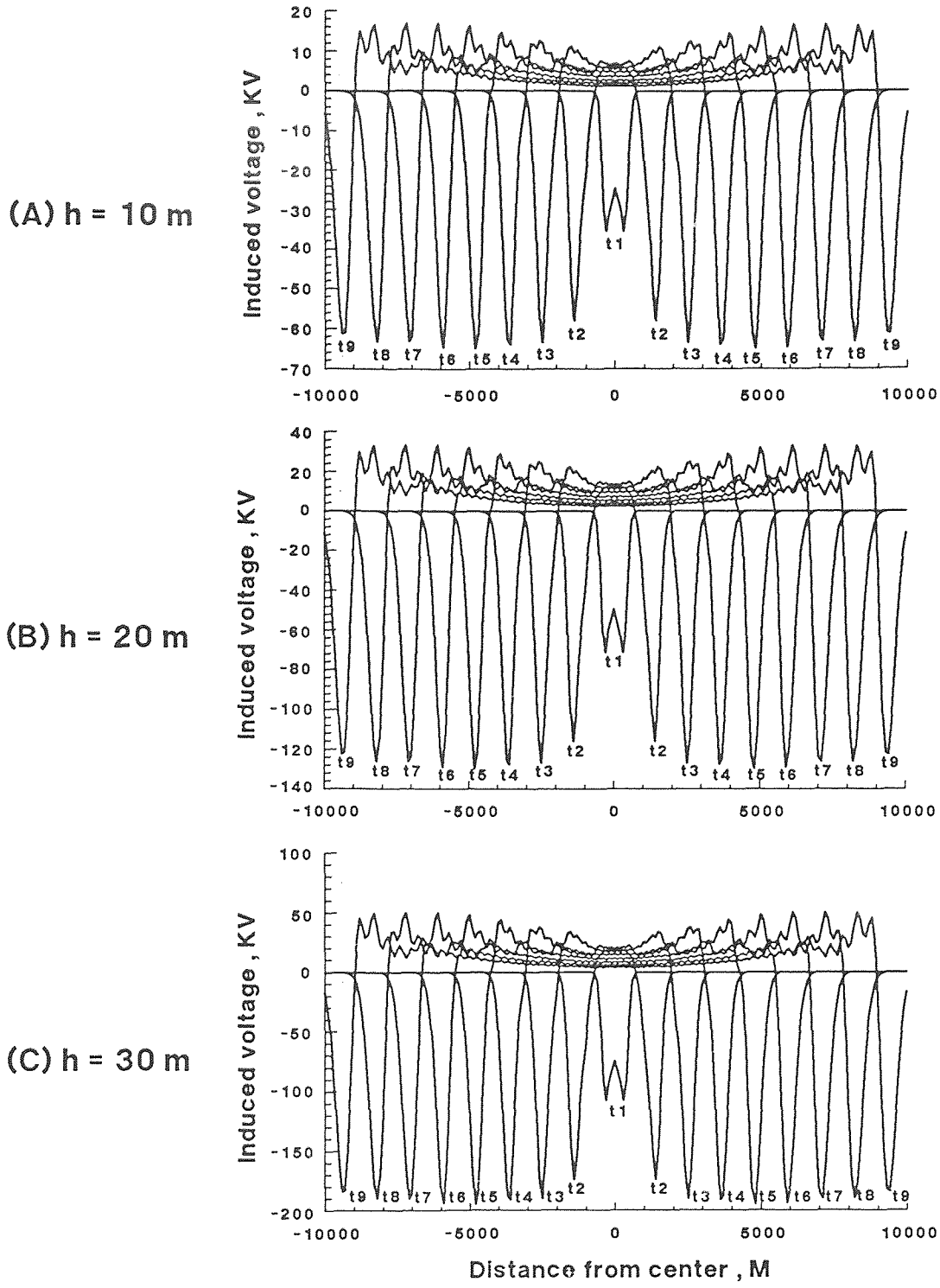

Figure 4.14 Induced voltage as a function of space at various times on an overhead power line caused by a vertical lightning stroke. Effect of height of the power line above ground, h.

$\beta = 0.3$, $I_0 = 10kA$, $t_f = 5\mu s$, $y_0 = 100m$, $h_c = 3km$

REFERENCES

[1] M. A. Uman, *Lightning*, McGraw-Hill, New York, (1969).

[2] Report of Joint IEEE-EEI Subject Committee on EHV Line Outage, Trans. IEEE, Vol. 86 (1967): 547.

[3] P. Chowdhuri, E. T. B. Gross, "Voltage Surges Induced on Overhead Lines by Lightning Strokes", Proc. IEE, Vol. 114, No. 12 (1967): 1899-1907.

[4] C. F. Wagner, G. D. McCann, "Induced Voltage on Transmission Lines", AIEE Trans., Vol. 61 (1942): 916-930.

[5] S. Rusck, "Induced Lightning Over-Voltages on Power-Transmission Lines with Special Reference to the Over-Voltage Protection of Low Voltage Networks", Tran. Royal Institute of Technology, Stockholm, Sweden (1958).

[6] S. Rusck, "Protection of Distribution Lines", *Lightning*, Vol. 2, ed. R. H. Golde, Academic Press, New York (1977): 747-771.

[7] G. Cornfield, Correspondence on "Voltage Surges Induced on Overhead Lines by Lightning Strokes", Proc. IEE, Vol. 119, No. 7 (1972): 893-894.

[8] A. C. Liew, S. C. Mar, "Extention of The Chowdhuri-Gross Model for Lightning Induced Voltage on Overhead Lines", IEEE Trans. Power Systems, Vol. PWRD-1, No. 2 (1986): 240-246.

[9] A. J. Eriksson, M. F. Stringfellow, D. V. Meal, "Lightning-induced Overvoltages on Overhead Distribution Lines", IEEE Trans. PAS, Vol. PAS-101, No. 4 (1982): 960-968.

[10] S. Yokoyama, K. Miyake, H. Mitani, A. Takanishi, "Simultaneous Measurement of Lightning Induced Voltages with Associated Stroke Currents", IEEE Trans. PAS, Vol. PAS-102, No. 8 (1983): 2420-2427.

[11] A. Sakakibara, "Calculation of Induced Voltages on Overhead Lines Caused by Inclined Lightning Strokes", IEEE Trans. Power Delivery, Vol. 4, No. 1 (1989): 683-689.

[12] S. Yokoyama, "Calculation of Lightning-Induced Voltages on Overhead Multiconductor System", IEEE Trans. PAS, Vol. PAS-103, No. 1 (1984): 100-107.

[13] K. S. Yee, "Numerical Solution of Initial Boundary Value Problems Involving Maxwell's Equations in Isotropic Media", IEEE Trans. AP, Vol. AP-14, No. 3 (1966): 302-307.

[14] A. Taflove, M. E. Brodwin, "Numerical Solution of Steady-State Electromagnetic Scattering Problems Using the Time-Dependent Maxwell's Equations", IEEE MTT, Vol. MTT-23, No. 8 (1975): 623-630.

[15] K. Berger, "The Earth Flash", *Lightning*, Vol. 1, ed. R. H. Golde, Academic Press, New York (1977): 119-190.

[16] P. Chowdhuri, "Analysis of Lightning-induced Voltages on Overhead Lines", IEEE Trans. Power Delivery, Vol. 4, No. 1 (1989): 479-489.

[17] A. Greenwood, *Electrical Transients in Power Systems*, Edition 2, John Wiley & Sons, Inc., New York (1991).